GLO 1150

DEPARTMENT OF GEOLOGY AND GEOPHYSICS

REPORT: FINAL: Volume 77-11

CONTRACT: EY-76-S-07-1601

AGENCY: DOE/DGE

TITLE: REGIONAL GRAVITY AND AEROMAGNETIC SURVEYS OF THE MINERAL MOUNTAINS AND VICINITY, MILLARD AND BEAVER COUNTIES, UTAH

AUTHORS: James A. Carter and Kenneth L. Cook

DATE: April 1978

UNIVERSITY OF UTAH SALT LAKE CITY, UTAH 84112

REGIONAL GRAVITY AND AEROMAGNETIC SURVEYS OF THE MINERAL MOUNTAINS AND VICINITY, MILLARD AND BEAVER COUNTIES, UTAH

by

James A. Carter and Kenneth L. Cook

PREFACE

The attached report was submitted by James A. Carter in partial fulfillment of the requirements for the degree of Master of Science in Geophysics, Department of Geology and Geophysics at the University of Utah. The work was performed under the direction of Dr. Kenneth L. Cook.

ABSTRACT

The results of gravity and aeromagnetic surveys of the Mineral Mountains and vicinity are presented as a terrain-corrected Bouguer gravity anomaly map (about 1450 stations with 1-mgal contour interval) and a total magnetic field intensity residual anomaly map (with contour interval 50 gammas), respectively. Combined interpretation of the gravity and aeromagnetic data was conducted based on comparing and contrasting various processed maps and interpretative geologic cross sections produced from each survey. Processing and modeling techniques which were used to faciitate the interpretation include:

1) Gravity--a) high-pass frequency filtering, b) polynomial fitting, c) pseudomagnetic filtering, d) strike filtering, e) upward continuation filtering, and f) two and one-half dimensional profile modeling.

2) Aeromagnetics--a) low-pass frequency filtering, b) polynomial fitting, c) pseudogravity filtering, d) strike filtering, and e) two and one-half dimensional profile modeling.

Broad structural features apparent from the interpretation include: 1) Basin and Range normal faults which strike generally north-south and lie along the eastern and western margins of the Mineral Mountains; 2) the grabens of Milford and Beaver valleys which border the Mineral Mountains horst on the west and east, respectively; and 3) an east-northeastward-trending lineation which corresponds with the

Black Rock offset of Crosby (1973) and passes through the County Line fault in the northern Mineral Mountains. This lineation probably corresponds to a major structural feature along which intrusive bodies have been emplaced. Modeling of the reduced gravity data using an assumed density contrast of 0.5 g/cc between the bedrock and valley fill resulted in a depth of alluvial fill of about 1.5 km at the deepest point in Milford Valley graben.

Quaternary rhyolite domes and flows are exposed along the crest of the Mineral Mountains. These volcanics are thought to be related to the heat source for the geothermal reservoir at Roosevelt Hot Springs. Roughly corresponding magnetic and gravity lows overlie the exposed volcanic domes which include Bearskin, Little Bearskin and North and South Twin Flat Mountains. These lows may be caused by a magma chamber at rather shallow depth, but are more likely caused by the lower density and magnetic susceptibility of the rhyolite. A gravity saddle in the area of Ranch Canyon and a roughly corresponding magnetic saddle are also possible expressions of a low-density, low-magnetic susceptibility body, but modeling has indicated that the gravity saddle may be caused by overlap of the gravity lows associated with Milford Valley and Beaver Valley grabens and the silicic volcanics. Removal of a different regional gravity could, however, alter this conclusion.

Over the known geothermal reservoir, possible expressions of hydrothermal magnetite alteration (a magnetic low area) and sediment

densification (a gravity high area) have been observed. A north-south-trending magnetic high, which overlies alluvium, corresponds with the Opal Mound fault, which marks the westward extent of the reservoir. A pronounced magnetic low, which may represent a sedimentary or metamorphic rock unit, is located just south of the high thermal gradient anomaly area and corresponds with the southern boundary of the reservoir.

ACKNOWLEDGEMENTS

I would like to thank my committee chairman, Dr. K. L. Cook, and the other members of my committee, Dr. J. A. Whelan, and Dr. R. T. Shuey for their guidance and assistance throughout this study.

University of Utah students W. D. Brumbaugh, R. F. Sawyer, and J. H. Snow assisted by providing helpful discussion and instruction in the data reduction and interpretation phases of this research.

Dr. J. R Montgomery of ASARCO generously provided the polynomial fitting programs used in processing the data.

My sincere appreciation is also given to my parents, Mr. and Mrs. R. B. Carter, who provided much encouragement and assisted in various ways in the completion of this thesis.

Financial assistance for this work was provided by the Energy Research and Development Administration (ERDA) and the Department of Energy, Division of Geothermal Energy (DOE/DGE) under Contract No. EY-76-S-07-1601.

TABLE OF CONTENTS

TABLE OF CONTENTS (CONT'D)

LIST OF ILLUSTRATIONS

Figures

LIST OF ILLUSTRATIONS (CONTINUED)

LIST OF ILLUSTRATIONS (CONTINUED)

LIST OF ILLUSTRATIONS (CONTINUED)

Tables

PLATE

INTRODUCTION

The Mineral Mountains and vicinity have been an area of active geothermal exploration since 1972. The focus of most of this exploration has been the Roosevelt Hot Springs Known Geothermal Resource Area (KGRA), which is located along the western flank of the Mineral Mountains approximately 20 km northeast of the town of Milford, Beaver County, Utah. To date (1978) two companies have drilled seven wells within the KGRA and the prospects for power production are now being evaluated.

Location and General Description of the Survey Area

The boundaries of the gravity and aeromagnetic surveys which comprise about 1075 km^2 and 540 km^2, respectively, are shown in Figures 1 and 2. The gravity survey area includes the Mineral Mountains, Milford Valley (a northern extension of the Escalante Desert), the Rocky Range, and portions of the Black Mountains, the Star Range, the Beaver Lake Mountains, the Beaver Mountains and Beaver Valley. The aeromagnetic survey area includes the Mineral Mountains and portions of both Milford Valley and Beaver Valley.

Topographic relief between the highest peaks of the northward-trending Mineral Mountains and the flanking valley floors is about 1.2 km. The characteristic features of the topography within the central Mineral Mountains are steep, narrow, eastward-trending canyons and sharp

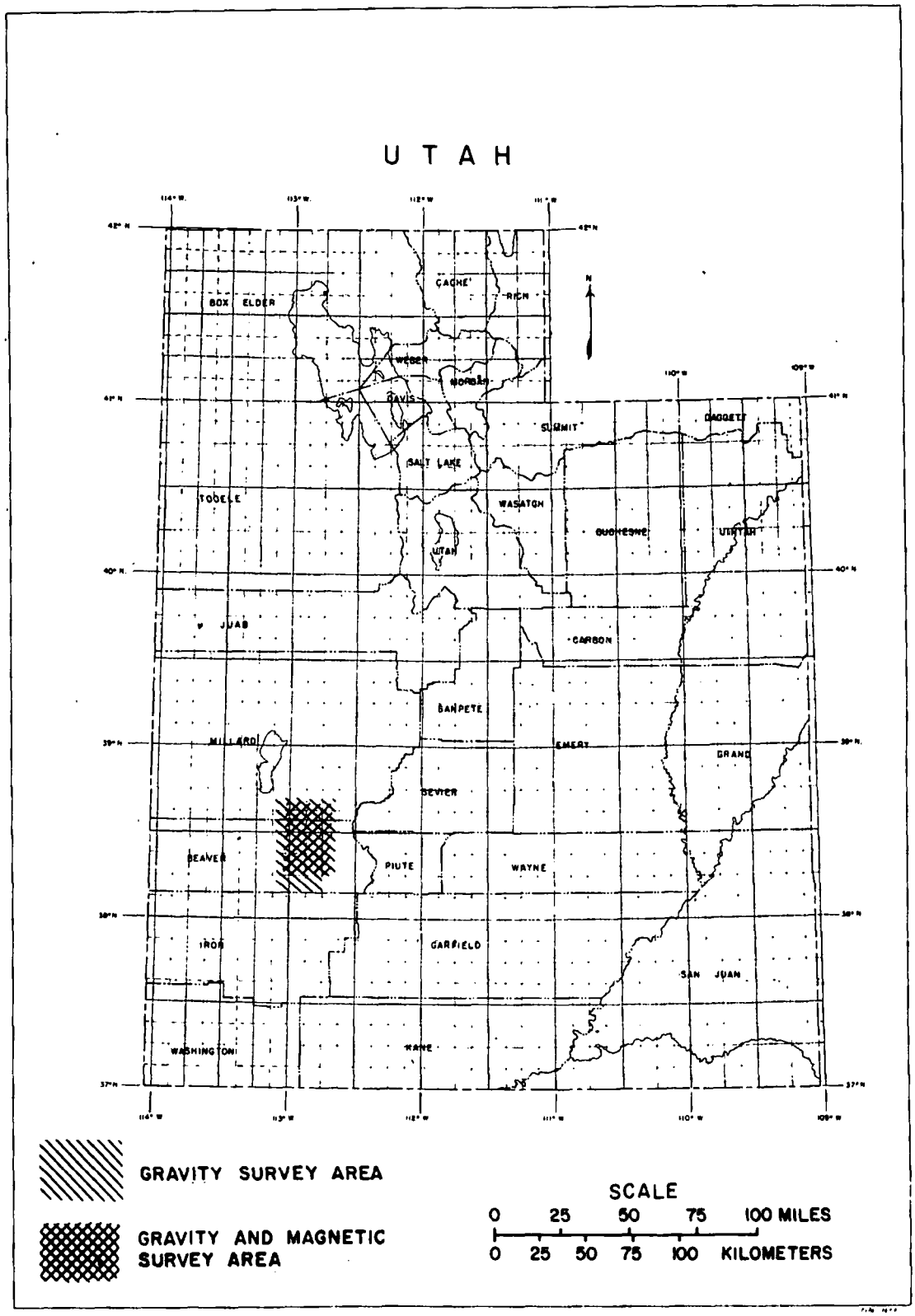

Figure 1. Map of Utah showing the surveyed area.

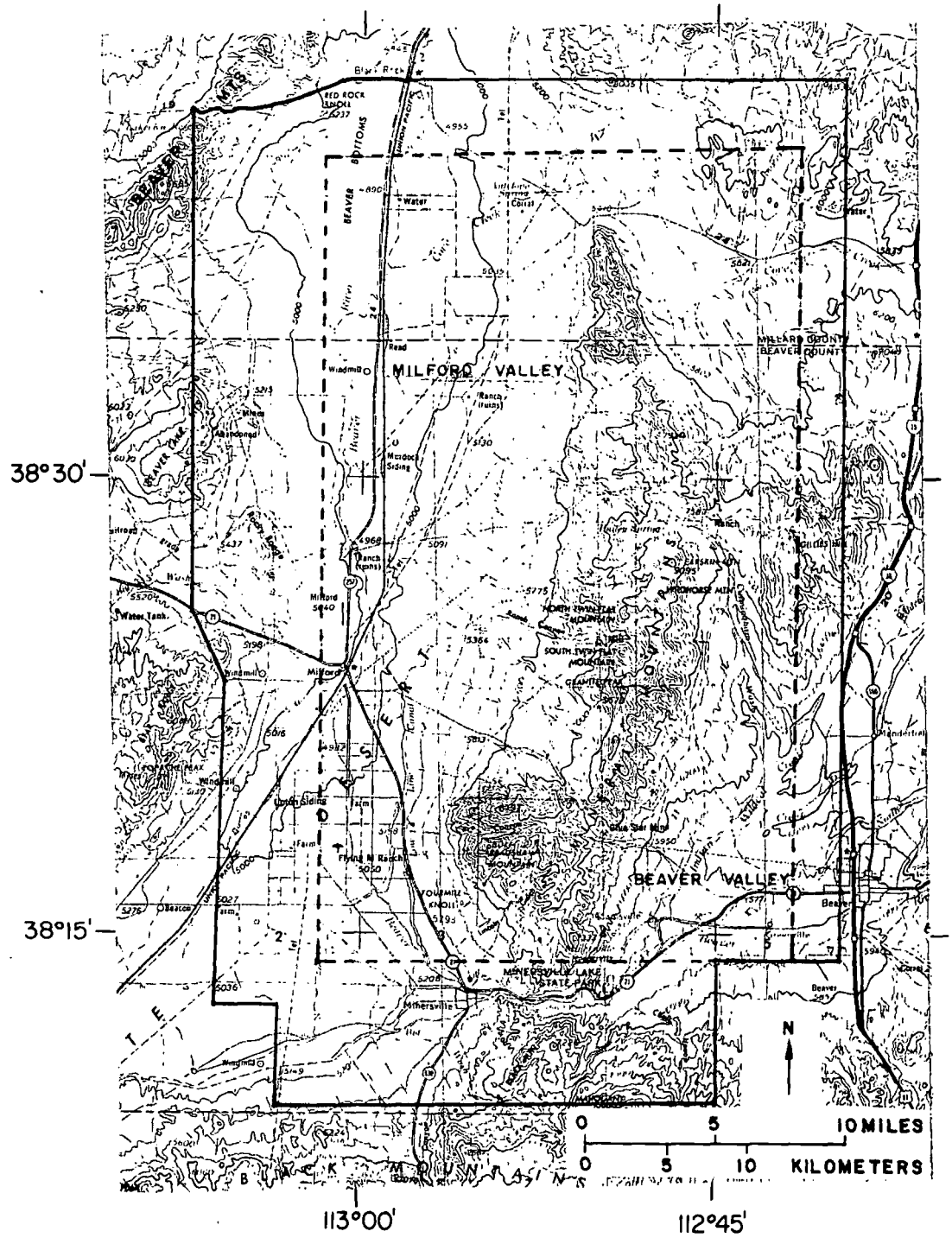

Figure 2. Index map showing outlines of the gravity and aeromagnetic surveys. Solid line-gravity survey; dashed line-aeromagnetic survey.

granite spires. The northern and southern parts of the Mineral Mountains are comprised mainly of metamorphic and sedimentary rocks, and the characteristic topography within these areas is not as rugged as in the pluton dominated central section.

Topographic relief between the highest peaks of the previously mentioned mountain ranges (other than the Mineral Mountains) and the adjacent valleys ranges from 0.3 km to 0.6 km and the characteristic topography within these ranges varies from very rugged topography in the volcanic Black Mountains to regularly undulating low peaks in the Beaver Mountains.

Previous Geologic, Geochemical and Geophysical Investigations

Early geologic investigations in the area of study include general geologic descriptions and mapping by Butler et al. (1920) and Crawford and Buraneck (1945), both of whom were interested primarily in the mineral resources of the area. The geology of the northern part of the Mineral Mountains was mapped by Liese (1957) and the central and southern parts were mapped by Earll (1957). The area including Roosevelt Hot Springs was mapped in detail by Petersen (1975a, 1975b) and Parry and Dedolph (1976). The northern and central Mineral Mountains have been remapped by Evans et al. (1977). The geology of portions of the Black Mountains has been mapped by Erickson and Dasch (1968), and Erickson (1973) described the volcanic rocks of most of the survey area. The Star Range was described and mapped in reports by Baer (1962), Abou-Zied (1968) and Baetcke (1969). The geology of

the Beaver Lake Mountains has been mapped and described by Barosh (1960) and Welsh (1973). The Rocky Range geology was mapped by Whelan (1973).

Geochemical investigations of alteration within the goethermal gradient anomaly area (Fig. 4) near Roosevelt Hot Springs have been conducted by Parry et al. (1976) and Bryant and Parry (1977).

Geophysical investigations include resistivity surveys near Roosevelt Hot Springs by Ward and Sill (1976) and heat flow studies by Sill and Bodell (1977). Regional gravity surveys with large station separations by Mudgett (1963) and Petersen (1972) obtained the gross features of the gravity field over Milford Valley. Schmoker (1972) analyzed the gravity and aeromagnetic fields over the western edge of the survey area using data obtained from the U.S. Geological Survey aeromagnetic and gravity maps (1966) for the San Francisco Mountains and vicinity. Additional aeromagnetic data are available from the state map which was compiled by Zietz et al. (1976).

The present study incorporates the gravity work of several investigators from the University of Utah. All or portions of the data from the following studies were incorporated into the present gravity study, which consists of data for 1468 gravity stations: Brumbaugh and Cook (1977), Crebs and Cook (1976), Sawyer and Cook (1977), Sontag (1965), and Thangsuphanich (1976). A map showing that portion of the study area surveyed by each of these investigators as

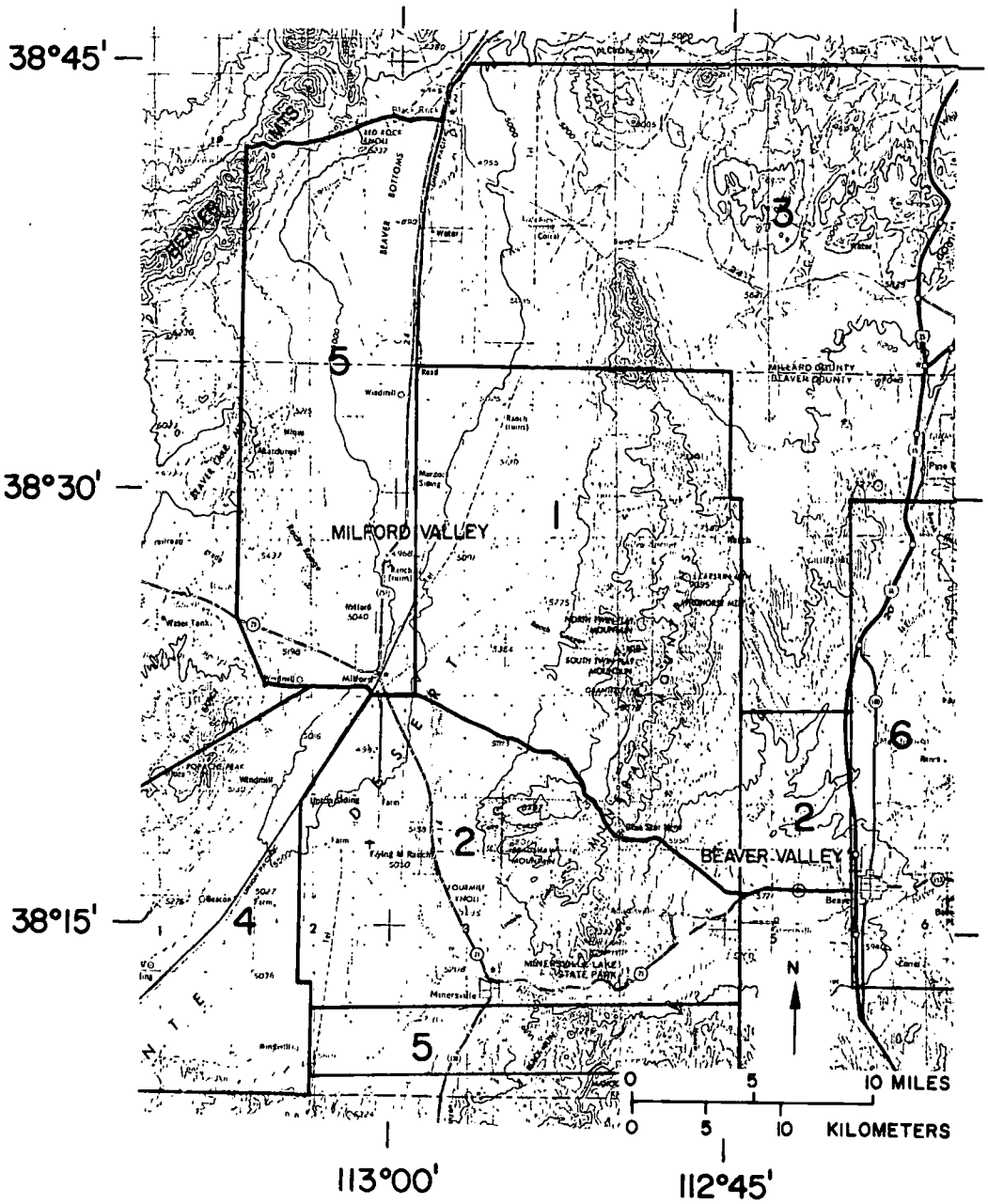

Figure 3. Gravity survey index map, for key see Table 1.

Table 1. Key to gravity surveys shown in Figure 3.

Map No.	Investigator	Distance to Which Stations Were Terrain-Corrected
1	Crebs (1976)	28.8 km [1/]
2	Thangsuphanich (1976)	28.8 km [1/]
3	Brumbaugh (1977)	20.0 km [2/]
4	Sawyer (1977)	18.8 km [1/]
5	Carter	20.0 km [2/]
6	Sontag (1965)	58.8 km [1/]

[1/] Terrain corrections were computed using U.S.C. & G.S. zone charts. Terrain corrections were computed for each station in mountainous terrain. In flat terrain, a judicious number of stations were terrain-corrected and the terrain corrections for remaining stations were contoured and interpolated from these values.

[2/] Terrain corrections were computed using U.S.C. & G.S. zone charts for inner zones (B through E) and a computer program (Kane, 1962 and Hardman, 1964) for the remaining distance to 20 km. Terrain corrections were computed for all stations.

well as those portions of the area surveyed by the author is shown in Figure 3.

Purpose and Scope of the Study

Gravity and magnetic methods have been used extensively in the investigation and interpretation of geothermal prospects. The primary contirbution of gravity and magnetic data in geothermal exploration lies in the delineation of the structural framework within which the geothermal resource is located. Insight into the structural setting can be derived from both qualitative inspection of gravity and magnetic maps and quantitative geologic modeling of anomalies.

In some cases the relationship between gravity and/or magnetic data and the geothermal prospect is more direct. However, anomalies which have been observed over known geothermal prospects are variable in character and must be carefully interpreted with attention to the geologic setting. At the Imperial Valley KGRA in southern California, small positive gravity anomalies observed over areas of high heat flow have been attributed to either an emplacement of higher density rhyolite domes or a densification process in which the loosely consolidated sediments are cemented and/or thermally metamorphosed by circulating hot fluids (Biehler and Combs, 1972). At the Geysers geothermal field, located 120 km north of San Francisco, a gravity low (about 20 km wide and with about 30 mgal closure) northeast of the steam field has been interpreted as a magma chamber (Isherwood, 1975), which is thought to be the heat source for the geothermal system. At

the Lake City KGRA in Modoc County, California, a strong gravity gradient of 25 mgal in 2 mi (3.3 km) is centered over a mud volcano and hot spring (Anderson and Axtel, 1972). The gradient is attributed to a fault with over 5,000 ft (1524 m) of vertical displacement which may serve as a conduit for the circulation of thermal fluids. Magnetic anomalies in geothermal areas are, in general, even less characteristic than gravity anomalies (Chapman, 1975). This is generally caused by the location of most geothermal areas in volcanic regions where information about the subsurface is scant and the possible causes of magnetic anomalies are many. Possible magnetic anomalies which are directly related to geothermal systems include magnetic lows caused by hydrothermal destruction of magnetite and characteristic magnetic anomalies which may indicate the location of unexposed igneous rocks related to the heat source.

The analyses of gravity and magnetic data in this study were performed in an attempt to 1) delineate the structural setting of the Roosevelt Hot Springs KGRA and 2) discover any direct gravity and/or magnetic expression of the geothermal system (either the steam reservoir or the heat source).

GEOLOGY

General Geology

The area of study is located in southwestern Utah (Fig. 1) in the Basin and Range physiographic province which is characterized by north-south trending horst block mountain ranges separated by alluvium-filled basins, which are generally grabens. The major topographic and geologic feature of the area is the graben-horst combination formed by Milford Valley (a northern extension of the Escalante Desert) and the Mineral Mountains (Figs. 2 and 4). The Mineral Mountains horst, which rises about 1 km above the floor of Milford Valley, is dominated geologically by the Mineral Mountains pluton. This pluton is the largest single outcropping intrusive body in Utah, covering nearly 250 km^2. Potassium-argon ages of 9 million years (m. y.) and 14 m. y. have been obtained from the pluton (Park, 1968; Armstrong, 1970). Both ages may be young due to reheating of the pluton by Quaternary volcanic activity. The dominant unit of the pluton is a light-colored granite which is medium to very coarse grained. In the northern portion of the area, granodiorite predominates and both units are gradational along the edges of the outcrop to a darker granitic rock which is fine to medium grained. The pluton is cut by mafic and aplitic dikes as well as a suite of Quaternary silicic volcanics (Parry et al., 1977). The northern terminus of the Mineral Mountains pluton has been designated the

FIGURE 4. GENERAL GEOLOGIC MAP OF THE MINERAL MOUNTAINS AND VICINITY, BEAVER AND MILLARD COUNTIES, UTAH. GEOLOGY COMPILED FROM EVANS (1977), HINTZE (1963), WHELAN (1973, 1977), BAER (1973), AND WELSH (1973).

EXPLANATION

SEDIMENTARY ROCKS

CENOZOIC	Qal	QUATERNARY ALLUVIUM
	Qos	QUATERNARY OPAL AND OPALINE SINTER
	Qcal	QUATERNARY CEMENTED ALLUVIUM
	C	CENOZOIC SEDIMENTARY ROCKS
MESOZOIC	M	MESOZOIC SEDIMENTARY ROCKS
PALEOZOIC	P	PALEOZOIC SEDIMENTARY ROCKS

METAMORPHIC ROCKS

PRECAMBRIAN	Pc	PRECAMBRIAN METAMORPHIC ROCKS

IGNEOUS ROCKS

CENOZOIC	Ti	TERTIARY INTRUSIVE ROCKS
	Qb	QUATERNARY BASALT
	Qrd	QUATERNARY RHYOLITE DOMES
	Qrf	QUATERNARY RHYOLITE FLOWS
	Qvt	QUATERNARY VOLCANIC TALUS
	Qra	QUATERNARY ASH FLOWS
	T_2bf	LATE TERTIARY BASALT FLOWS
	T_2rf	LATE TERTIARY RHYOLITE FLOWS
	Tvrp	TERTIARY ROGER PARK BRECCIA
	Tvu	TERTIARY VOLCANICS, UNDIFFERENTIATED
	Tvbc	TERTIARY BULLION CANYON RHYOLITE
	Tvdh	TERTIARY DRY HOLLOW LATITE
	Tvmb	TERTIARY MOUNT BELKNAP RHYOLITE
	Tvji	TERTIARY JOE LOTT TUFF
	Tvnr	TERTIARY NEEDLES RANGE LATITIC IGNIMBRITES
	Tvl	TERTIARY ISOM ANDESITIC-LATITIC IGNIMBRITES
	T_2ap	LATE TERTIARY ANDESITE-TRACHYTE-LATITE PYROCLASTICS

GEOLOGY CONTACT

NORMAL FAULT (BALLS INDICATE DOWNTHROWN SIDE)

STRIKE-SLIP FAULT (ARROWS INDICATE DIRECTION OF RELATIVE MOTION)

THRUST FAULT, BARBS ON THRUST SHEET

RAILROAD

HIGHWAY

ROAD

HIGH THERMAL GRADIENT ANOMALY AREA, OUTLINE FOLLOWS 300°C/KM CONTOUR

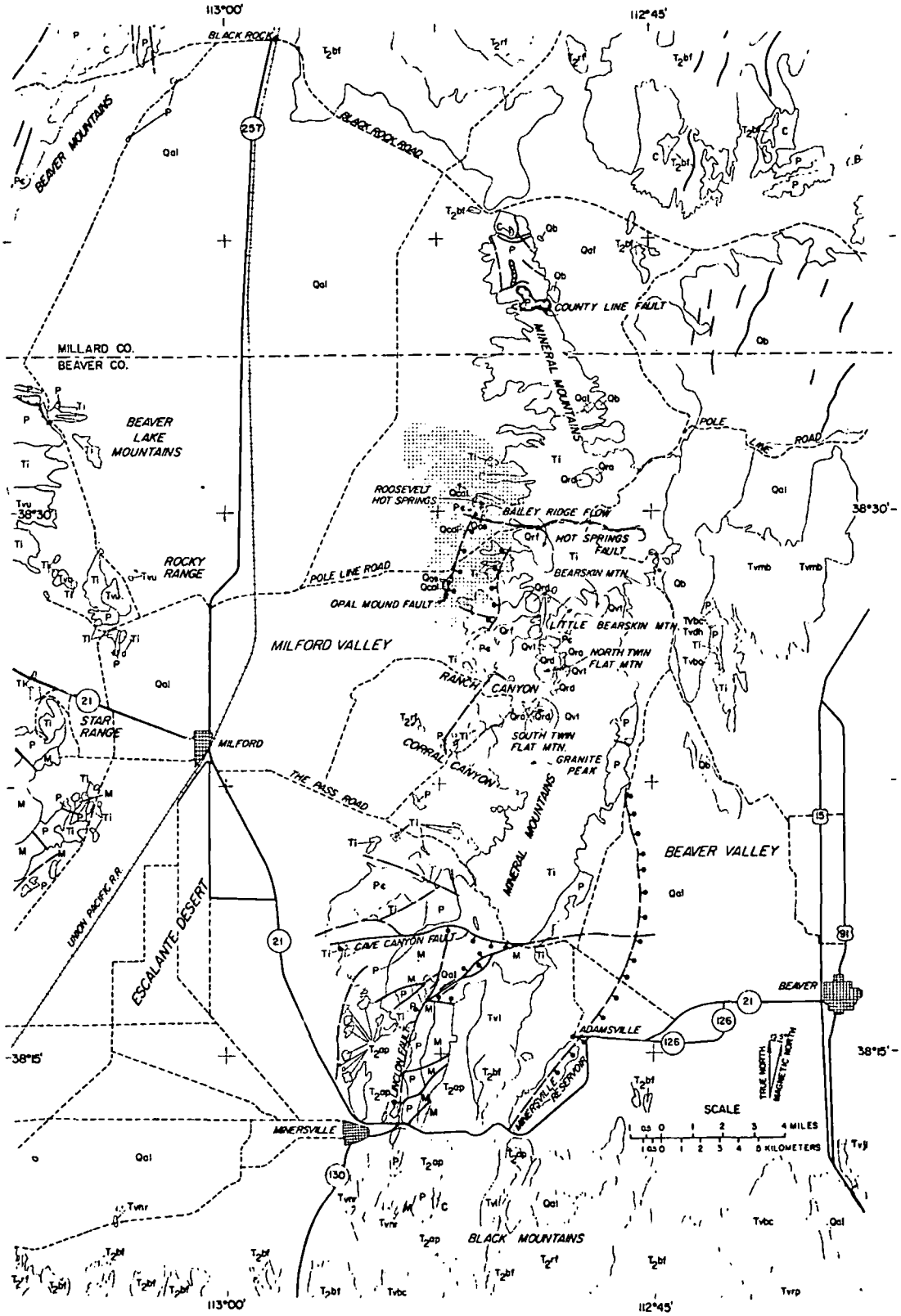
113°00'
112°45'
BLACK ROCK
BLACK ROCK ROAD
BEAVER MOUNTAINS
COUNTY LINE FAULT
MINERAL MOUNTAINS
MILLARD CO.
BEAVER CO.
BEAVER LAKE MOUNTAINS
POLE LINE ROAD
ROOSEVELT HOT SPRINGS
BAILEY RIDGE FLOW
HOT SPRINGS FAULT
BEARSKIN MTN.
OPAL MOUND FAULT
LITTLE BEARSKIN MTN
NORTH TWIN FLAT MTN.
ROCKY RANGE
MILFORD VALLEY
RANCH CANYON
SOUTH TWIN FLAT MTN.
GRANITE PEAK
CORRAL CANYON
STAR RANGE
MILFORD
THE PASS ROAD
BEAVER VALLEY
UNION PACIFIC R.R.
ESCALANTE DESERT
CAVE CANYON FAULT
ADAMSVILLE
BEAVER
MINERSVILLE
BLACK MOUNTAINS
SCALE
MILES
KILOMETERS
TRUE NORTH
MAGNETIC NORTH
38°30'
38°15'

County Line fault (Fig. 4) and north of this fault the Mineral Mountains horst is composed of sedimentary units predominantly of Cambrian age. The Cambrian formations as mapped by Liese (Petersen, 1973) are a quartzite (30 m thick), a shale (10-30 m thick), and two limestone formations (total thickness about 540 m). One conglomerate unit about 35 m thick, crops out in the northern Mineral Mountains and is dated as Tertiary (?) by Petersen (1973). The central Mineral Mountains (north of Cave Canyon fault and south of the County Line fault) is comprised largely of pluton; however, limited sedimentary outcrops of Permian age occur on the eastern and western flanks of the pluton. On the eastern flanks, both a limestone and a sandstone formation are exposed, whereas only the limestone formation occurs on the western flank. In addition to the sedimentary units and the pluton, other lithologic units exposed in the central Mineral Mountains are hot spring deposits, Quaternary silicic volcanics (both of these features will be discussed later) and an irregular belt of gneiss and schist (900 m thick) (Earll, 1957, p. 9) which is exposed along the west side of the range both north and south of Cave Canyon fault. These metamorphic rocks are assigned a Precambrian (?) age on the basis of lithologic similarity to other rocks of known Precambrian age in Utah. South of Cave Canyon fault in the southern Mineral Mountains, only three small intrusives are exposed and Earll (1957) maps the western two outcrops as quartz monzonite and not an extension of the main pluton. The sedimentary formations of the southern Mineral Mountains range in age from Mississippian to Jurassic and include limestones, sandstones, and shales. There is also one

conglomerate formation which Earll (1957) dated as Cretaceous (?) but which has been dated as Tertiary (?) by Petersen (1973). The Mississippian formation is limestone (825 m thick). The Pennsylvanian - early Permian is represented by an undifferentiated limestone (280 m thick). The later Permian is represented by quartzite (370 m thick) and limestone (210 m thick). The Triassic is represented by units of limestone and shale (total thickness of 390-520 m). The Jurassic is represented by two sandstone formations (total thickness of 640 m). Exposures of volcanic rocks are found south of Cave Canyon fault along the eastern border of the range. These volcanics, which grade from basal andesite flows to quartz latite flows with some olivine basalt flows in the upper layers of the stratigraphic column (Earll, 1957; Petersen, 1973), are of Tertiary age.

South of the Mineral Mountains, across highway 21, are the Black Mountains. These mountains are comprised mostly of late Tertiary volcanics, although limited exposures of Paleozoic and Mesozoic sedimentary rocks occur. These sediments are postulated to underlie the extrusives at fairly shallow depths of about 300 m (Erickson, 1968).

Along the western margin of Milford Valley are three mountain ranges which trend generally north-south. They are from south to north the Star Range, the Rocky Range, and the Beaver Lake Mountains. All three ranges consist of intrusive and extrusive igneous bodies which have metamorphosed adjacent Paleozoic and Mesozoic sediments near the zones of contact. Potassium-argon age dates indicate that the intrusion in

the Star Range is 21 m. y. old, the intrusion in the Rocky Range is 27 m. y. old and the intrusion of the Beaver Lake Mountains is 28 m. y. old (Lemmon et al., 1973). North of the Beaver Lake Mountains are the Beaver Mountains which consist of Precambrian rocks, Paleozoic sediments and a Tertiary conglomerate formation. North and east of the Mineral Mountains, basalt and rhyolite flows predominate, although some outcrops of Paleozoic sediments are found.

Structural Geology

The dominant structural features of this area are those of the Basin and Range province. As noted before, the Basin and Range structure is characterized by north-south trending horst block mountain ranges separated by deep valleys with normal faulting forming the boundaries between horst and graben. The Mineral Mountains and Milford Valley of this study are a good example of this horst-graben structure. Another prominent structural feature in this area is overthrusting and folding, which took place during the Sevier orogeny of late Cretaceous age. The well-defined leading edge of the thrust sheet, which advanced from the northwest and placed Cambrian rock over younger rock, is right laterally offset along an east-northeast-trending line which passes through the County Line fault in the northern Mineral Mountains (Fig. 4). This offset, designated the Black Rock offset by Crosby (1973), extends eastward from well-defined exposures of the leading edge of the thrust in the Beaver Lake Mountains (Fig. 4), across the mapped thrusting in the northern Mineral Mountains, to the next exposure of the leading edge of the thrust in the southern Pavant

Range (about 8.5 km east-northeast of the small Paleozoic outcrop near the northeast corner of Fig. 4). Crosby (1973) considers the scattered sedimentary exposures south of this offset as part of a "disturbed belt" in which deformation and local thrusting caused by the advancing thrust sheet account for the complex relationships of the exposed sedimentary sections. This disturbed belt, which encompasses the entire area of study south of the offset line, is defined as a transition zone between the undeformed strata of the Colorado plateau and the severely deformed rocks of the fold and thrust belt (Crosby, 1973). The Black Rock offset also marks the apparent northern termination of an east-west belt of igneous intrusions (Butler, 1920, Schmoker, 1972) which were probably emplaced along a major structural feature.

Geology of Roosevelt Hot Springs Thermal Area

The major near-surface thermal gradient anomaly, determined from thermal gradient measurements in about 50 drill holes of varying depths, is located just west of the Mineral Mountains pluton, largely over alluvium (Fig. 4). Detailed geologic mapping of this area was done by Petersen (1975a, 1975b) and Parry and Dedolph (1976). Mapping of the surrounding areas in the central and northern Mineral Mountains has been done by several investigators from the University of Utah and this work has been compiled by Evans (1977). The following discussion is based largely on these studies.

At one time a group of hot springs discharged in the high thermal

gradient area and water samples were taken as recently as 1957, but all of the springs were dry by 1966 (Mundorff, 1970). Hot spring deposits consist largely of siliceous sinter and sinter cemented and altered alluvium. Sulfur is also present in localized areas. These hot spring deposits lie along the north-south-striking Opal Mound fault (Fig. 4) which is the most conspicuous of numerous north-south and east-west trending faults that cut through the thermal gradient anomaly area. Some of these faults, which have been mapped or inferred by various geophysical and geological techniques, appear to control the shape of the near-surface thermal anomaly (Sill and Bodell, 1977).

Other rocks which crop out in the area surrounding the thermal gradient anomaly include granite of the pluton, Precambrian (?) metamorphic rocks, and a suite of Quaternary silicic volcanic flows and domes of which the granite and Precambrian (?) rocks were discussed earlier. The suite of rhyolite volcanics extends discontinuously for about 15 km along the crest of the Mineral Mountains (Fig. 4). Potassium-argon radiometric dates indicate that the two flows (which display reversed magnetic polarity) are about 800,000 yr old and the domes (which display normal magnetic polarity) are about 500,000 yr old. Chemical and mineralogical data indicate that the rhyolite domes and flows may have originated from the same magma batch by the fractionation of feldspar (Parry et al., 1977). Water fugacities indicate that the flows were extruded from a magma chamber at a depth of 11 km while the domes were extruded from a depth

of 1.6 km. The disparity in depth of origin of the flows and domes indicates that there may be two magma chambers. The earlier and deeper chamber having extruded the flows while the second chamber (possibly derived from the first by feldspar fractionation) extruded the domes. The similarity in the petrologic and chemical composition of the domes suggests that they all originated from the same relatively shallow magma chamber (Parry et al., 1977).

INSTRUMENTS AND FIELD TECHNIQUES

Data Acquisition

The gravity data acquired and used in this study were obtained by several researchers from the University of Utah. These researchers used instruments and field techniques similar to those used by the author so only the author's instruments and field techniques will be discussed. The aeromagnetic data used in this study were acquired by Aerial Surveys, under contract to, and satisfying the requirements of the University of Utah, Department of Geology and Geophysics. The product supplied to the University of Utah by Aerial Surveys was a total magnetic field intensity residual anomaly map with the earth's main field (as established by the International Geophysical Reference Field, updated to 1975) removed. This map (contour interval 25 gammas) was used as raw data for the study.

Instrumentation

All gravity readings taken by the author were obtained using LaCoste and Romberg model G geodetic gravity meter no. 264 which has a precision capability of 0.001 mgal. The aeromagnetic survey was conducted using a Geometrics proton precession magnetometer with 1 gamma accuracy.

Gravity Field Techniques

Gravity stations were located on published or preliminary 7-1/2 minute U.S.G.S. topographic quadrangle maps at easily identified positions such as road intersections, bench marks, section corners, and spot elevations. Elevations for most stations were taken directly from the maps since positions with known elevations were occupied whenever possible. When station elevations were not indicated on the topographic map, two Wallace and Tierman altimeters (read to the nearest foot) were used to find the station elevation. The altimeters were read at a station of known elevation, at the station for which the elevation was being calculated, and then at another station of known elevation. This loop of readings was corrected for linear drift as a function of time and the elevation of the unknown station was calculated. This elevation was compared with the elevation of the station indicated by the contour lines of the topographic map and if the computed elevation fell within the contour lines bracketing the station, the altimeter elevation was used. If the altimeter elevation fell outside the elevation indicated by the contour lines, the station elevation was linearly interpolated from the contour lines of the topographic map. The elevations of eleven stations which formed part of a north-south profile across Ranch Canyon (Fig. 4) were surveyed using a Keuffel and Esser wye level. The wye level was read to the nearest 0.01 ft and closure error was 1.63 ft (0.5 m).

All of the author's gravity readings were tied to the Milford gravity base station in the Utah Gravity Base Station Network (Cook et al.,

1971). The initial and final readings of each day were taken at this base. In addition, temporary field bases were established in the area of study. These temporary bases were tied to the Milford base by a series of loops represented by the sequence ABABA where A represents Milford base and B represents the field base. Where practical, several field bases were tied to the Milford base in the same loop so that the sequence may have been ABCDABCDA where A represents Milford base and B, C and D represent field base stations. Each base station loop was completed in a short period of time (usually not more than 2 hr between readings at Milford base) so that errors due to earth tides and instrument drift were accurately corrected for by assuming linear drift between rereadings at Milford base.

Gravity readings at stations other than the temporary field bases were also taken in looping sequences and linear drift corrections applied. These loops were somewhat longer (usually about 5 hr between loop closures) and loop closures were made at temporary field bases rather than at Milford base.

Aeromagnetic Survey Specifications and Initial Data Reduction

The aeromagnetic survey was drape-flown with specified mean terrain clearance of 1000 ft. Altitude was maintained to within 50 ft with the aid of a radar altimeter. Flight lines were flown in east-west directions with north-south flight line spacing of 1/4 mi. Navigation and recovery of aircraft location was accomplished with aerial photography. After checking the observed readings for possible

misrecorded points and drift correcting the readings to account for diurnal variation of the magnetic field, the flight line picks were input to a gridding program which produced a square mesh of magnetic field points. The main magnetic field of the earth (International Geophysical Reference Field, updated to 1975) was then removed from the gridded data producing a square mesh of toal magnetic field intensity residual anomaly values. This grid was then machine contoured to produce the final aeromagnetic map (Fig. 9) used in this study.

DATA PREPARATION

Gravity Data Reduction

Reduction of gravity meter readings to simple Bouguer gravity anomaly values utilized a gravity reduction program developed by previous researchers at the University of Utah. This program converts meter readings to milligals using the manufacturer's supplied instrument constants and corrects for tidal variation and instrument drift by assuming linear drift between loop closures. Theoretical gravity values at mean sea level are calculated by the International Gravity Formula (Swick, 1942) and mean sea level was selected as datum for the survey. The density for the Bouguer correction was chosen as 2.67 gm/cc for the following reasons: 1) this is a good approximation of the average density of crustal rocks to a depth of about 2 km below the surface (Nettleton, 1976, p. 280); 2) density measurements of field samples (Table 2 and Appendix 1) indicate that this is a reasonable average density for the sedimentary rocks of the surveyed area; and 3) this density was assumed by previous investigators whose data were incorporated into the terrain-corrected Bouguer anomaly map (Fig. 7). The assumptions of 2.67 g/cc for the Bouguer density and 0.30861 mgal/m for the free air correction imply that the total elevation correction was 0.19683 mgal/m or 0.05999 mgal/ft.

Each of the author's stations was terrain corrected out to a distance of 20 km with an assumed rock density of 2.67 g/cc. Terrain corrections were made in two steps. In the first step, the inner zones (zones B through E) were hand calculated using U.S. Coast and Geodetic Survey terrain correction charts (Swick, 1942). In the second step, the outer zone corrections were calculated using a computer program developed by Hardman (1964) who modeled his program after an algorithm published by Kane (1962). Use of the computer program required digitizing the topography by estimating the average elevation in each 1 km square to a distance of 20 km beyond the edges of the surveyed area. The UTM (Universal Transverse Mercator) grid, which is marked on recent U.S.G.S. topographic maps, was a convenient choice for this terrain matrix. Elevation estimates were made from U.S.G.S. 15-minute topographic maps when available and 7-1/2-minute topographic maps otherwise. Two simple computer program subroutines were added to Hardman's programs which eliminated the necessity of locating staions in both geographic coordinates (required for reduction to simple Bouguer values) and UTM coordinates (required for making terrain corrections). The first subroutine (originally programmed by R. T. Shuey, 1976, personal communication) converts geographic coordinates to UTM coordinates and the second subroutine locates the station in the terrain matrix. Using these subroutines allowed the author to use the output of the simple Bouguer reduction program to calculate the terrain correction for the outer zones with a minimum of tedious and mistake-prone station locating. The template and computer-calculated terrain corrections were added to give the

total terrain correction for each station and the resulting terrain correction was added to the simple Bouguer gravity value to give the values on the terrain-corrected Bouguer gravity anomaly map (Fig. 7). This map was hand contoured (with a 1 mgal contour interval at a scale of 1:62500) from gravity data stations with an estimated average station separation of 1.5 km. The terrain-correction methods used by the other investigators whose data were used in this map are indicated in Table 1 and the explanation for Figure 7.

Gravity Data Accuracy

The total gravity data error is an accumulation of several small errors. The gravimeter used in the survey gave repeatable readings within 0.004 mgal. The maximum amplitude change due to earth tides is about 0.3 mgal in 6 hr. The tidal effect is non-linear so the linear drift correction applied in reducing the gravity values is a source of error although this error is reduced by shortening the time between loop closures. Both the reading error and the error due to the non-linearity of the tidal force will appear in the differences between the simple Bouguer values of reoccupied stations. A total of 85 stations, including 63 stations occupied originally by previous investigators and 22 stations occupied and reoccupied by the author, were used to compute a mean error of 0.051 mgal and a pooled standard deviation of $\pm$ 0.054 mgal for simple Bouguer gravity values. The maximum difference between any two readings of the same station was 0.26 mgal and about 85 percent of the differences were less than 0.10 mgal.

Other sources of error in the gravity readings are imprecise horizontal locations and elevations of gravity stations. Horizontal locations were picked from USGS 7-1/2-minute topographic quadrangle maps to the nearest 0.01 minutes of arc. A reasonable maximum error in horizontal station location of 0.05 minutes (about 90 m) would result in an error of 0.074 mgal if the mislocation were entirely in a north-south direction. Because station locations were chosen at easily located sites, the error due to horizontal station mislocation is probably less than 0.1 mgal. The least accurate station elevations occur when the elevation is obtained by altimeter readings or when the elevation is taken directly from the map by linear interpolation between contour lines. The elevation accuracy in these cases depends on the contour interval of the topographic map used. The largest contour interval on any of the maps used in this area is 40 ft (12 m). Assuming a reasonable station elevation error of 20 ft (6 m) which is one-half of the largest contour interval, the error in gravity values from this source is probably less than 1.2 mgal.

The final source of error in the gravity data is the terrain corrections, which ranged from nearly zero in the flat areas of Milford Valley to slightly over 20 mgal for stations located on peaks in the Mineral Mountains. The assumption of an accuracy of 10 percent of the terrain correction value, results in errors between 0 and 2 mgal from terrain corrections.

The sum of the above errors results in a probable maximum error for stations in the Mineral Mountains approaching 3-1/2 mgal. In

comparison, stations in the flat areas of Milford Valley have a probable maximum error of about 1 mgal.

The above analysis of gravity data errors involves only the author's field work. However, similar error estimates have been obtained by other investigators (Brumbaugh and Cook, 1977; Crebs and Cook, 1976) whose data were incorporated into the terrain-corrected Bouguer anomaly map (Fig. 7).

It should be noted that although terrain corrections were computed to different distances by different researchers (Table 1 and Figure 7), comparisons of the terrain corrections of 50 stations corrected to 20 km with the same stations corrected to 28 km showed differences of less than the probable error of the terrain corrections. Furthermore, the errors showed no consistent trend, i.e., the 28-km corrections were smaller than the 20 km corrections as often as they were larger. The conclusion is that using different terrain correction distances (i.e., 28 km in comparison with 20 km, as used by the author) did not significantly degrade the accuracy of the terrain-corrected Bouguer gravity anomaly values.

Magnetic Data Accuracy

The methods used by Aerial Surveys to produce the aeromagnetic map of the study area were described earlier. These data were not critically analyzed in detail and the accuracy of the survey is assumed to be about 12-1/2 gammas (half the contour interval of the aeromagnetic map).

GEOLOGIC CONTROL

Sample Collection and Physical Property Determination

Rock samples of the common rock types in the study area were collected and the bulk density and magnetic susceptibility measured. Most of the samples were slightly to moderately weathered and a few were very weathered. A beam balance was used to measure bulk density and a Geophysical Specialties Co. model MS-2 susceptibility bridge was used to measure magnetic susceptibility. Susceptibility measurements were made using rock chips that were approximately pea-size and volume corrections were made according to the manufacturer's instructions.

The results of sample measurements made by the author and other investigators (Crebs and Cook, 1976; Brumbaugh and Cook, 1977; Thangsuphanich, 1976) in the area are summarized in Table 2, in which the samples are grouped by location and rock type. The density, magnetic susceptibility and source location (latitude and longitude) for each of the author's samples are listed in Appendix 1. References are cited for listings of individual sample data acquired by other investigators.

Drill Hole Information

Drill hole information consists of shallow water wells drilled in the alluvium of Milford Valley, several dry oil wells drilled south of

Table 2. Bulk densities and magnetic susceptibilities.

Rock type	Bulk Density: No. of Samples	Bulk Density: Range (gm/cc)	Bulk Density: Mean (gm/cc)	Magnetic Susceptibility: No. of Samples	Magnetic Susceptibility: Range (units of 10^{-6} cgs)	Magnetic Susceptibility: Mean (units of 10^{-6} cgs)
Tertiary Intrusive						
Granitic [1]	30	2.45-2.71	2.59±.07	25	38-3750	1245±1143
Granitic [2]	4	2.63-2.77	2.67±.07	4	260-4300	2044±1702
Quaternary Volcanic [1]						
Rhyolite	8	2.22-2.38	2.31±.07	7	149-415	222±89
Perlite	7	1.90-2.31	2.11±.16	7	34-234	108±76
Obsidian	8	2.15-2.35	2.30±.07	6	34-105	88±27
Tertiary Volcanic						
Rhyolite [1]	7	2.18-2.35	2.24±.07	3		546±280
Quartz latite [2]	1	---	2.67	1	---	1403
Andesite [3]	4	2.17-2.52	2.40±.16	4	44-820	381±381
Basalt (vesicular)	1	---	2.42	1	---	1067
Metamorphic						
Gneiss [1], [4]	5	2.63-2.74	2.69±.04	4	1580-3330	2600±842

Table 2. (Continued)

Rock type	Bulk Density: No. of Samples	Bulk Density: Range (gm/cc)	Bulk Density: Mean (gm/cc)	Magnetic Susceptibility: No. of Samples	Magnetic Susceptibility: Range (units of 10^{-6} cgs)	Magnetic Susceptibility: Mean (units of 10^{-6} cgs)
Metamorphic (cont.)						
Gneiss [1]/	1	---	2.69	1	---	35
Marble [1]/	1	---	2.85	1	---	20
Quartzite [2]/	5	2.50-2.74	2.62±.09	5	0-14	8±5
Sedimentary						
Limestone [1]/	9	2.55-2.97	2.71±.13	5	0-49	14±20
Limestone [1]/	2	2.70-2.76	2.73±.04	2	5-19	12±9
Sandstone [1]/	3	2.47-2.76	2.62±.15	3	12-28	18±9

[1]/ Samples taken from the Mineral Mountains.

[2]/ Samples taken from the Star Range, Rocky Range, Beaver Lake Mountains, or Beaver Mountains.

[3]/ Samples taken from the Black Mountains.

[4]/ Samples taken by Crebs (1976) from outcrops now mapped as predominantly granite with gneiss fingers (Evans, 1977, personal communication). The magnetic susceptibilities of the gneiss might be higher than normal because of intense reworking by the granite intrusion.

Table 3. Drill hole geologic control.

Drill Hole Designation	Drill Hole Location Latitude Deg.	Min.	Longitude Deg.	Min.	Well Depth (m)	Depth Bedrock Encountered (m)	Type of Bedrock
OIL [1]	38	36.88	112	59.55	1030	--	[7]
TG-5 [2]	38	32.94	112	49.56	52	45	Fractured Granite
DDH 1976-1 [3]	38	30.38	112	51.22	62	36	Fractured Granite
DDH-1a [4]	38	29.40	112	51.60	66	35	Precambrian (?) Gneiss
HF-1 [2]	38	38.98	112	46.75	155	30	Granite
HF-3 [2]	38	31.18	112	48.68	149	9	Granite
13-10 [5]	38	28.72	112	51.58	[6]	83	[6]
3-1 [5]	38	29.39	112	51.02	[6]	87	[6]

[1] Source: Hansen and Scoville, 1955

[2] Source: Whelan, 1977

[3] Source: Bryant and Parry, 1977

[4] Source: Parry, et al., 1976

[5] Source: Crebs and Cook, 1976

[6] Data not yet available.

[7] Drill hole bottomed in alluvium. Bedrock not penetrated.

Black Rock in northern Milford Valley and shallow thermal gradient and core holes drilled in the vicinity of the high geothermal gradient area shown on Figure 4. Although Phillips Petroleum Company and Thermal Power Company have drilled deep steam-production wells into the geothermal reservoir, lithologic logs for these wells have not been made available to the author. Selected drill hole locations, depth of bedrock, if encountered, and type of bedrock are shown in Table 3.

Summary of Geologic Control

To construct an interpretative geologic model, as much geologic control (either density and magnetic susceptibility contrast or depth to the anomaly causing bodies) as possible must be known. Consideration of the geologic control data specified above leads to the following conclusions:

1. The average density of crustal rocks above sea level which Nettleton (1976, p. 257) gives as 2.67 gm/cc is a good estimate of average bedrock density in this area.

2. The density of the alluvium in this area was estimated by Crebs and Cook (1976, p. 22) as 2.0 gm/cc, which results in a reasonable density contrast of about 0.5 gm/cc between the bedrock and alluvium.

3. The magnetic susceptibility of the intrusive rocks is highly variable and, due to the weathered nature of most samples, the average susceptibility is probably low. Due to the near-zero magnetic susceptibilities of the sedimentary rocks and alluvium, the typical magnetic susceptibility contrast for the area is essentially the value of the average magnetic susceptibility of the intrusive rocks.

4. Drill-hole information provides a minimum depth of alluvial fill in the Milford Valley graben at the location of the hole designated "oil" in Table 2. This drill hole is

located about 5.0 km north of the Millard-Beaver County line and about 0.5 km west of the railroad tracks (see Fig. 4) near the deepest part of the valley. The depth of alluvium penetrated by this well is about 1.0 km; and since the well did not penetrate bedrock, this is a minimum depth of valley fill.

5. Drill-hole information also defines rather well the throw of the Opal Mound Fault (Fig. 4). Drill holes DDH-1976-1 and DDH-1a are located on the west side of the fault and drill holes 13-10 and 3-1 are located on the east side of the fault. Comparison of depths to bedrock (from Table 2) shows a downthrow of about 50 m on the east side of the Opal Mound Fault.

Interpretative geologic models were constructed along several profiles using the above geologic controls as guidelines.

MAP PROCESSING

To facilitate interpretation, polynomial fitting and wavelength filtering were used to enhance different features of the terrain-corrected Bouguer gravity anomaly map (Fig. 7) and the total magnetic field intensity residual anomaly map (Fig. 9). All of the maps produced by processing digitized values were machine-contoured using a contouring program which was generously supplied by John Hawkins.

Preparation of Gridded Maps

Processing the maps, using fast Fourier transforms to carry out wavelength filtering, required digitization of the gravity and magnetic maps. These digitized maps were also used to do the polynomial fitting.

The hand-contoured gravity map (with a contour interval of 1 mgal and map scale of 1:62,500) was hand-digitized on the Universal Transverse Mercator (UTM) grid at 1 km intervals. The resulting gravity grid (57 north-south points and 38 east-west points) was machine-contoured and careful comparison with the original contour map allowed the detection and correction of erroneous values at a few grid points. Aliasing of the hand-contoured gravity map (resulting from the 1 km grid interval) was evident in a few places; but the overall quality of the map was not seriously degraded.

Although the contractor supplied a grid (1000-ft grid interval) of digitized aeromagnetic values, the grid used by the contractor was not the UTM grid and the grid interval was not an even multiple of the 1-km grid interval chosen for the gravity grid. To maintain consistency between the gravity and magnetic grids, the machine-contoured aeromagnetic map (with a contour interval of 25 gammas and map scale of 1:24,000) was hand-digitized and verified in the same manner as the gravity map. The digitization interval for the aeromagnetic map was reduced to 1/2 km to avoid significant aliasing of the smaller magnetic anomalies. The resulting grid of total magnetic field intensity residual anomaly values has 98 north-south points and 57 east-west points.

Preparation of Gridded Maps for Wavelength Filtering

All wavelength filtering was implemented in the frequency domain by multiplying the frequency response of spatial filters by the discrete Fourier transform of the gravity and magnetic grid values. The programs used for wavelength filtering were developed largely by Dr. R. T. Shuey and others at the University of Utah.

The two-dimensional discrete Fourier transform was calculated using a one-dimensional fast Fourier transform which operated on the values along each row of the grid and then operated on the values along each column of the grid (Oppenheim and Schafer, 1975, p. 118). Prior to transforming, several modifications of the gridded data values were necessary. To eliminate a large zero-frequency component and to

lessen edge effects, the mean and trend of both grids were removed by subtracting a least-squares-best-fit plane (first order polynomial surface) from the gridded data. This was accomplished by using the polynomial fitting program described below. To further eliminate edge effects, constant values were extrapolated for five grid points around the edges of each grid and a full cosine bell operator was applied to the five-point border. This operator tapered all edges of each extrapolated grid smoothly to zero. The one-dimensional fast Fourier transform, which was used in calculating the two-dimensional transform, required that the number of points in each grid dimension be an even power of two. This was accomplished by extending each grid dimension to a higher power of 2 by adding zeros. All grid dimensions for both the gravity and magnetic grids were extended to 128 points. This number was selected for both grids because it resulted in a rather large zero pad for all grids. (The minimum number of zeros in any dimension was 20 in the north-south dimension of the magnetic grid.) A large zero pad is necessary because filtering in the frequency domain by multiplication corresponds to circular convolution, not the desired linear convolution, in the space domain. In particular, a zero pad of 20 points allows a space domain filter length of 20 points or less with no circular convolution. The filters used in this study were all designed in the frequency domain and were not checked or truncated in the space domain to insure that the spatial filters consisted of 20 or less non-zero points. However, the assumption was made that all of the filters used would have near-zero values for points greater than 20 grid-units from the origin resulting

in low magnitude effects due to circular convolution. A good discussion of the zero padding technique to eliminate circular convolution is given by Oppenheim and Schafer (1975, p. 119).

Reduced to-the-Pole-Magnetic Map

The total magnetic field intensity residual anomaly map (Fig. 9) was converted to a reduced-to-the-pole magnetic intensity residual map (Fig. 10) by wavelength filtering. This process produces a residual magnetic anomaly map under the double assumption of magnetization and an inducing magnetic field direction both vertical. The anomalies on this map will thus look as if the survey had been conducted at the north magnetic pole and the magnetization direction of each body was in the direction of the inducing field. The Fourier transform of the reduced-to-the-pole residual magnetic anomaly map is calculated by multiplying the Fourier transform of the total magnetic field intensity map by the factor:

$$\frac{1}{\left[\sin(I) + i\cos(I)\,\frac{f_x\cos(D) + f_y\sin(D)}{\sqrt{(f_x^2 + f_y^2)}}\right]^2}$$

where I and D are the inclination and declination, respectively, of the earth's main magnetic field in the survey area; f_x and f_y are the frequencies (cycles/grid interval) in the x and y directions, respectively; and i is the square root of -1.

The advantages of using this map for interpretation include:

1) Anomalies tend to be smoother because the high-low effect caused by an inclination of less than 90^{o} is eliminated; and

2) The peaks of anomalies tend to overlie the center of the causative body.

The reduced-to-the-pole magnetic anomaly map was used for all further interpretation and processing of the data.

Residual and Regional Maps

The separation of gravity and magnetic maps into a regional component caused by deep sources and a residual component caused by shallower sources, has long been an accepted step in the interpretation of potential field data. The ambiguity inherent in this process (because broad shallow sources can produce the same anomaly as deep sources) has led to the development of several techniques for extracting regional fields. Techniques used in this study include polynomial fitting and wavelength filtering.

The method of polynomial fitting assumes that the regional field can be approximated by a low-order polynomial surface. The residual map is what remains after the regional surface is subtracted from the original map.

In this study, the implementation of the polynomial fitting technique involved the use of programs developed and supplied by Dr. J. R

Montgomery. This package of programs calculates a polynomial surface of desired order which is a least-squares best-fit to the input data. Polynomial surfaces of orders 1 through 10 were computed for the gravity data.

In order to determine which polynomial surface best approximated the regional gravity field, a plot of the root mean square error versus polynomial order (Fig. 5) was made. It is apparent from Figure 5 that the misfit between the polynomial surface and the gravity data decreases by smaller amounts for orders higher than 5. This feature indicates that for orders higher than 5, the polynomial surface is trying to fit rather small residual anomalies and the smooth regional effects have already been closely approximated. Accordingly the fifth order polynomial surface was chosen to make the fifth-order polynomial residual gravity anomaly map shown in Figure 11.

A modification of the polynomial technique was also used to remove a regional gravity component which was approximated by a planar surface with the following characteristics: 1) a strike that was chosen parallel to the direction of strike of the assumed regional gravity surface and 2) a least-squares best-fit slope in the direction perpendicular to this strike. The strike of the assumed regional gravity surface was established as N 25° E by visually approximating the average trend of the gravity contours from a low-pass filtered terrain-corrected Bouguer gravity anomaly map of southern Utah compiled by John Snow (1977, oral communication). The least-squares best-fit surface with dip direction perpendicular to the strike was

then calculated using a computer program. This program projected each gravity grid value onto a line perpendicular to the assumed strike of the regional gravity surface and then computed the least-squares best-fit straight line approximation to the projected grid values. A residual map was then generated by subtracting the best-fit straight line from the projected gravity grid values and this map (called the "residual gravity anomaly map with best-fit projected regional removed") is shown in Figure 8.

Gravity and magnetic fields can be thought of as a superposition of anomalies caused by bodies with different physical properties (densities and magnetic susceptibilities). The use of wavelength filtering to separate these anomalies into a regional component caused by deep sources and a residual component caused by shallower sources is based on the assumption that deep sources will produce long-wavelength anomalies and shallow sources will produce short-wavelength anomalies. Although all anomalies, whether due to shallow or deep sources, have spectra which overlap significantly toward the lower frequencies (Grant, 1972), the many anomalies in a map may tend to separate according to wavelength into a deep source (long wavelength) ensemble and a shallow source (short wavelength) ensemble.

An examination of the power spectrum of a map will assist in determining whether the data can be separated into long- and short-wavelength anomalies. If the map is easily separated into a collection of deep sources and a collection of shallow sources, the natural logarithm of the power spectrum will show a break in slope at

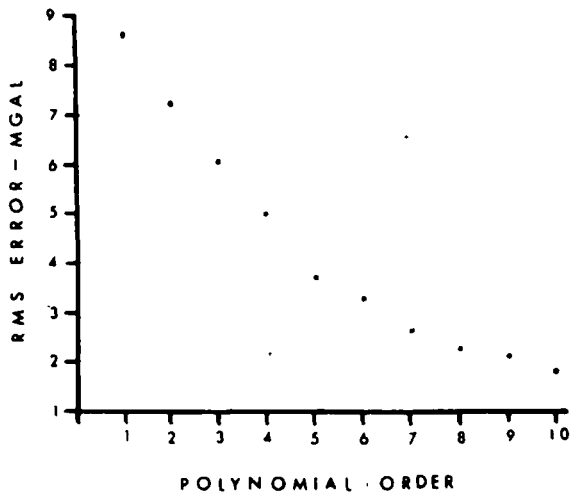

Figure 5. Plot of the root-mean-square values of the difference between the terrain-corrected Bouguer gravity anomaly values and the least-squares best-fit polynomial values versus polynomial order. The fifth-order polynomial was selected as the best regional gravity approximation.

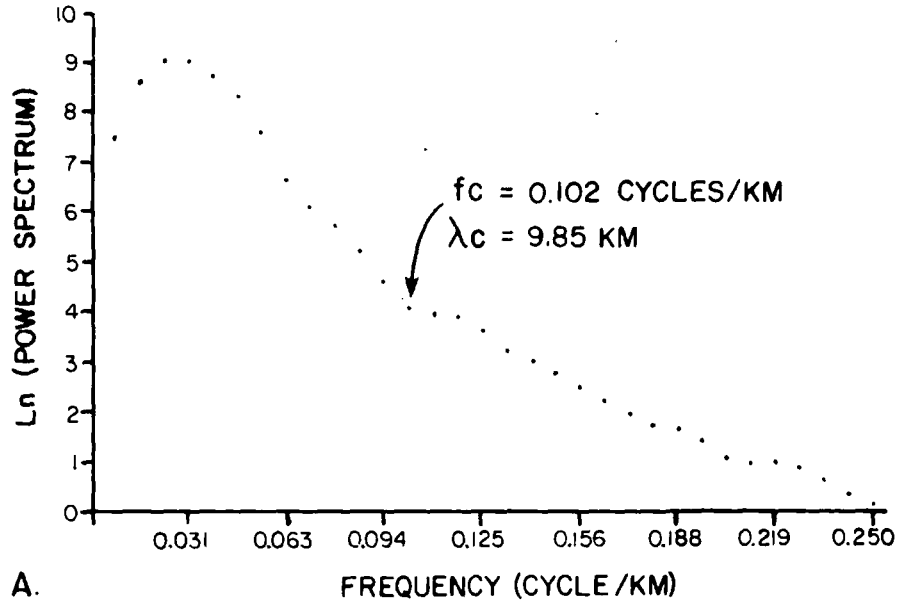

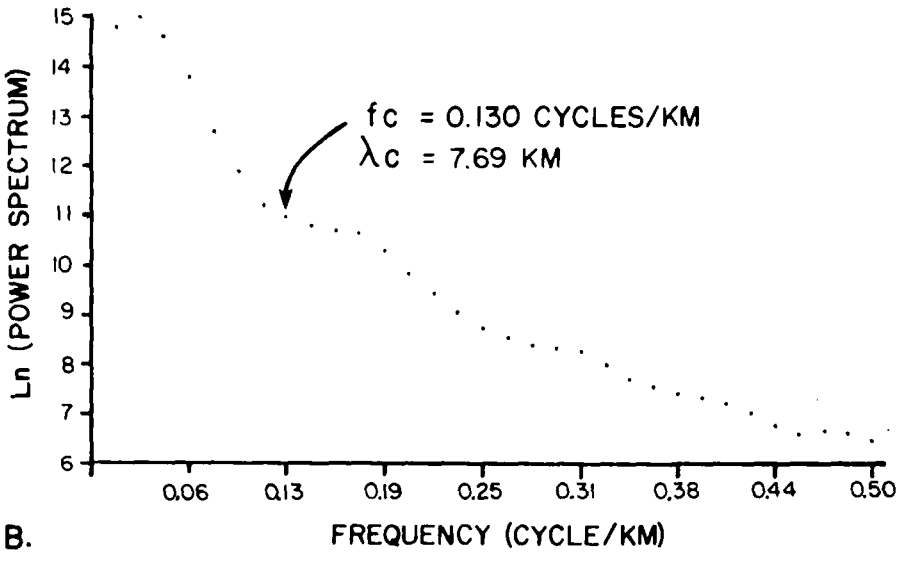

Figure 6. Plots of the natural logarithm of the power spectrum averaged over azimuth versus frequency for: A. gridded terrain-corrected Bouguer gravity anomaly values, and B. gridded reduced-to-the-pole magnetic values. The arrow indicates the selected cutoff frequency; f_c = cutoff frequency, λ_c = wavelength corresponding to f_c.

the frequency or wavelength which separates the map into these collections.

The power spectra of the gridded gravity data and the reduced-to-the-pole gridded magnetic data were computed by multiplying the Fourier transform of each grid by its complex conjugate and dividing by the area of the original map. Then these power spectra were averaged over azimuth and smoothed. Plots of the natural logarithm of the power spectra, with the chosen frequency which best separates the residual and regional components indicated, are shown in Figure 6.

The frequencies selected from the power spectra were used as cutoff frequencies when designing high- and low-pass filters to separate the regional and residual components of the gravity and reduced-to-the-pole magnetic maps. High-and low-pass filters were designed in the frequency domain by constructing ideal filters (with a value of 1 for the frequency range to be passed and a value of 0 for the frequency range to be rejected) and then applying a full cosine bell taper to a specified percentage of the filter pass band to reduce the Gibb's effect.

The maps produced using this method were: 1) a high-pass filtered gravity anomaly map (Fig. 12) with a cutoff frequency of 0.102 cycles/km (corresponding to a wavelength of 9.80 km) and a taper of 25 percent of the pass band, and, 2) a low pass filtered gravity anomaly map (Fig. 13) with a cutoff frequency of 0.140 cycles/km

(corresponding to a wavelength of 7.14 km) and a taper of 12.5 percent of the pass band.

Strike-filtered Maps

Enhancement of gravity and magnetic gradients and trends with selected strike directions can be accomplished by strike filtering in this frequency domain (Fuller, 1967, p. 692-696). This procedure provides a useful interpretive aid by emphasizing obvious trends and bringing out more subtle trends that might have been overlooked on the original map. The strike filters for each map were designed in the frequency domain. For each filter a "pie slice" of 90^{o}, centered on the selected strike direction, was passed (multiplied by 1) and the remainder was rejected (multiplied by 0). A full cosine bell taper was applied to a band 30^{o} wide at each side of the pie slice to minimize the Gibb's effect. In the frequency domain, linear trends (directions) are shifted by 90^{o}, and therefore a north-south wavevectors would be passed to produce an east-west strike-filtered map. The following strike-filtered maps were produced by strike filtering:

1) North-south strike-filtered gravity anomaly map (Fig. 17).

2) East-west strike-filtered gravity anomaly map (Fig. 19).

3) Northeast-southwest strike-filtered gravity anomaly map (Fig. 21).

4) North-south strike-filtered magnetic anomaly map (Fig. 18).

5) East-west strike-filtered magnetic anomaly map (Fig. 20).

Pseudomagnetic, Pseudogravity and Upward Continued Maps

The gridded gravity data and the gridded reduced-to-the-pole magnetic data were converted to a pseudomagnetic map (Fig. 14) and a pseudogravity map (Fig. 15), respectively, by wavelength filtering. The frequency responses used to calculate these maps are based on the assumptions used in the derivation of Poisson's relation between the gravity and magnetic fields. For a single-anomaly-causing body, Poisson's relation will hold if the density and magnetic susceptibility contrasts are constant throughout the causative body. When these assumptions are extended to an area composed of a superposition of many anomalies, each causative body must produce proportional magnetic and gravity anomalies. This means that each anomaly causing body must have constant density and magnetic susceptibility within the body boundaries, and the density-magnetic susceptibility ratio of each causative body in the area must equal the same constant. Although this requirement is geologically unreasonable for areas in even simple geologic settings, comparison of a pseudomagnetic or pseudogravity map with its counterpart may prove valuable in the interpretation process by revealing areas where these assumptions are approximately correct.

In order to produce a reduced-to-the-pole pseudomagnetic map, the Fourier transform of the gridded gravity data is multiplied by the following frequency response or filter factor (designated the pseudomagnetic filter factor):

(A) $$(kH/\gamma\rho)\ (2\pi c\sqrt{f_x^2 + f_y^2})$$

where f_x is the frequency (in cycles/grid interval) in the x direction, f_y is the frequency (in cycles/grid interval) in the y direction, c is the number of cm/grid interval, k is the magnetic susceptibility contrast (in cgs units), ρ is the density contrast (in g/cc), H is the magnetic intensity of the earth's main field (in oersteds) and γ is the gravitational constant (in cgs units). In order to produce a pseudogravity map from the gridded reduced-to-the-pole magnetic data, the Fourier transform of the gridded data is multiplied by a "pseudogravity filter factor" which is the inverse of the pseudomagnetic filter factor given in expression (A). The pseudomagnetic filter factor enhances high-frequency components so the map it produces will resemble a residual magnetic anomaly map, whereas the pseudogravity filter factor acts as a smoothing filter and will resemble a regional gravity anomaly map. The density and magnetic susceptibility contrasts (0.5 gm/cc and 0.025 cgs units, respectively) were chosen to approximate the contrasts between the alluvial fill of Milford Valley and the granite of the Mineral Mountains pluton.

In order to compare the pseudogravity map with the gravity map or the reduced-to-the-pole pseudomagnetic map with the magnetic map, it was necessary to upward continue the gravity map and the pseudomagnetic map to the elevation of the aeromagnetic survey (1,000 ft i.e., 304.8

m). This is a smoothing operation and is readily implemented in the frequency domain by multiplying the Fourier transform of the gridded map values by the filter factor:

$$\exp\left(-2\pi h\sqrt{f_x^2 + f_y^2}\right)$$

where h is the desired amount of upward continuation (in grid intervals), f_x is the frequency (in cycles/grid interval) in the x direction, and f_y is the frequency (in cycles/grid interval) in the y direction. The maps which were upward continued in this manner are the pseudomagnetic map (Fig. 14) and the upward-continued gravity map (Fig. 16).

PROFILE MODELING

Computation of Profile Models

Modeling of selected gravity and aeromagnetic profiles was accomplished using computer programs developed by J. H. Snow (1977). These programs employed two phases in finding a model which fit the observed data. The first phase performed a one-dimensional direct search over user-specified model parameters to minimize the sum of the square of the differences between the computed and observed anomalies. The second phase linearized the forward problem by expanding the forward solution in a Taylor series and then used linear inversion with a Marquardt step to fit better the computed anomalies to the observed anomalies. The forward gravity problem was computed using a 2-1/2 dimensional algorithm developed by Cady (1977) and the forward magnetic problem was computed using a 2-1/2 dimensional algorithm developed by Shuey and Pasquale (1973).

Specification of the strike length (or 1/2 dimension) of model bodies differed between the gravity and magnetic modeling programs. The gravity program allows one to specify a different strike length in each direction perpendicular to the profile. Furthermore, negative strike lengths are permitted so that a body can be shifted to one side or the other of the profile. The magnetic program allows only the specification of one strike length and the effect of the body is

computed as if the profile traversed the center of the body. Modeling bodies which are not traversed by the profile is not possible when using the magnetic modeling program.

Profile Selection and Regional Gravity Removal

Three east-west gravity and magnetic profiles were selected for modeling with the previously mentioned modeling programs. Gravity and magnetic profiles were taken from the residual gravity anomaly map with best-fit projected regional removed (Fig. 8) and the reduced-to-the-pole magnetic map (Fig. 10), respectively, by reading the gridded map values at each grid point along the desired traverse. This procedure resulted in gravity profiles with residual values spaced 1 km apart and magnetic profiles with residual values spaced 1/2 km apart. In order to smooth the effects of peak or trough values, and obtain a more "representative" anomaly profile, several east-west grid lines were averaged (or "stacked") to give the observed values along each profile. The number of grid lines which were averaged was determined by the north-south extent of anomalies of interest along the profile so that destructive interference caused by averaging adjacent high and low anomaly centers together was avoided. The grid lines, which were averaged and the designation given each profile, are indicated on Figure 8 for gravity profiles and Figure 10 for magnetic profiles. The regional gravity values, which were removed from each gravity profile prior to modeling, are the gravity values at each grid point along the profile of the plane which was removed from the residual gravity anomaly map with best-fit projected

regional removed (Fig. 8). This regional gravity has a gradient of 0.81 mgal/km with gravity values decreasing to the east.

INTERPRETATION OF GRAVITY AND MAGNETIC DATA

Map Interpretation

To facilitate the analysis of anomalies, the terrain-corrected Bouguer gravity anomaly map (Fig. 7) and the total magnetic field intensity residual anomaly map (Fig. 9) were digitized and the resulting gridded data were operated on using various techniques to produce the previously mentioned (see "MAP PROCESSING") processed maps. As an aid in discussion, prominent anomalies or geologically important features have been designated by numbers on the processed maps.

Terrain-corrected Bouguer gravity anomaly map (Fig. 7) and residual gravity anomaly map with best-fit projected regional removed (Fig. 8) -- Since the residual gravity anomaly map with best-fit projected regional removed was used as the primary gravity base map for comparison with the other processed maps, and since the anomaly patterns of this map and the terrain-corrected Bouguer gravity anomaly map are very similar, the two maps are discussed together.

The large oval-shaped gravity low (with about 15 mgal of closure) in the west-central portion of each map (number 6 in Fig. 8), overlies the alluvium in Milford Valley (Fig. 4). The rather strong gravity gradient across the eastern and western margins of this low indicate that Milford Valley is probably an alluvium-filled graben with normal faulting forming the east and west sides of the graben. This prominent gravity low (number 6 in Fig. 8) is designated the "Milford

Figure 7. Terrain-corrected Bouguer gravity anomaly map of the Mineral Mountains and vicinity, Beaver and Millard Counties, Utah

Explanation

Gravity data sources: W. D. Brumbaugh, J. A. Carter, T. J. Crebs R. F. Sawyer, R. J. Sontag, I. Thankgsuphanich, and University of Utah gravity class of 1974

A density of 2.67 gm/cc was assumed for both the Bouguer and terrain corrections. Terrain corrections were computed using the following:

Data Source	Distance to which stations were terrain-corrected	
Brumbaugh	20.0 km	2/
Carter	20.0 km	2/
Crebs	28.8 km	1/
Sawyer	18.8 km	1/
Sontag	58.8 km	1/
Thangsuphanich	28.8 km	1/

Datum is mean sea level.

Contour interval is 1 milligal.

1/ Terrain corrections computed using U.S.C. & G.S. zone charts

2/ Terrain corrections computed using U.S.C. & G.S. zone charts for inner zones (B through E) and a computer program (Kane, 1962 and Hardman, 1964) for the remaining distance to 20 km.

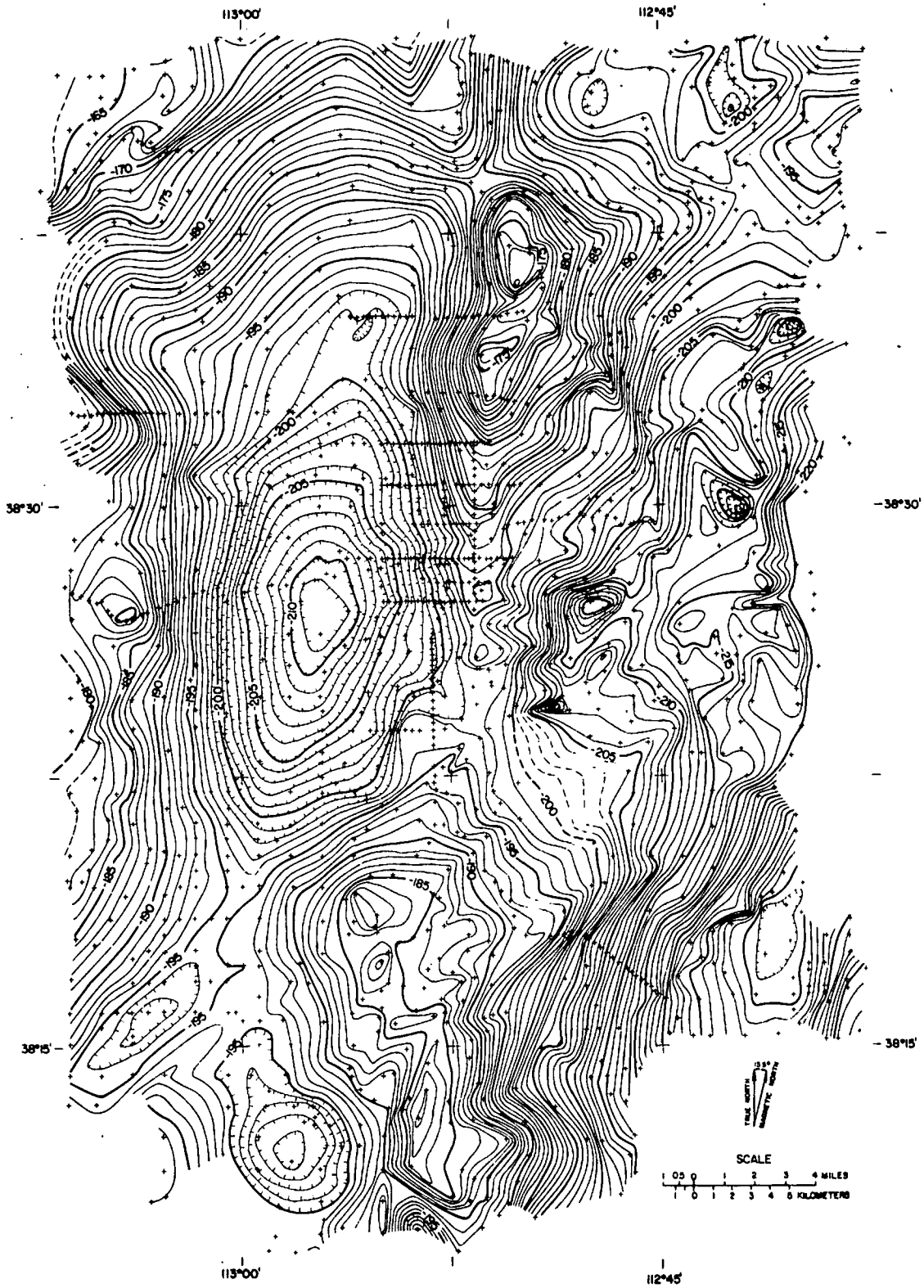
113°00'
112°45'
38°30'
38°15'
SCALE
1 0.5 0 1 2 3 4 MILES
1 0 1 2 3 4 5 KILOMETERS

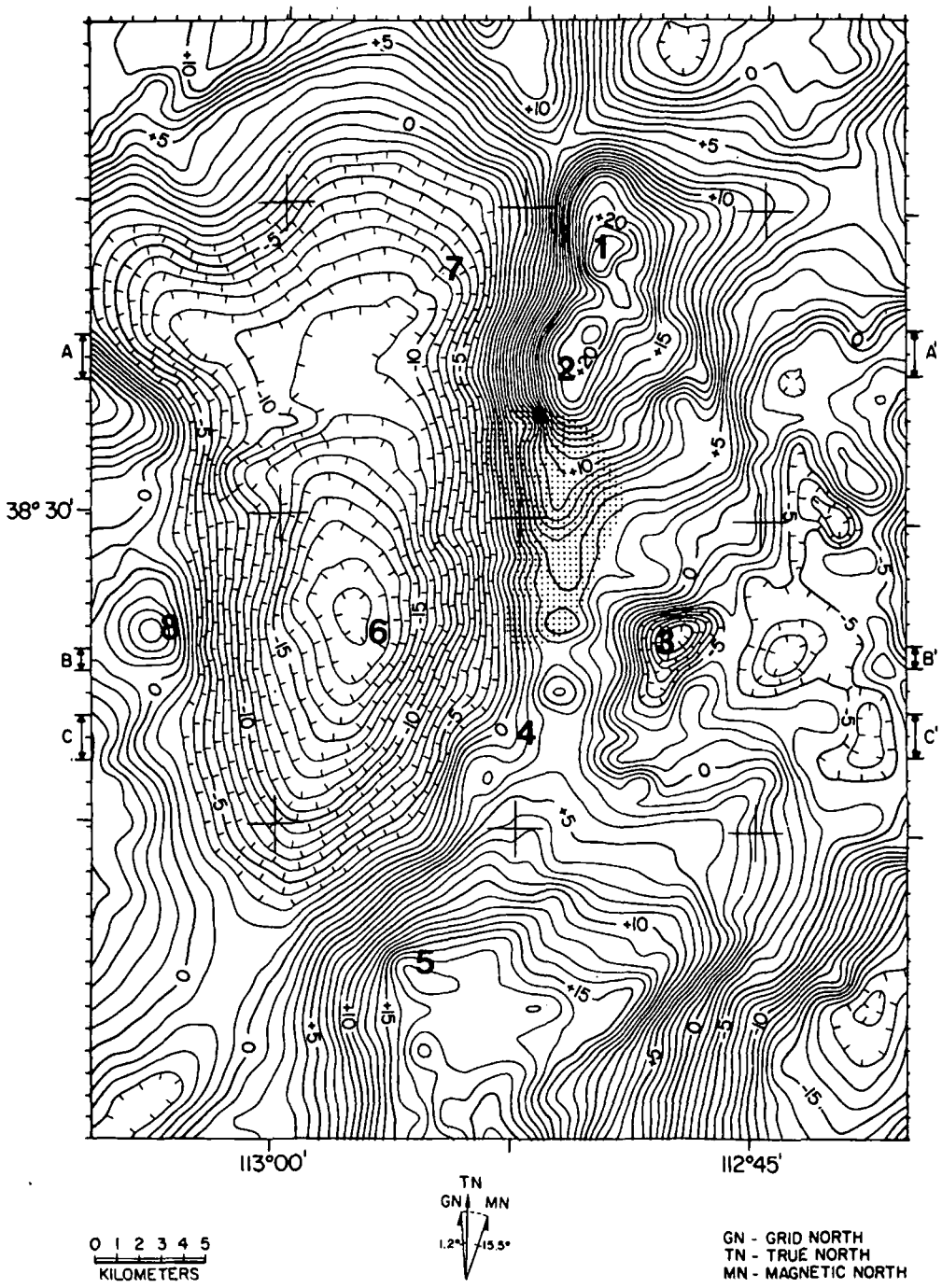

Figure 8. Residual gravity anomaly map with best-fit projected regional removed; contour interval = 1 mgal. Grid lines selected for gravity profiles are indicated by lettering along map border. Grid values along grid lines, indicated by arrows, were averaged to give the observed profile values. Dotted pattern indicates the high thermal gradient anomaly area.

Valley gravity low."

The Milford Valley gravity low is bordered on the west by a high gravity area which overlies the Star Range, the Rocky Range and the Beaver Lake Mountains (Fig. 4). The small gravity high (number 8 in Fig. 8) over the Rocky Range, is designated the "Rocky Range gravity high."

North of the gravity high area, along the western edge of the maps is an arm of the Milford Valley gravity low which overlies alluvium separating the Beaver Lake Mountains from the Beaver Mountains (Fig. 4). North of this arm is a high gravity area (in the northwestern corner of the maps) which overlies the Beaver Mountains.

Extending eastward from the northwestern corner of the maps (Figs. 7 and 8), the gravity contours trend generally east-west to a point about half way across the map, where the trend of the gravity contours changes abruptly to north-south. The generally east-west trending contours north of Milford Valley gravity low indicate that the depth of alluvial fill in Milford Valley graben is decreasing to the north and the suggestion of a southeastward trending gravity nose near the center of the maps indicates that the Paleozoic and Precambrian rocks of the Beaver and/or Mineral Mountains extend under the volcanics and alluvium at rather shallow depth.

In the southeastern portion of the map, south of Milford Valley gravity low (number 6 in Fig. 8), is a gravity saddle and a northeastward-trending gravity nose which separates the Escalante

Desert south of the Star Range into two gravity lows.

Adjacent to the eastern edge of Milford Valley gravity low is a large northward-trending gravity high which overlies the exposed rock of the Mineral Mountains. This gravity high is separated into two major highs by a gravity saddle (number 4 in Fig. 8 and designated the "Ranch Canyon gravity saddle") in the area of Ranch Canyon (Fig. 4). The southern major gravity high (not entirely shown on Fig. 8) overlies predominantly Precambrian (?), Mesozoic, and Paleozoic rocks in the southern Mineral Mountains and extends southward across state highway 21, where it closes abruptly near the southernmost exposure of sedimentary rocks in the predominantly volcanic Black Mountains (Fig. 4). Near the northern end of the southern major gravity high, a gravity saddle which overlies the Cave Canyon fault (Fig. 4) separates the high into two small gravity highs. The northernmost of these gravity highs (number 5 in Fig. 8) is designated the "southern Mineral Mountains gravity high." The northern major gravity high is similarly separated into two small highs by a gravity saddle which overlies the County Line fault (Fig. 4). This fault occurs where the exposed granite of the Mineral Mountains pluton terminates against the Cambrian rocks of the northern Mineral Mountains. Hence, the northernmost of these small gravity highs (number 1 in Fig. 8 and designated the "northern Mineral Mountains gravity high") overlies Cambrian sedimentary rocks, whereas the southern high (number 2 in Fig. 8 and designated the "central Mineral Mountains gravity high") overlies granite and alluvium along the western margin of the Mineral

Mountains. A southward-trending elongate gravity nose extends from the central Mineral Mountains gravity high (number 2 in Fig. 8) to the Ranch Canyon gravity saddle (number 4 on Fig. 8). This nose lies along the western margin of the Mineral Mountains and is located primarily over alluvium in some places. Where the east-west striking Hot Springs fault (Fig. 4) intersects the gravity nose (along the -190 mgal contour of Fig. 7), the smoothly elongate nature of the contours is disrupted. This feature is not apparent in Figure 8 because the digitization interval (1 km) was too large to accurately reproduce such a small disturbance in the contours.

Northeast of the Ranch Canyon gravity saddle is a pronounced north-northeastward-trending elongate low gravity zone (about 8 km in length and consisting of two gravity lows) that overlies a series of silicic volcanic domes, including Bearskin and Little Bearskin Mountains, and North and South Twin Flat Mountains. The northernmost low in this zone is centered over Bearskin and Little Bearskin Mountains and is designated the "Bearskin gravity low" (number 3 on Fig. 8).

The southeastern portion of the maps is dominated by a generally north-south trending gravity contour with gravity values decreasing eastward toward the alluvial deposits in Beaver Valley (Fig. 4). A small gravity low, with closure of 1 mgal, along the eastern border of the maps overlies what is probably the deepest part of the alluvial fill in Beaver Valley.

North of the gravity low over Beaver Valley and east of the high gravity area overlying the Mineral Mountains, the gravity contours are rather disturbed with several small gravity highs and lows overlying an area geologically dominated by Quaternary basalt and Tertiary rhyolite flows.

In the northeast portion of the gravity maps an eastward-trending gravity nose which originates over the northern Mineral Mountains gravity high (number 1 on Fig. 8) ends in a gravity saddle near the eastern border of the map. This nose overlies primarily alluvium, but east of the gravity saddle, where a gravity high extends off the maps to the northeast, limited exposures of Paleozoic sedimentary rocks (Fig. 4) indicate that the nose and saddle may be caused by Paleozoic sedimentary units underlying the alluvium at shallow depth. North of the gravity saddle is a low gravity zone which extends off the maps to the north. This low overlies primarily late Tertiary basalt flows and is bounded on the east by a strong east-west gravity gradient located just north of the sedimentary gravity high (number 1 on Fig. 8).

West of the major northern gravity high, comprised of the northern Mineral Mountains gravity high (number 1 on Fig. 8) and the central Mineral Mountains gravity high (number 2 on Fig. 8) is a northern extension of Milford Valley graben-gravity low (number 7 on Fig. 8 and designated the "northern Milford Valley gravity low") which is separated from the Milford Valley gravity low (number 6 on Fig. 8) by an area of disturbed contours which tend to form a gravity saddle between the two lows. This area of disturbed contours lies along a

line connecting the northern terminus of the Mineral Mountains pluton with the northernmost exposures of intrusive rocks in the Beaver Lake Mountains (Fig. 4) and is attributed to the continuation of this contact (between the intrusive rock and the sedimentary rock) under the alluvium and extending entirely across Milford Valley.

Although the anomaly patterns of the terrain-corrected Bouguer gravity anomaly map (Fig. 7) and the residual gravity anomaly map with best-fit projected regional removed (Fig. 8) were similar enough to allow discussing the maps together without difficulty, it should be noted that there are significant differences between the two maps. The most obvious of these differences is the gravity values which range from -163.7 mgal to -236.7 mgal on Figure 7 and from +22.7 mgal to -19.4 mgal on Figure 8. This difference in gravity values is caused by the removal of an average value by subtracting a least-square best-fit plane (see "Map Processing") from the reduced and digitized gravity values on Figure 7. A less obvious but more significant difference between the two maps is apparent in the southeastern portion of the maps, where the strong east-west gravity gradient on Figure 7 has a total decrease to the east of about 44 mgal, whereas the decrease across the same area on Figure 8 is only about 34 mgal. This demonstrates that a rather significant regional gravity with gravity values decreasing to the east and south, has been removed from the residual gravity anomaly map with best-fit projected regional removed (Fig. 8).

Total magnetic field intensity residual anomaly map (Fig. 9) and reduced-to-the-pole residual magnetic anomaly map (Fig. 10) -- The reduced-to-the-pole residual magnetic anomaly map (Fig. 10) was produced from the digitized total magnetic field intensity residual anomaly values by wavelength filtering (see "MAP PROCESSING"). As previously mentioned, the anomalies on the reduced-to-the-pole residual magnetic anomaly map will tend to overlie the centers of the causative bodies. This means that the anomalies in Figure 10 are shifted slightly north-northeastward (relative to the anomalies of Figure 8) along the direction of magnetic north (N15.5^{o}E). This anomaly shift (amounting to about 1 km for most anomalies) is not readily apparent when the two maps are compared, but this small shift produced a significantly better correlation between the mapped geology features and the anomalies. The difference between the magnetic values on the two maps in due primarily to the removal of a least-squares best-fit plane from the digitized total magnetic field intensity residual anomaly values prior to filtering (see "MAP PROCESSING"). Removal of this plane was necessary because, although the (International Geophysical Reference Field) has been removed from the total magnetic field data, the average value of the total magnetic field data is negative and an average data value other than zero is unacceptable for wavelength filtering. Despite the above differences between the reduced-to-the-pole residual magnetic anomaly map and the total magnetic field intensity residual anomaly map, the anomaly patterns are similar enough to discuss the two maps together.

Figure 9. Total magnetic field intensity residual anomaly map of the Mineral Mountains and vicinity, Beaver and Millard Counties, Utah

Explanation

Data collected, reduced and machine contoured by Aerial Surveys.

Survey was drape-flown at mean terrian clearance of 1000 ft.

International Geophysical Reference Field (IGRF), updated to 1975, was removed from data.

Contour interval is 50 gammas.

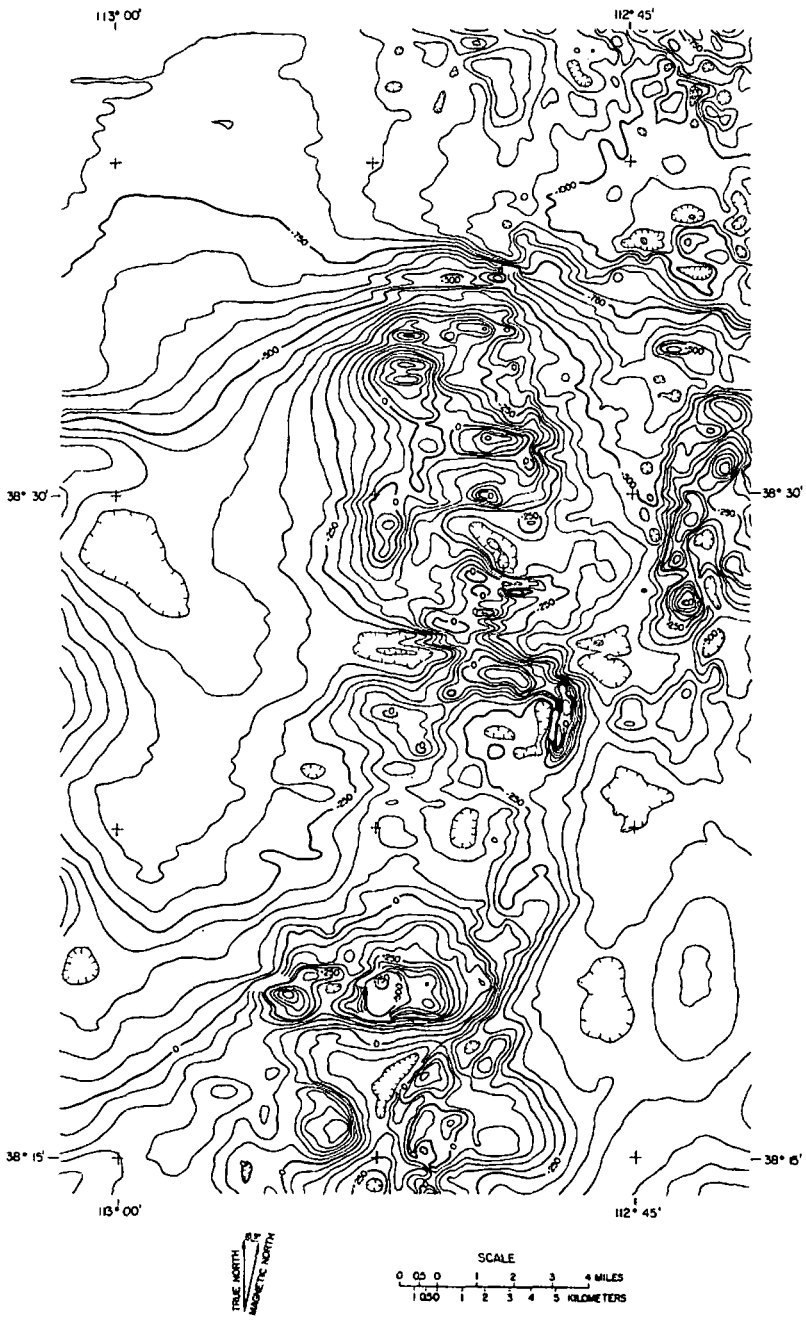
113° 00'
112° 45'
38° 30'
38° 15'
TRUE NORTH
MAGNETIC NORTH
SCALE
0 0.5 0 1 2 3 4 MILES
1 0 1 2 3 4 5 KILOMETERS

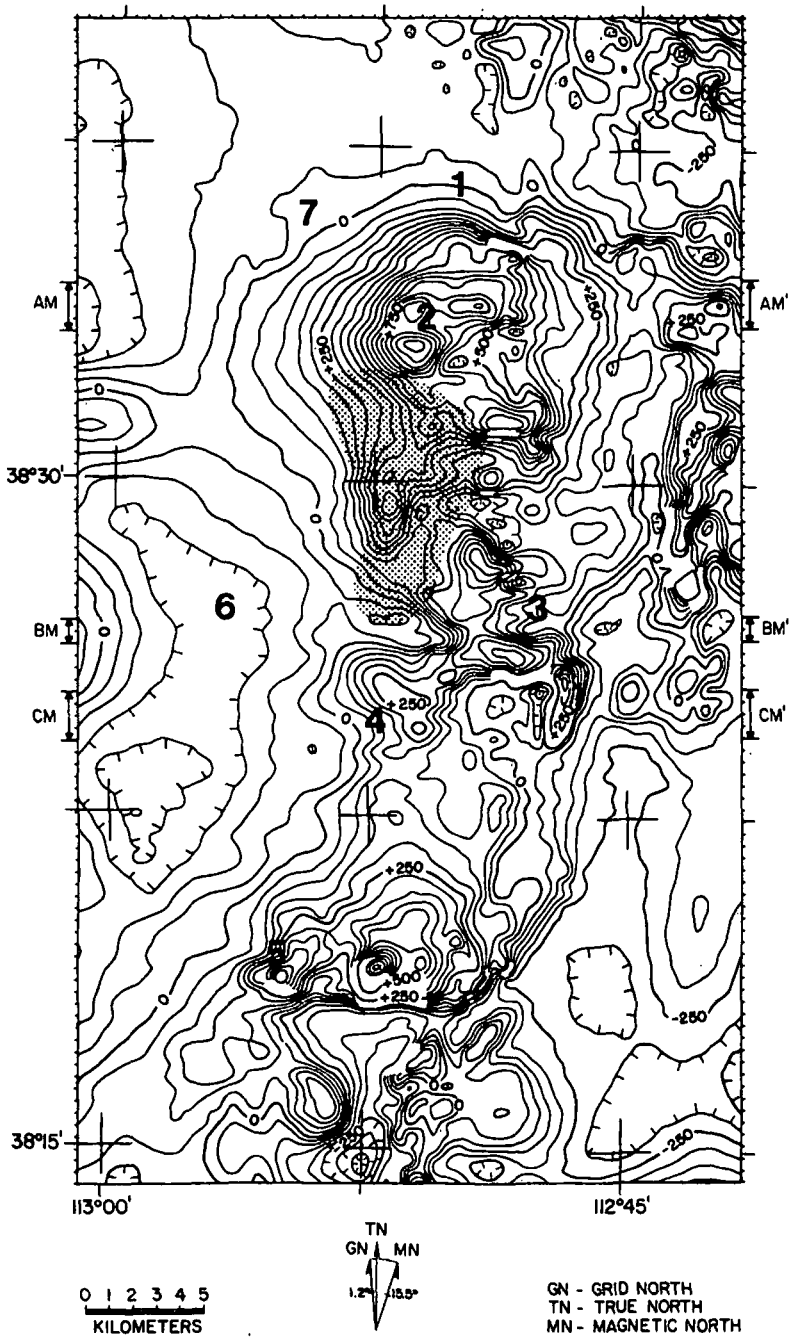

Figure 10. Reduced-to-the-pole residual magnetic anomaly map; contour interval = 50 gammas. Grid lines selected for magnetic profiles are indicated by lettering along map border. Grid values along grid lines, indicated by arrows, were averaged to give the observed profile values. Dotted pattern indicates the high thermal gradient anomaly area.

In the central portion of both maps is a northward-trending magnetic high which overlies, primarily, the exposed granite of the Mineral Mountains pluton. On the north, this high (designated the "central Mineral Mountains magnetic high") is bounded by east-west trending contours with a large relief of about 350 gammas (just south of number 1 on Fig. 10) which correspond with the northern end of the Mineral Mountains pluton at the County Line fault (Fig. 4). On the south, the pluton magnetic high is also bounded by east-west trending contours with a large relief of about 500 gammas (just south and east of number 5 on Fig. 10) that corresponds with the Cave Canyon fault (Fig. 4).

In the northeastern portion of the central Mineral Mountains magnetic high is a localized magnetic high (number 2 on Fig. 10) which corresponds well with the central Mineral Mountains gravity high. This magnetic high overlies granite and alluvium along the western margin of the central Mineral Mountains.

In the central portion of the central Mineral Mountains magnetic high, is a constriction of the high which corresponds to a constriction of the exposed granite of the pluton. The magnetic low area causing this constriction (number 3 on Fig. 10) from the east overlies the rhyolite domes of Bearskin and Little Bearskin Mountains (Fig. 4), whereas the magnetic low causing the constriction from the west overlies mostly alluvium and extends into the high along the axis of a reversed magnetic polarity rhyolite flow (Fig. 4). Approximately 3 km north of the low magnetic area overlying Bearskin and Little Bearskin Mountains (number 3 on Fig. 10), is a magnetic low which corresponds well with

the mapped exposure of the Bailey Ridge flow (Fig. 4), another reversed magnetic polarity rhyolite flow.

West of the low over the Bailey Ridge flow is a magnetic high which overlies alluvium along the western margin of the Mineral Mountains. This high is separated from the magnetic high to the north by a saddle which overlies a northwestward-trending line of hot spring deposits about 1.75 km long. The low magnetic area extending southward from this saddle lies within the high thermal gradient anomaly area (patterned area on Fig. 10) and may be caused, in part, by hydrothermal alteration of magnetite formerly in the rocks above or within the reservoir. This hypothesis is weakened, however, by the fact that this entire area overlies alluvium and the magnetic low may therefore be caused by the low magnetic susceptibility of the alluvium alone.

In the southern portion of the central Mineral Mountains magnetic high, an area of high magnetic intensity lies north of and adjacent to the previously mentioned east-west magnetic trend overlying Cave Canyon fault. This high magnetic area is comprised of several separate magnetic highs; and the highest anomaly peaks are located near mapped contacts between the sedimentary and/or Precambrian (?) rocks and the pluton. A magnetic nose extends northward from this high area and separates into two smaller noses. The easternmost of these noses trends north-northeast, and the end of this nose overlies Granite Peak (Fig. 4), which is the highest mountain in the Mineral Mountains. The westernmost nose overlies primarily alluvium along the

western margin of the Mineral Mountains and terminates in a saddle (about 2 km south-southeast of number 4 in Fig. 10) in the area of Corral Canyon (Fig. 4). North of these noses is a broad low magnetic intensity area which is bounded on the north, east, and west by magnetic highs. The magnetic low area is centered approximately over South Twin Flat Mountain (Fig. 4), which is the southernmost of the previously mentioned rhyolite domes. The magnetic highs which bound this magnetic low area are attributed to locally high areas of magnetic susceptibility within the granite of the pluton.

South of the central Mineral Mountains magnetic high, which terminates at the Cave Canyon fault (Fig. 4), a magnetic low area overlies the Mesozoic and Paleozoic sedimentary rocks of the southern Mineral Mountains. Bounding this low on the east, a magnetic high area overlies outcrops of Tertiary volcanics and one small outcrop of Tertiary intrusive rocks. An eastward extension of this magnetic high area overlies alluvium south of Minersville Reservoir (Fig. 4) and indicates that the volcanics probably extend under the alluvium at shallow depth. Bounding the magnetic low on the west, a magnetic high overlies a limited outcrop of intrusive rock.

In the southwestern corner of the maps, a magnetic high area in the form of a magnetic nose trends southwestward from the magnetic high area (number 5 on Fig. 10) north of Cave Canyon fault. This magnetic nose is attributed to the southwestward extension of the pluton under the alluvium at rather shallow depth.

In the west central part of the map is a magnetic low (number 6 on Fig. 10) which overlies the Milford Valley gravity low. This magnetic low is attributed to the low magnetic susceptibility of the alluvium in Milford Valley. The magnetic low over Milford Valley terminates in an area of generally east-west-trending magnetic contours which cross the valley over alluvium. These east-west-trending magnetic contours, which merge with the previously noted east-west contours that correspond with the County Line fault, are thought to indicate the northern terminus of the intrusive rocks underlying the alluvium of Milford Valley. North of this lineament is a broad magnetic low area which extends across the entire northern part of the map. As expected, due to the low magnetic susceptibility of sedimentary rock, no magnetic expression of the northern Mineral Mountains gravity high (number 1 on Fig. 10) appears within the magnetic low area.

Along the eastern edge of the maps opposite the northern half of the central Mineral Mountains magnetic high is a magnetic high area, which consists of many small magnetic peaks. This area overlies an extensive Quaternary basalt flow.

In the southeastern portion of the maps, a northward-trending elongate magnetic low area overlies, and is attributed to, the alluvium of Beaver Valley (Fig. 4).

Residual and regional maps--The reduced gravity data were used to produce two residual gravity anomaly maps. Figure 11 shows a fifth-order polynomial residual gravity anomaly map and Figure 12 shows a high-pass filtered gravity anomaly map. The reduced-to-the-pole residual magnetic anomaly data were used to produce a low-pass filtered (regional) magnetic anomaly map, shown in Figure 13.

On the fifth-order polynomial residual gravity anomaly map (Fig. 11), the areal extent of the low gravity zone surrounding the Bearskin gravity low (number 3) has increased significantly. This suggests that the silicic volcanic domes and flows, which crop out in the central Mineral Mountains, have been extruded from a rather extensive body of low-density material underlying the eastern portion of the Mineral Mountains pluton. On this map, the Ranch Canyon gravity saddle (number 4) reveals an apparent right lateral offset of about 1.5 km. The gravity nose, which extends into the saddle area from the south, overlies alluvium and is attributed to Paleozoic sedimentary and/or Precambrian(?) metamorphic rocks which may extend into this area from exposures in the southern Mineral Mountains. Two small outcrops of Paleozoic sedimentary rock (Fig. 4) in this area support this conclusion. The broad gravity low over Milford Valley is clearly separated into two lows (number 6 and number 7) on this map. The previously proposed contact zone between the sedimentary rocks (to the north) and the igneous rocks (to the south) in the floor of Milford Valley occurs near the northern part of the gravity saddle which

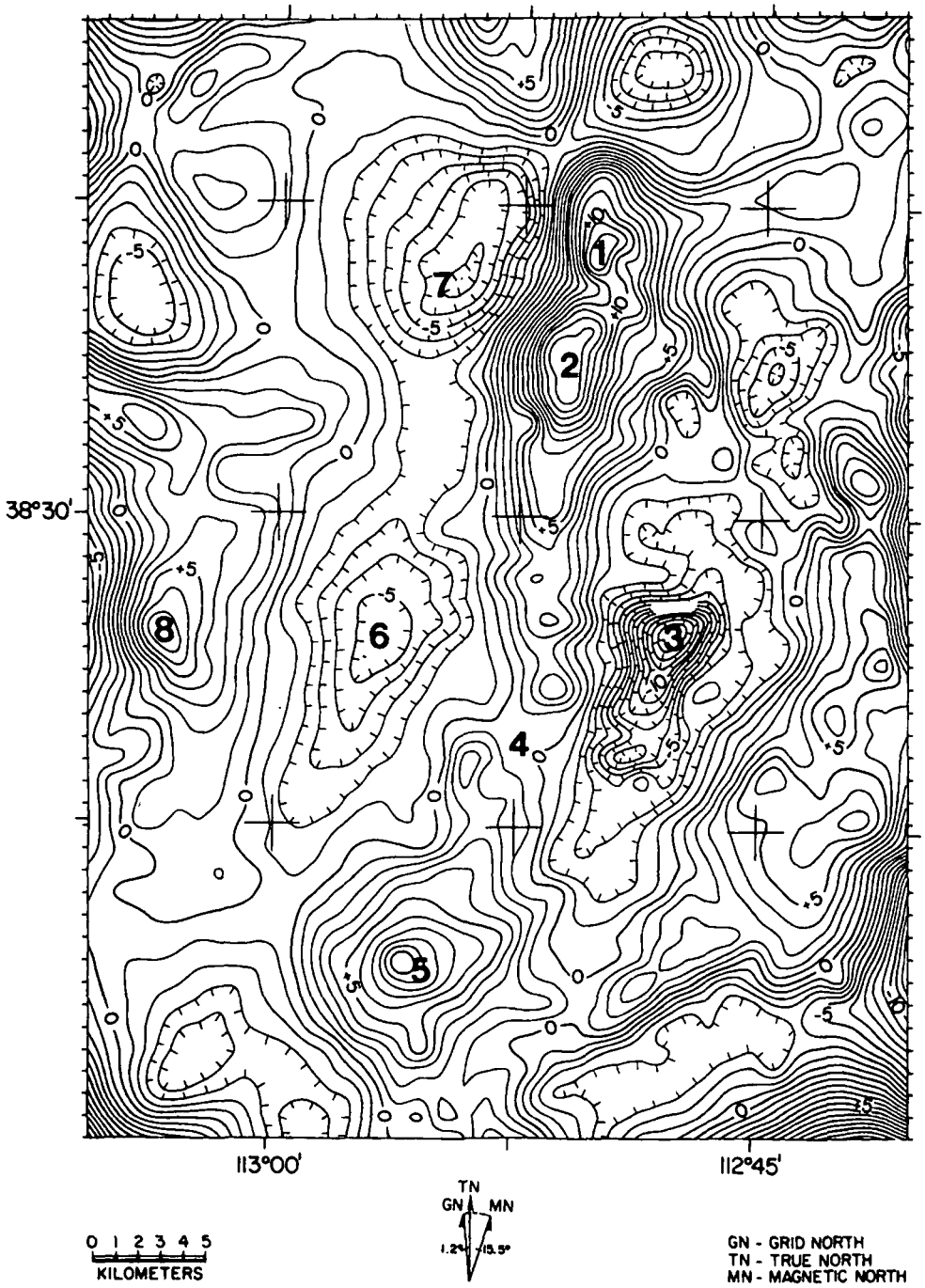

Figure 11. Fifth-order polynomial residual gravity anomaly map; contour interval = 1 mgal.

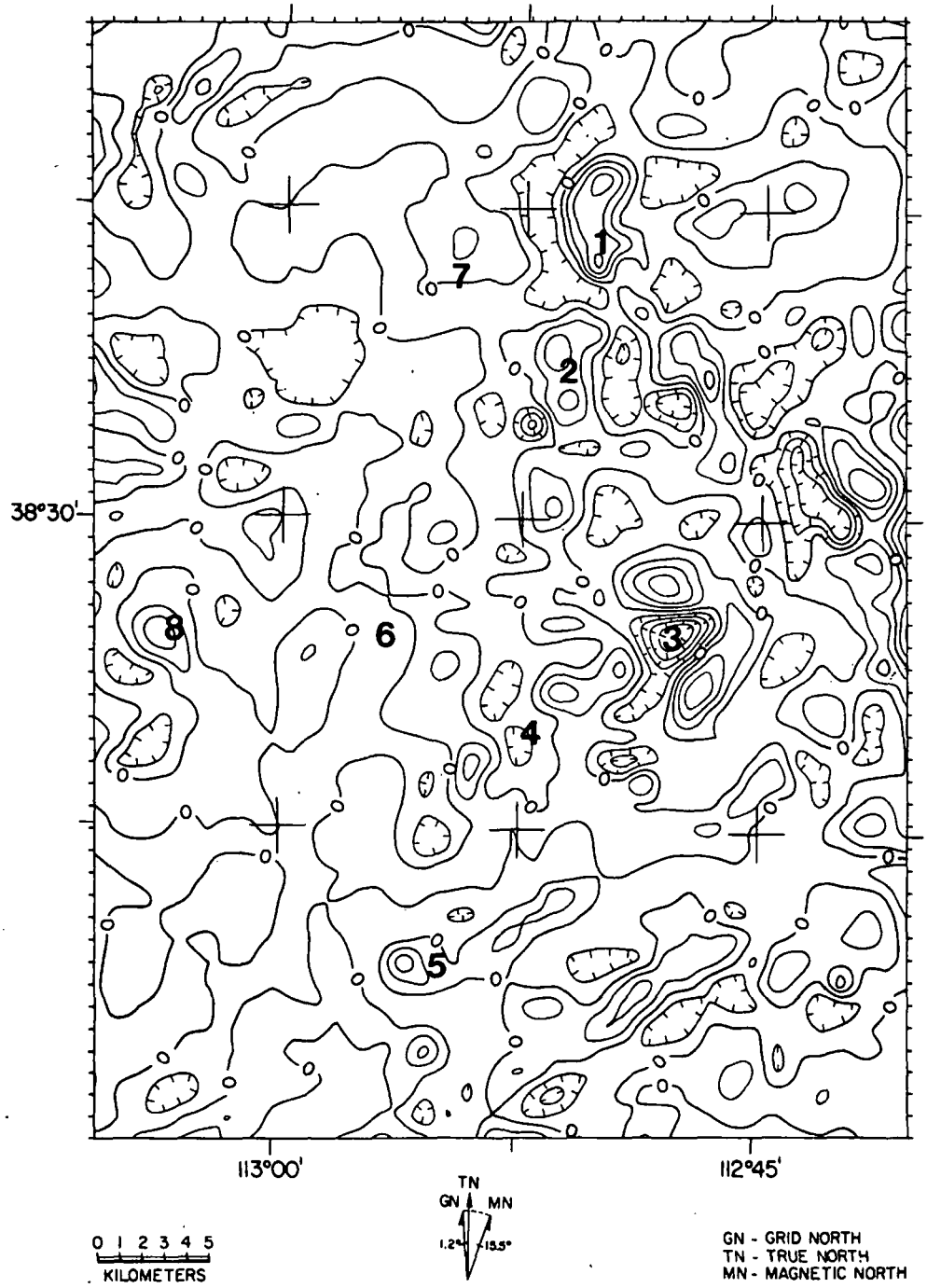

Figure 12. High-pass filtered gravity anomaly map; contour interval = 1 mgal.

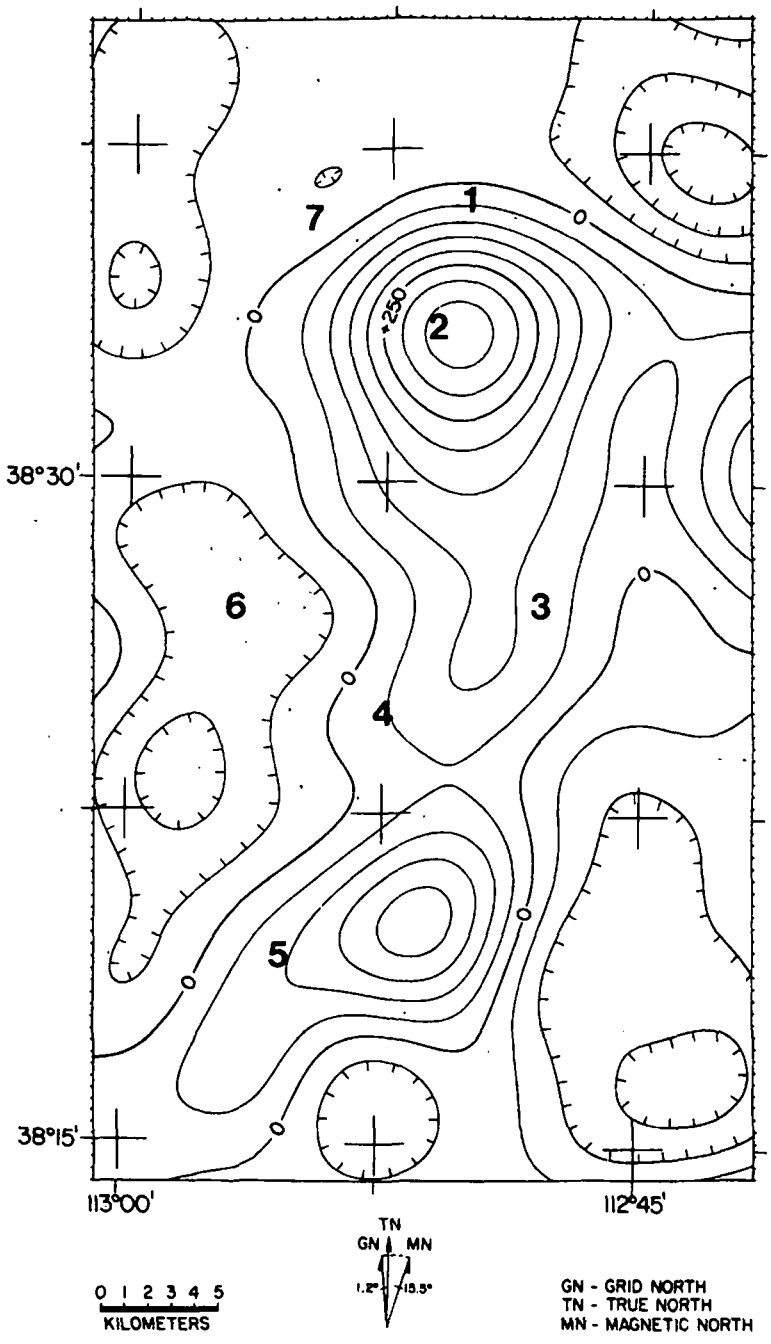

Figure 13. Low-pass filtered magnetic anomaly map; contour interval = 50 gammas.

separates these two lows.

On the high-pass filtered gravity anomaly map (Fig. 12), the broad gravity low area overlying Milford Valley and the northward-trending gravity high area overlying the Mineral Mountains are conspicuously absent. This absence is caused by the fact that these broad anomalies, whose power spectral content are primarily in the lower frequencies, were filtered out by the application of the selected high-pass filter. The anomalies remaining on this map may therefore be viewed as anomalies related to small localized density contrasts, probably at rather shallow depth. Trending south-southeastward from the northern Mineral Mountains gravity high (number 1) are a series of gravity highs which follow the mapped geology of the Mineral Mountains pluton. Adjacent to the eastern margin of the Bearskin gravity low (number 3) is a south-southwestward-trending elongate gravity high which also lies near the exposed eastern edge of the pluton. Southeast of this high is an elongate gravity high which extends northeastward from a limited exposure of Paleozoic sedimentary rocks along the western margin of the Mineral Mountains over the alluvium of Beaver Valley. This gravity high probably indicates an extension of the Paleozoic sedimentary rocks at shallow depth under the alluvium. In the southern Mineral Mountains, several small gravity highs also tend to follow the geologic boundaries of the mapped bedrock outcrops. About 3 km northeast of the Ranch Canyon gravity saddle (number 4), an elongate gravity high, trending generally east-west, overlies outcrops of Precambrian metamorphic rocks and the granite of the pluton. A

gravity high lying south of the middle Mineral Mountains gravity high (number 2) overlies a northwesterly trending series of hot spring deposits. This area was previously observed to be a magnetic saddle between two magnetic highs which may be related to hydrothermal magnetite alteration. A consistent explanation for a gravity high in this area would be that it is caused by the densification of the alluvium by cementation with hot spring deposits.

On the low-pass filtered residual magnetic anomaly map (Fig. 13), the magnetic high over the Mineral Mountains pluton is separated into two highs by a saddle located southeast of the Ranch Canyon gravity saddle (number 4). The southern magnetic high shows a pronounced southwesterly-trending magnetic nose which was previously attributed to an extension of intrusive rock under the alluvium in this area.

Upward-continued pseudomagnetic, pseudogravity and upward-continued gravity maps--The upward-continued pseudomagnetic map (Fig. 14) was produced from the gridded reduced gravity values and is compared with the reduced-to-the-pole residual magnetic anomaly map (Fig. 10). In general, there is a high degree of correlation between the central Mineral Mountains magnetic high (Fig. 10) and the high pseudomagnetic area of the upward-continued pseudomagnetic map (Fig. 14). There is also rather good correlation between the low magnetic area (number 6) over Milford Valley and the corresponding low pseudomagnetic area. This correlation indicates that Poisson's relation holds rather well in this area with respect to the granite of the Mineral Mountains pluton and the alluvial fill of Milford Valley.

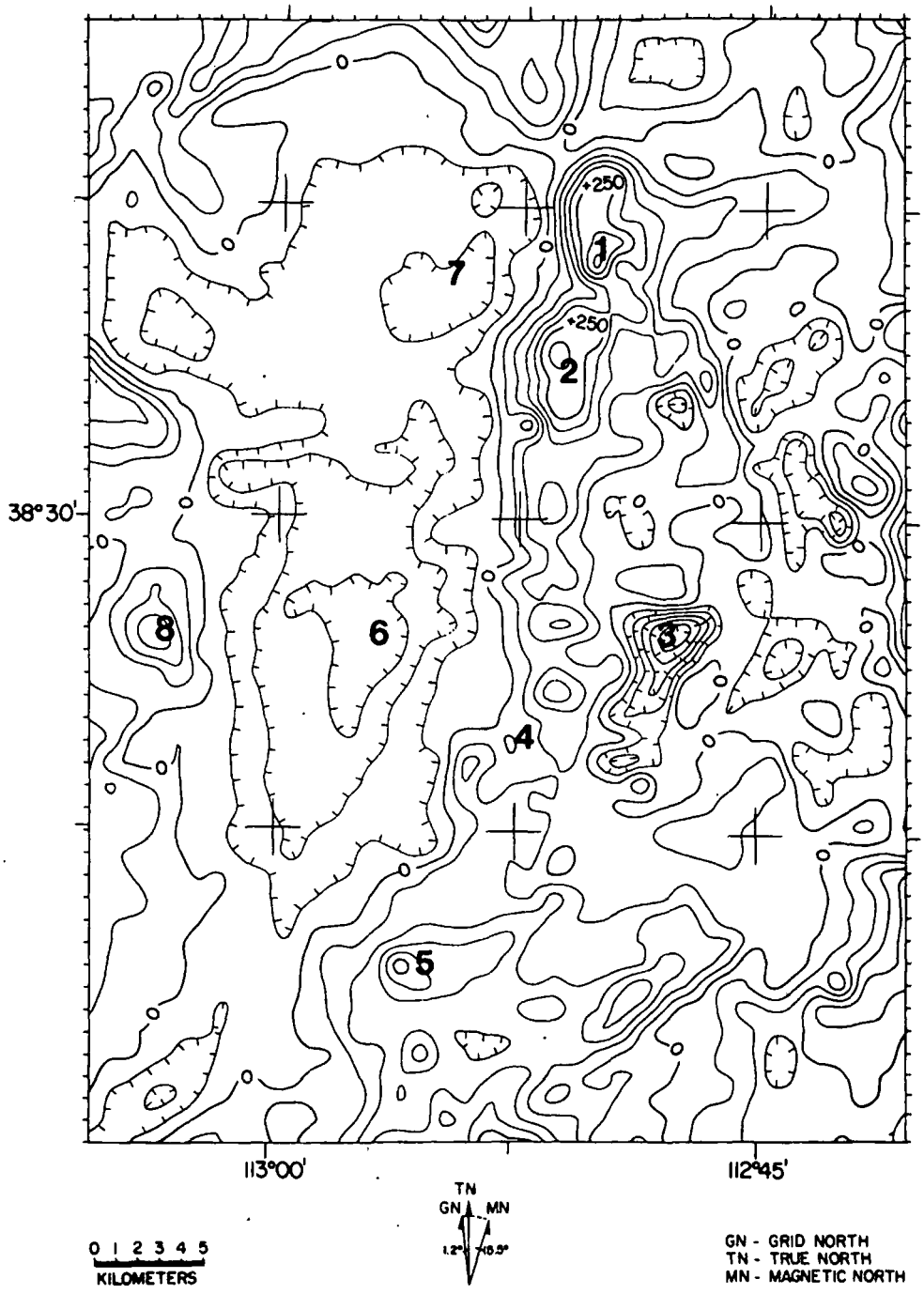

Figure 14. Upward-continued pseudomagnetic; contour interval = 50 gammas.

Although the highs over the Mineral Mountains on both maps correlate well, closer inspection reveals several differences. The pseudomagnetic high overlying the northern Mineral Mountains gravity high (number 1) corresponds to a magnetic low area on Figure 10, which is caused by the high-density; low-magnetic-susceptibility sedimentary rocks of the northern Mineral Mountains. An east-west trending magnetic high south of number 3 on Figure 10 shows no corresponding pseudomagnetic high. The magnetic high is thought to be caused by an area of high magnetic susceptibility within the pluton. About 8 km southeast of number 3, a northeastward-trending pseudomagnetic high overlies the magnetic low associated with the northern part of Beaver Valley. The pseudomagnetic high is probably caused by an eastward extension of high-density, low-magnetic-susceptibility Paleozoic sedimentary rocks at shallow depth under the alluvium of Beaver Valley. About 3 km southwest of number 4, a pseudomagnetic high, which overlies alluvium, also corresponds to a magnetic low area and is probably caused by a northward extension of the Paleozoic and/or Precambrian (?) metamorphic rocks exposed in the southern Mineral Mountains. The pseudomagnetic nose, which extends southward from number 2 and terminates southeast of number 4, contains three rather circular pseudomagnetic highs. The southernmost of these pseudomagnetic highs overlies the Mineral Mountains pluton, alluvium, and Precambrian (?) metamorphic rocks near the western margin of the Mineral Mountains, and is centered about 1 km north of a magnetic high which overlies alluvium and granite. The northerly offset between the centers of these two highs is attributed to the Precambrian (?) rocks

having a slightly higher density and a lower magnetic susceptibility than the granite of the pluton. Although measurements made by Crebs and Cook (1976) indicate a high magnetic susceptibility for Precambrian (?) gneiss samples, a similar relationship between the center of a pseudomagnetic high centered over Precambrian (?) rock and a magnetic high centered over intrusive rock occurs in the southern Mineral Mountains (number 5). In the area between the two southernmost of the above-mentioned three circular pseudomagnetic highs is a pseudomagnetic saddle. This pseudomagnetic saddle, which overlies primarily alluvium and granite, corresponds with a small, but deep, magnetic low. This magnetic low, which is centered over alluvium, may be caused by a reversed magnetic polarity rhyolite flow at shallow depth beneath the alluvium. This hypothesis is proposed due to the proximity of a reversed magnetic polarity rhyolite flow (Fig. 4) which corresponds with the eastern edge of the magnetic low. This proposed flow would probably issue from a separate vent, and not be an extension of the exposed flow because the toe of the exposed flow is readily accessible and does not appear to be significantly eroded (Evans, 1978, personal communication). An alternate and favored explanation for the magnetic low would be a rather thick unit of high-density, low-magnetic-susceptibility rock which overlies the granite of the pluton at shallow depth beneath the alluvium. The correspondence of the magnetic low with the southern end of the high thermal gradient anomaly area (dot pattern on Fig. 10) suggests that this unit controls the southward extent of the geothermal reservoir.

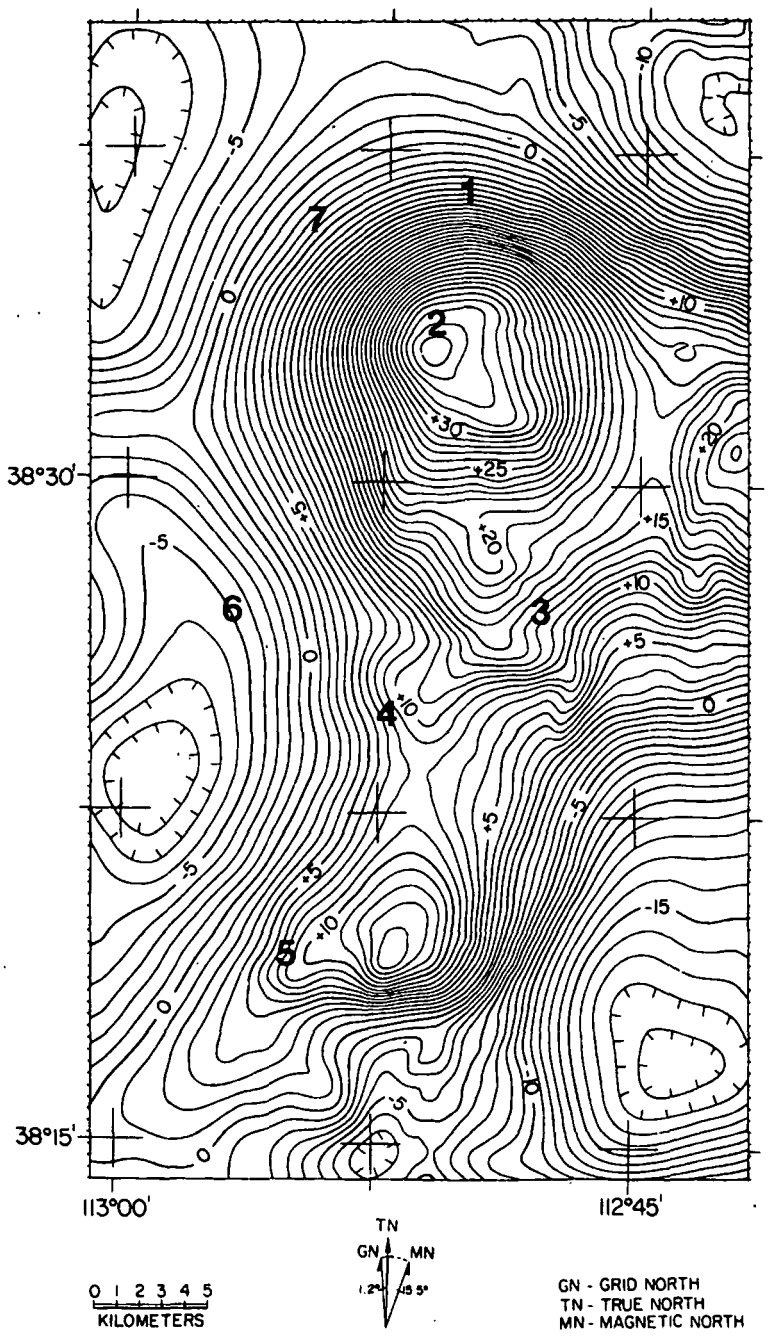

Figure 15. Pseudogravity map; contour interval = 1 mgal.

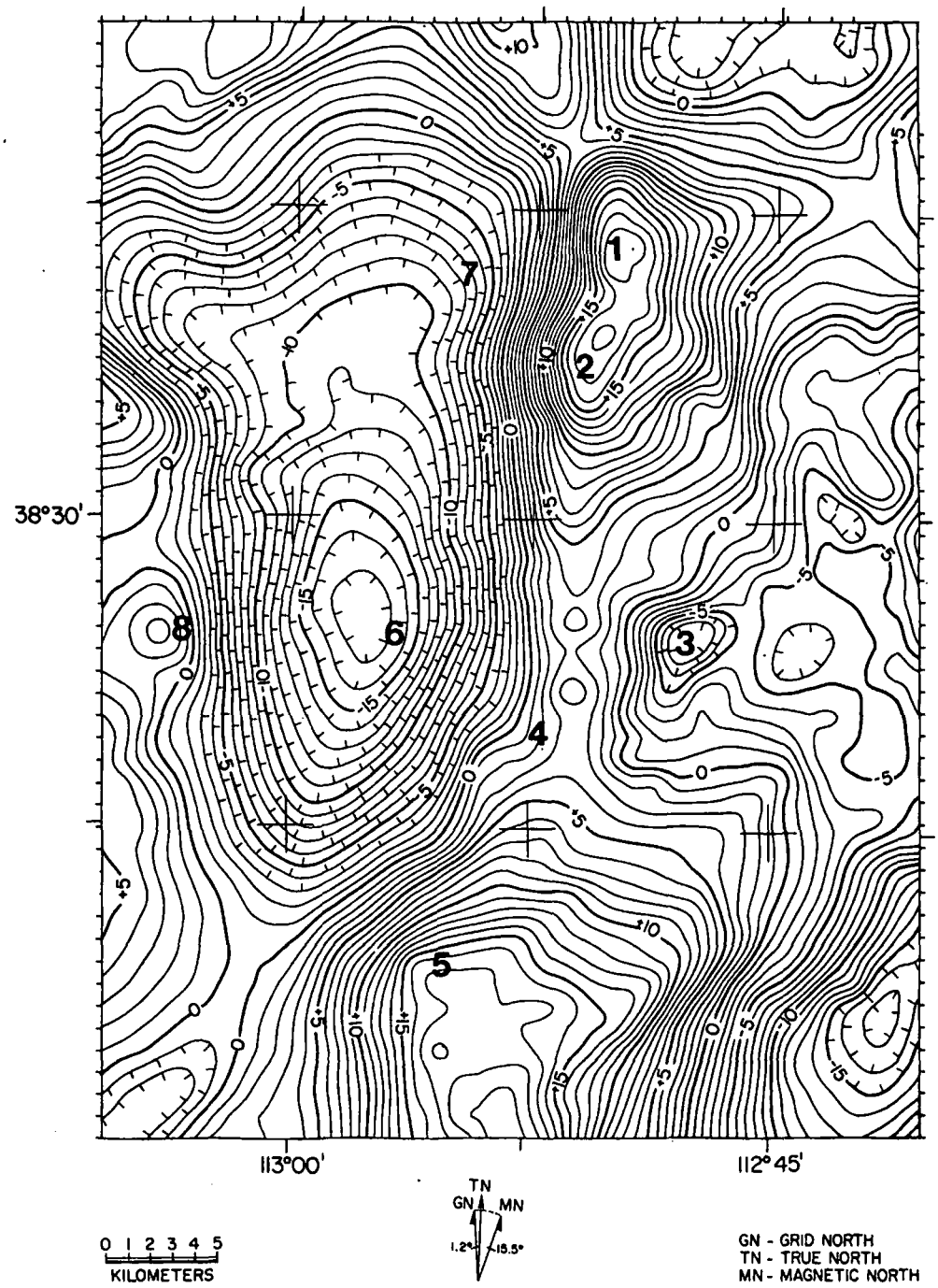

Figure 16. Upward-continued gravity map; contour interval = 1 mgal.

The pseudogravity map (Fig. 15) was produced from the gridded reduced-to-the-pole residual magnetic anomaly values and is compared with the upward-continued gravity map (Fig. 16). The pseudogravity low area overlying Milford Valley generally agrees well with the corresponding highs and lows on the upward-continued gravity map (Fig. 16). The location of the Ranch Canyon gravity saddle (number 4) correlates well with a similar saddle on the pseudogravity map. This correlation suggests the possibility of a low-density, low-magnetic-susceptibility body located beneath the surface exposure of the Mineral Mountains.

Strike-filtered maps--North-south (Fig. 17), east-west (Fig. 19), and northeast-southwest (Fig. 21) strike-filtered gravity maps and north-south (Fig. 18) and east-west (Fig. 20) strike-filtered magnetic maps were produced from the gridded reduced gravity data and the gridded reduced-to-the-pole residual anomaly data, respectively.

The purpose of these maps was to emphasize contour trends in the direction of the strike filter. Both the north-south strike-filtered gravity map (Fig. 17) and the north-south strike-filtered magnetic map (Fig. 19) show north-south trends which lie along the eastern and western margins of the Mineral Mountains. These trends have already been attributed to Basin and Range normal faulting which is believed to flank the Mineral Mountains horst on both its eastern and western margins. The north-south strike-filtered gravity map also shows a north-south trend along the western side of Milford Valley which is probably caused by normal faulting along the eastern flanks of the

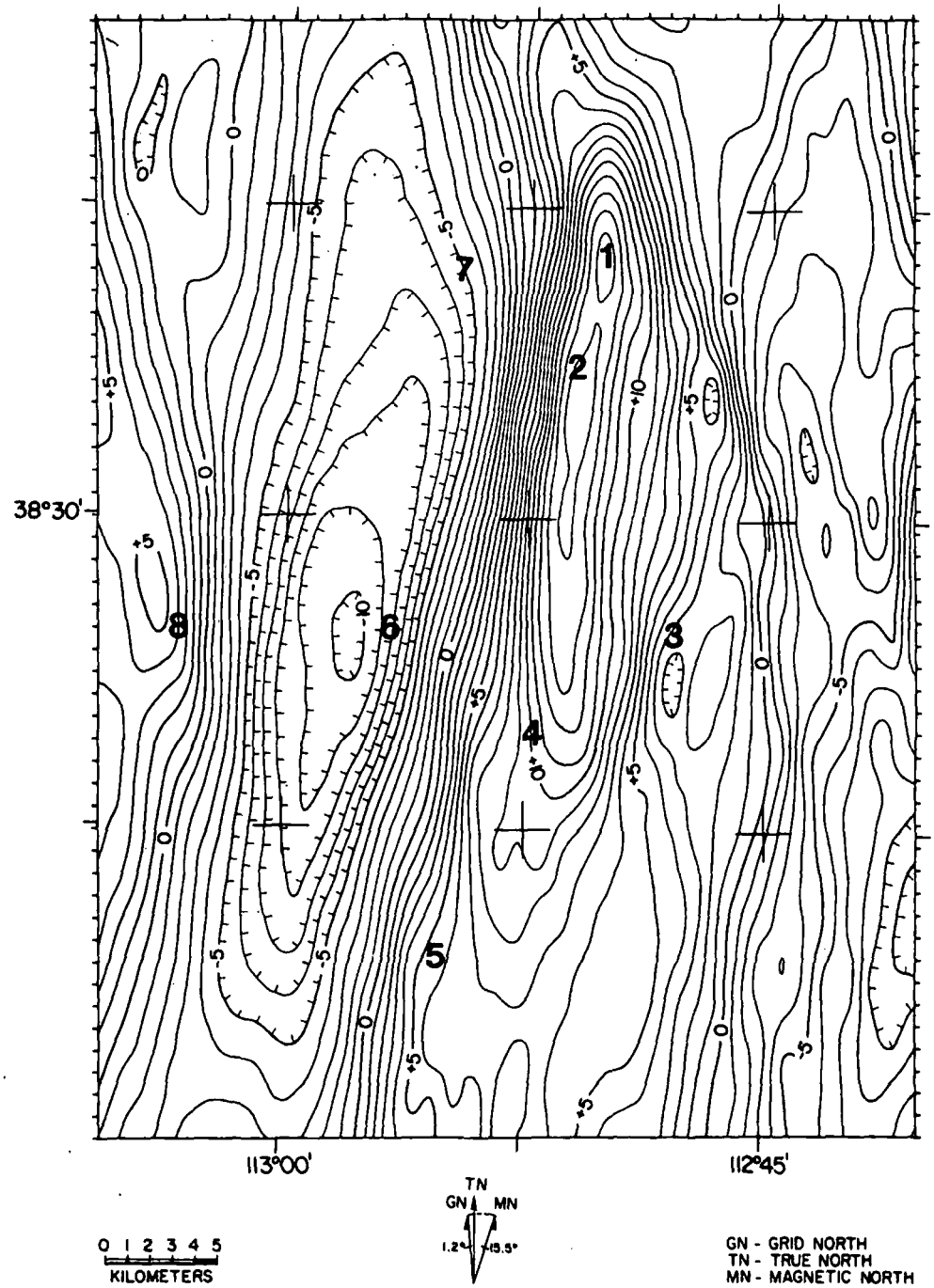

Figure 17. North-south strike-filtered gravity anomaly map; contour interval = 1 mgal.

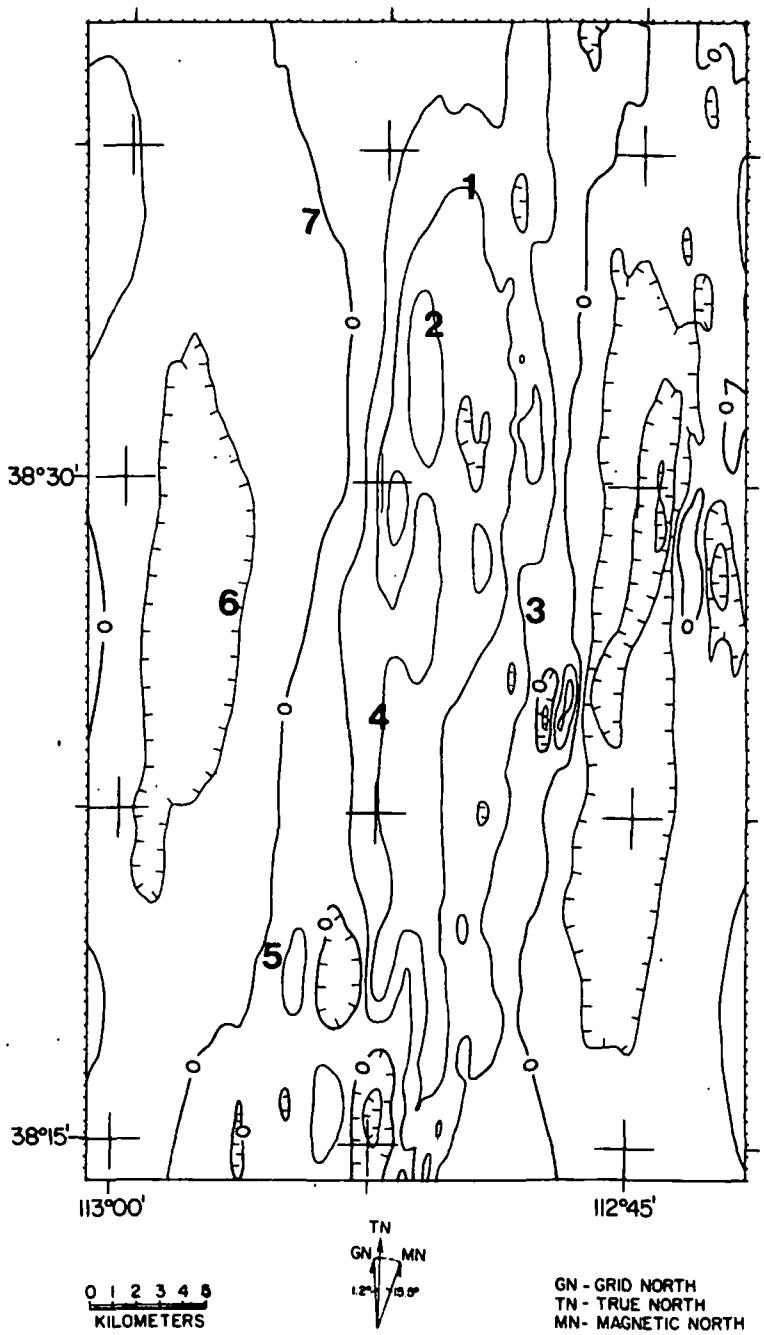

Figure 18. North-south strike-filtered magnetic anomaly map; contour interval = 50 gammas.

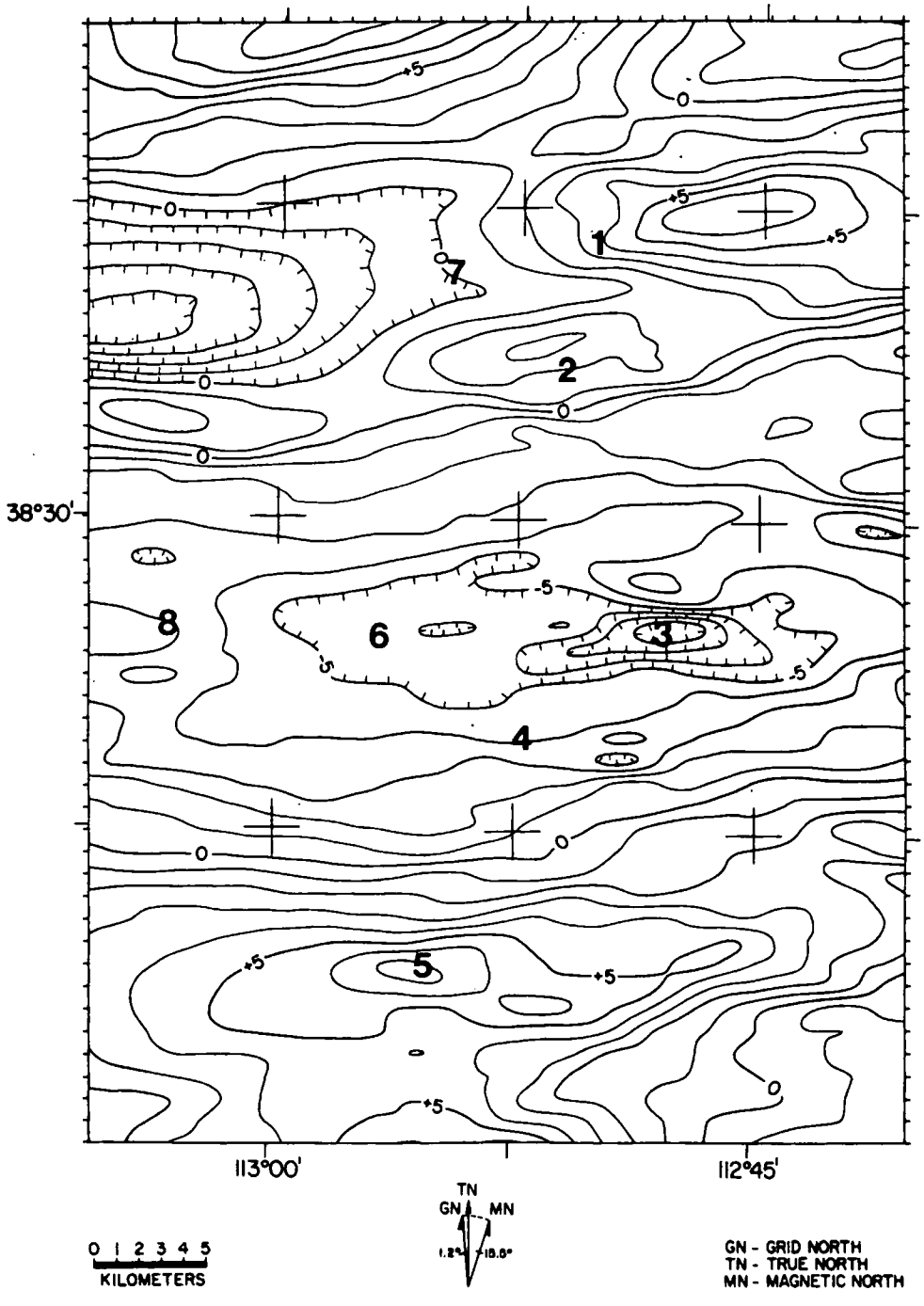

Figure 19. East-west strike-filtered gravity anomaly map; contour interval = 1 mgal.

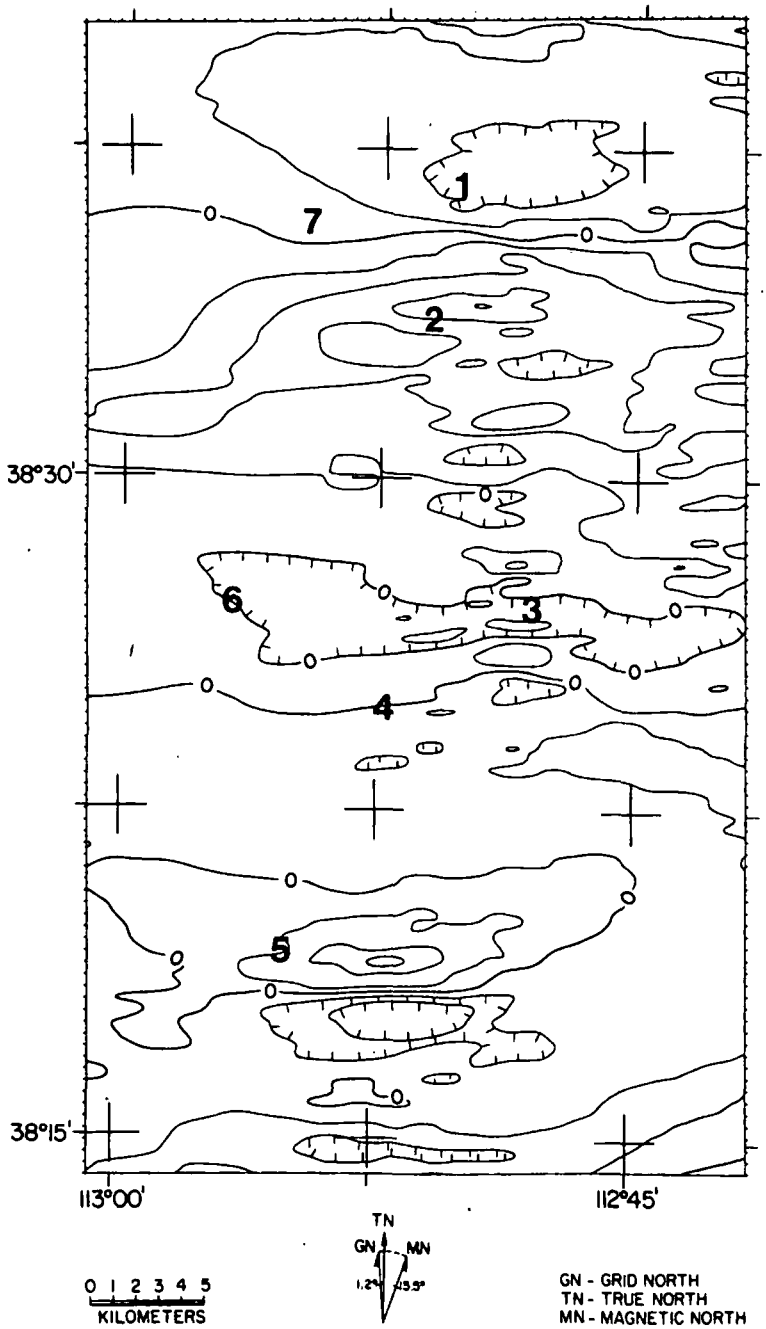

Figure 20. East-west strike-filtered magnetic anomaly map; contour interval = 50 gammas.

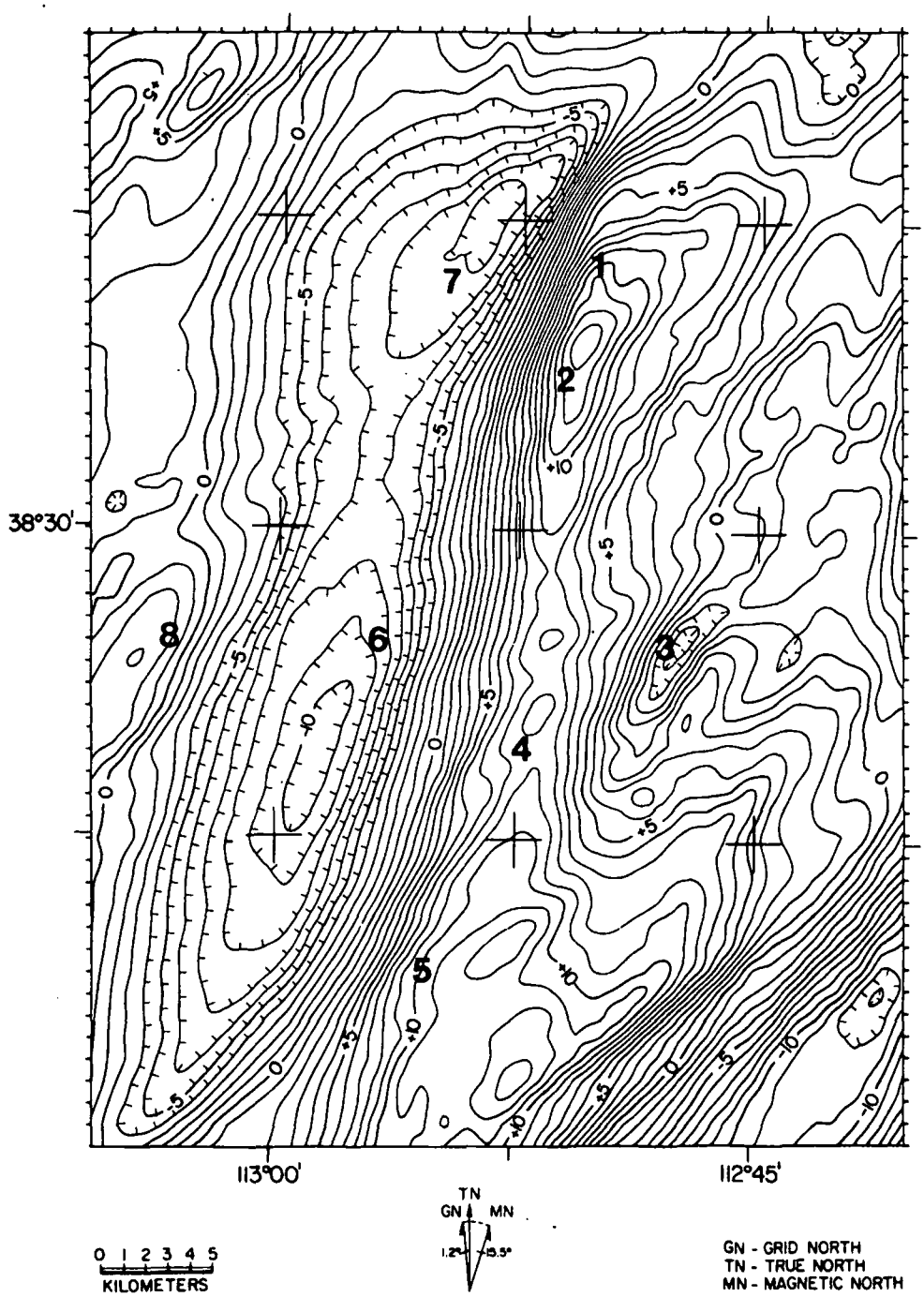

Figure 21. Northeast-southwest strike-filtered gravity anomaly map; contour interval = 1 mgal.

Star Range, Rocky Range, and Beaver Lake Mountains (Fig. 4).

The east-west strike-filtered gravity map (Fig. 19) and the east-west strike filtered magnetic map (Fig. 20) show strong east-west trends which pass through the area of the County Line fault (between numbers 1 and 2) and continue across Milford Valley. These trends have already been interpreted as indicative of the sedimentary rock-intrusive rock contact which is believed to continue across the floor of Milford Valley from its exposure at the County Line fault. On the east-west strike-filtered magnetic map (Fig. 20), the east-west trending contours associated with Cave Canyon fault (south of number 5) are also apparent.

The northeast-southwest strike-filtered gravity map (Fig. 21) reveals a strong northeastward trend near the southeastern corner of the map. The fact that this strong trend, which has previously been mentioned as evidence of range-flanking normal faulting, does not continue northward, may indicate that the range-bounding normal faults along the eastern margin of the central and northern Mineral Mountains are less extensive than the normal faults along the other flanks of the Mineral Mountains.

Interpretative Geologic Modeling of Gravity and Magnetic Profiles

Three profiles were selected for interpretative geologic modeling of the residual gravity and magnetic values (see "PROFILE MODELING"). Models for each profile were constrained using: 1) geologic mapping, 2) sample density or magnetic susceptibility measurements, and 3)

drill hole information when available. The interpretative geologic cross sections shown are not unique, but are considered reasonable for the geologic setting. The modeled gravity and magnetic profiles are indicated on Figures 8 and 10, respectively.

The interpretative geologic cross section for gravity profile A-A' is shown on Figure 22. The model for this profile is not entirely shown as the southward extent of Milford Valley and the bedrock of the Beaver Lake Mountains were modeled using a body whose northern face was positioned 1 km south (out of the paper) of the profile and extended to the south for 100 km. This body had a density contrast of -0.5 g/cc and a depth of 0.0 km at the first point on the profile. All other body points were common with the westernmost body shown. Profile A-A' traverses the northern part of Milford Valley and the graben underlying the valley is modeled with a maximum depth of alluvial fill of about 1.4 km. The eastern margin of the graben was modeled using step faults, but could have been modeled with a single sloping side. The step faults were placed where the strongest gradients on the residual gravity map with projected regional removed (Fig. 8) indicated possible faulting. The gravity high over the western margin of the Mineral Mountains was modeled using a high density block (+0.1 g/cc) with strike lengths that approximated the north-south extent of the northern and central Mineral Mountain gravity highs (numbers 1 and 2). East of the Mineral Mountains, the density contrast is decreased to -0.4 g/cc to account for the presence of volcanics in the alluvium of this area.

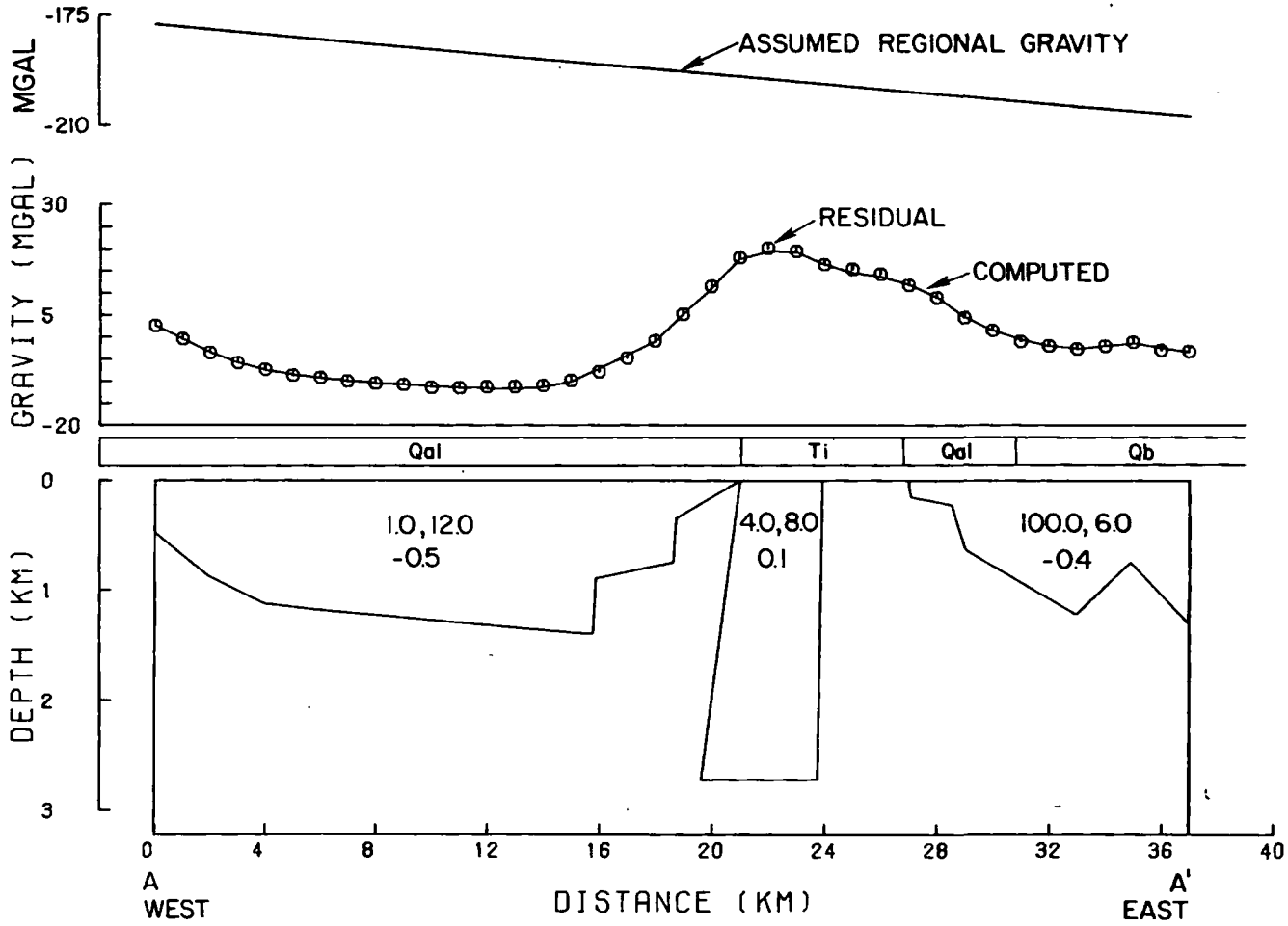

Figure 22. Interpretative geologic cross section along gravity profile A-A'. The upper numbers in each body are the strike lengths (km) of the body out of and into the paper, respectively. The lower number is the density contrast (g/cc). The mapped surface geology symbols are those used in Figure 4.

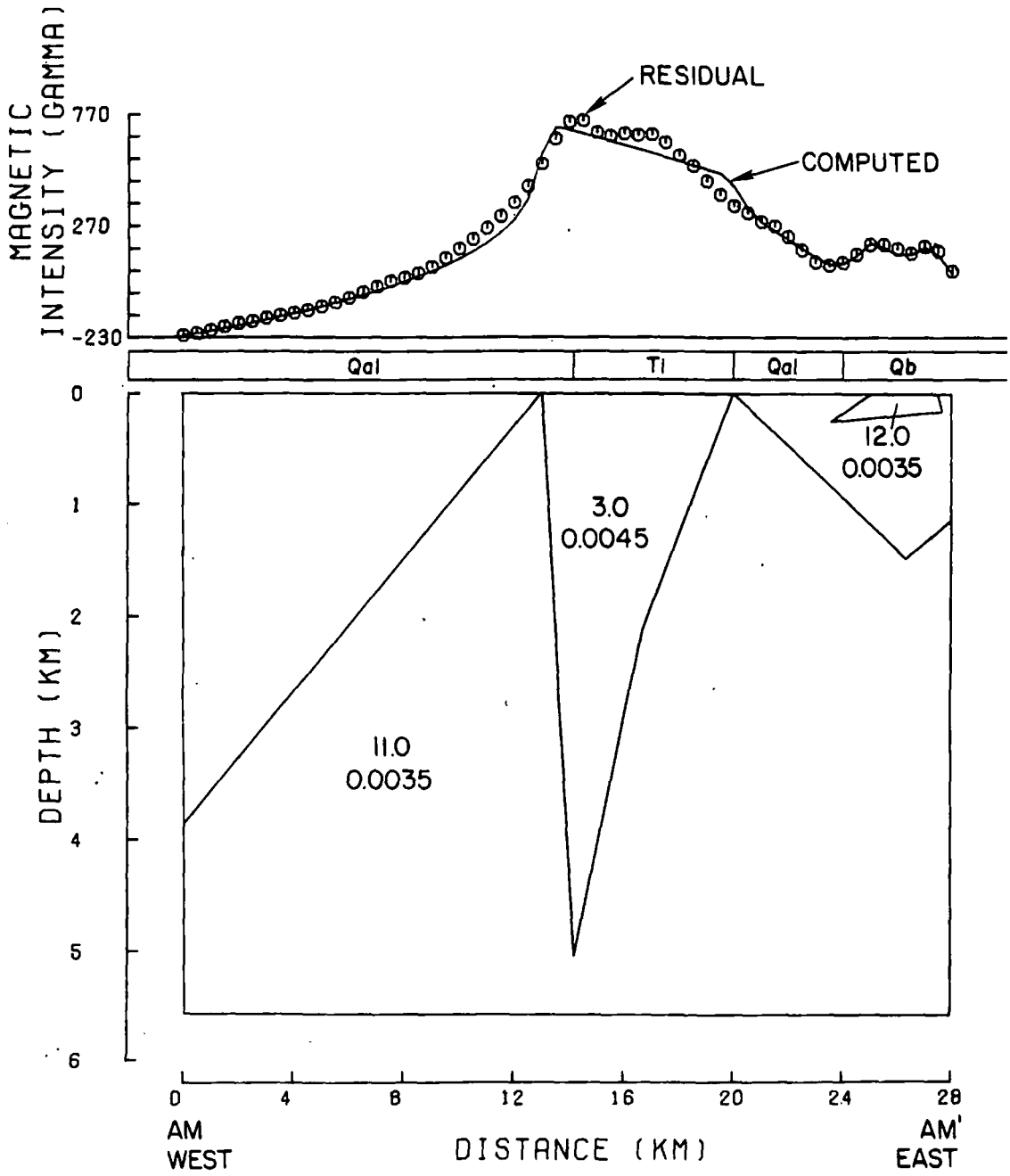

Figure 23. Interpretative geologic cross section along magnetic profile AM-AM'. The upper number in each body is the half-strike length (km) of the body. The lower number is the magnetic susceptibility contrast (cgs units). The mapped surface geology symbols are those used in Figure 4.

The interpretative geologic cross section for magnetic profile AM-AM' is shown on Figure 23. The model for this profile shows a continuous decrease of the depth of Milford Valley to the west and this is attributed to the fact that profile AM-AM' crosses the previously hypothesized contact between the low-magnetic susceptibility rocks on the north and the high-magnetic susceptibility rocks on the south. The increasing depth of magnetic bedrock under Milford Valley is therefore caused by the absence of high magnetic susceptibility material in the western part of the floor of Milford Valley.

The interpretative geologic cross section for gravity profile B-B' is shown on Figure 24. This profile crosses exposed Paleozoic rock in the southern Rocky Range and extends across Milford Valley, which is modeled as a graben with sloping sides and a maximum depth of alluvial fill of about 1.4 km. Where profile B-B' crosses the Bearskin gravity low (number 3 on Fig. 8), a body with a density contrast of -0.2 g/cc and strike lengths which approximate the north-south extent of the gravity low has been modeled. This body extends to a depth of 4.3 km and approximately underlies the low density rhyolite domes of Bearskin and Little Bearskin Mountains which intrude the pluton in this area. East of the Mineral Mountains the density contrast is decreased to -0.4 g/cc to approximate the density of the mixed volcanics and alluvium in this area.

The interpretative cross section for profile BM-BM' is shown on Figure 25. The model for this profile indicates a maximum depth of the alluvial fill in Milford Valley of 1.5 km, which agrees well with the

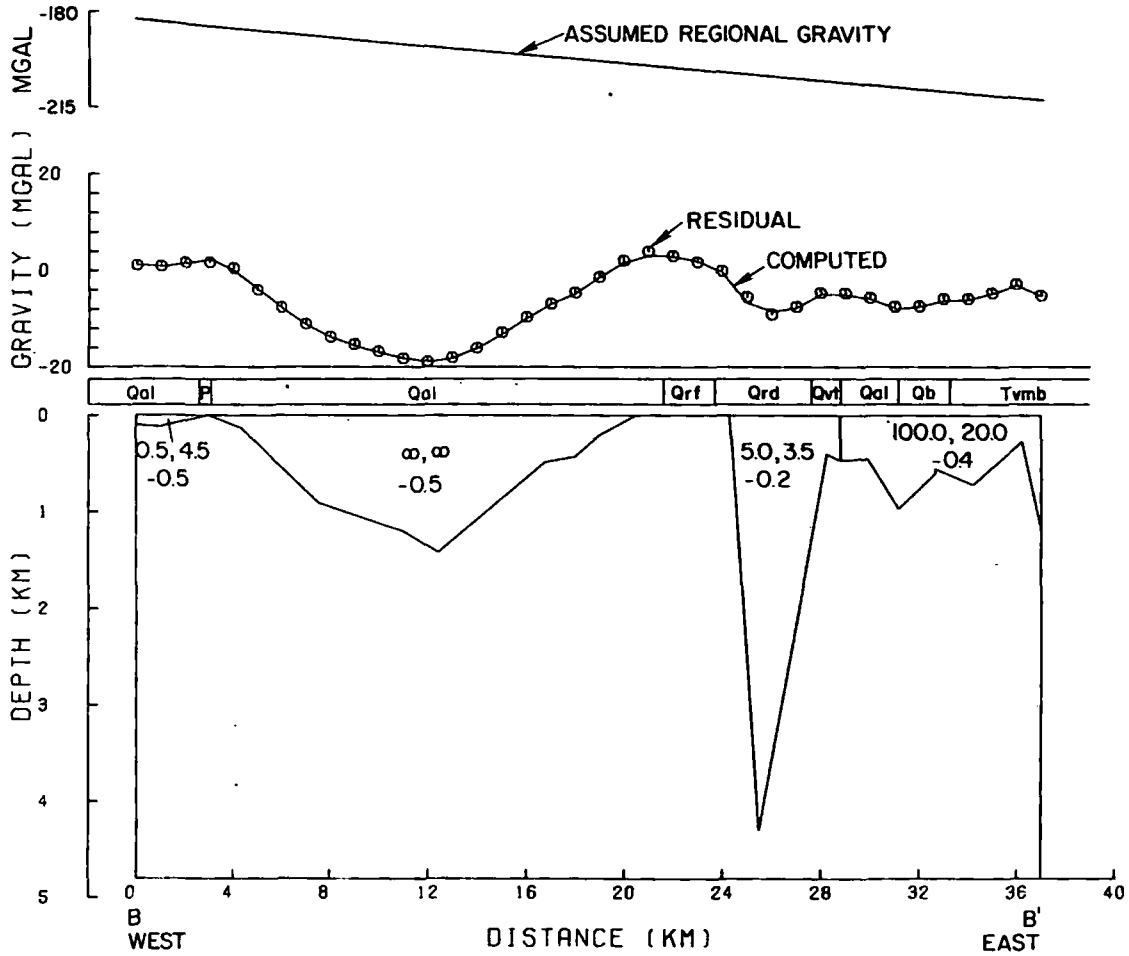

Figure 24. Interpretative geologic cross section along gravity profile B-B'. The upper numbers in each body are the strike lengths (km) of the body out of and into the paper, respectively. The lower number is the density contrast (g/cc). The mapped surface geology symbols are those used in Figure 4.

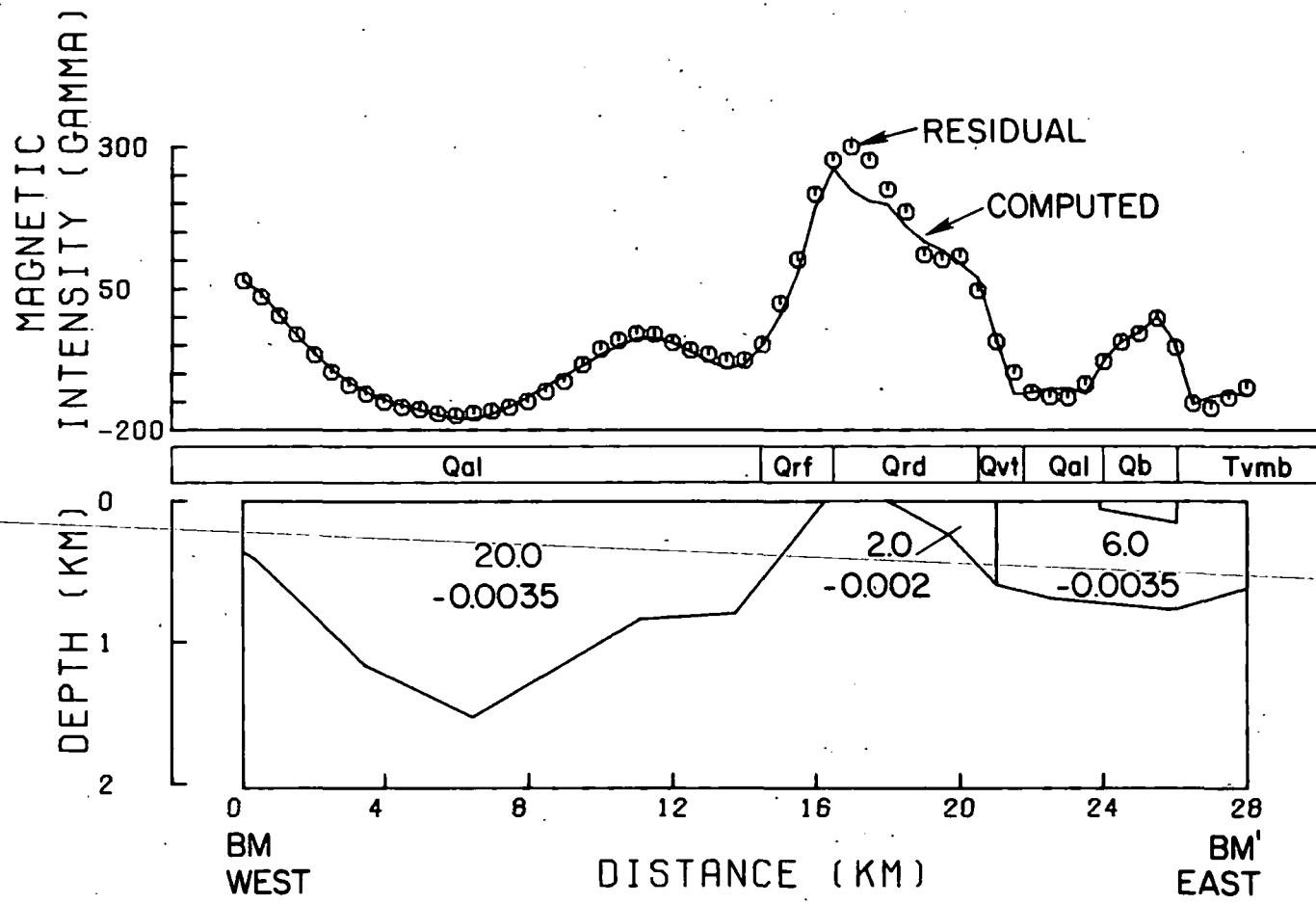

Figure 25. Interpretative geologic cross section along magnetic profile BM-BM'. The upper number in each body is the half-strike length (km) of the body. The lower number is the magnetic susceptibility contrast (cgs units). The mapped surface geology symbols are those used in Figure 4.

depth as determined by gravity profile B-B'. Near the eastern edge of the graben, however, the models diverge. The magnetic model indicates that a low-magnetic susceptibiity material overlies or comprises the eastern edge of the graben in this area. This disparity between the gravity and magnetics was noted during the map interpretation and was attributed to either a reversed magnetic polarity rhyolite flow overlying the pluton or a low-magnetic susceptibility unit of sedimentary or metamorphic rock. Part of this low magnetic intensity area underlies a mapped reversed magnetic polarity flow (Qrf) which undoubtedly accounts for part of the magnetic low. The area underlying the exposed rhyolite domes (Qrd) along profile BM-BM' has been modeled with a magnetic susceptibility contrast which is intermediate between the low magnetic susceptibility of the alluvium and the high magnetic susceptibility of the granite. The body modeled to represent the rhyolite domes is much smaller on the magnetic model than on the gravity model for profile B-B', and this is partly attributed to the averaging of grid lines which included some values over the east-west trending magnetic high south of number 3 (Fig. 10).

The interpretative geologic cross section for gravity profile C-C' is shown on Figure 26. This profile begins at the eastern margin of the Star Range and crosses Milford Valley, which is modeled as a graben with sloping sides and a maximum depth of alluvial fill of about 1.2 km. Where the profile crosses South Twin Flat Mountain (the southernmost exposed rhyolite dome), a large low-density body has been modeled as extending eastward under exposed intrusive rock to the

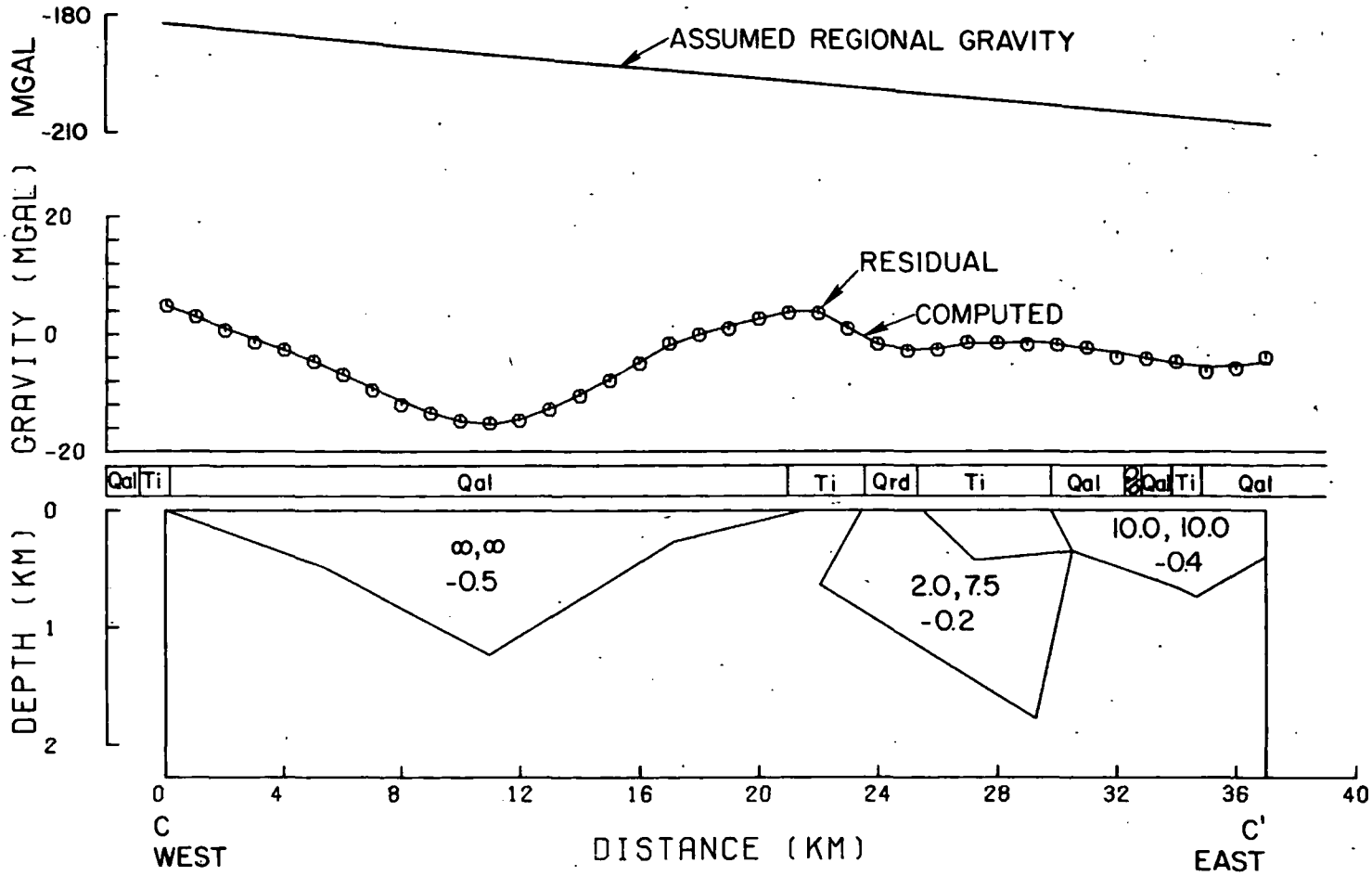

Figure 26. Interpretative geologic cross section along gravity profile C-C'. The upper numbers in each body are the strike lengths (km) of the body out of and into the paper, respectively. The lower number is the density contrast (g/cc). The mapped surface geology symbols are those used in Figure 4.

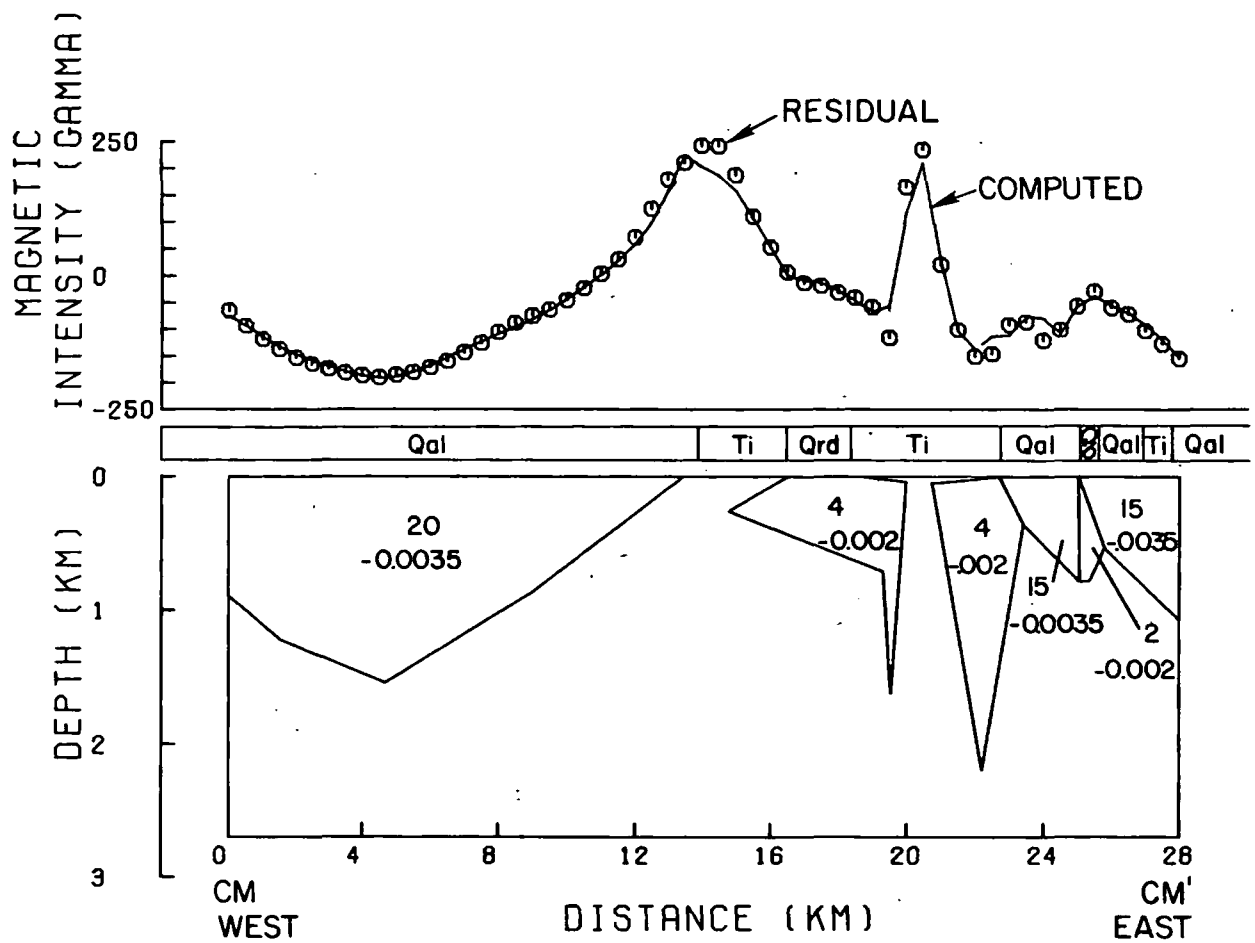

Figure 27: Interpretative geologic cross section along magnetic profile CM-CM'. The upper number in each body is the half-strike length (km) of the body. The lower number is the magnetic susceptibility contrast (cgs units). The mapped surface geology symbols are those used in Figure 4.

eastern margin of the Mineral Mountains and has a maximum depth of about 1.8 km.

The interpretative geologic cross section for magnetic profile CM-CM' is shown on Figure 27. The model for this profile indicates a maximum depth of alluvial fill in Milford Valley of about 1.5 km, which agrees rather well with the depth indicated by the model for gravity profile C-C'. Where the profile crosses South Twin Flat Mountain, a body with a magnetic susceptibility contrast between the high magnetic susceptibility of the granite and the low magnetic susceptibility of the alluvium, has been modeled. This body is broken into two bodies by high magnetic values which overlie the north south trending magnetic high south of number 3 on Figure 10, but the general shape of the two bodies compares rather well with the shape of the low density body modeled along gravity profile C-C'.

SUMMARY AND CONCLUSIONS

The gravity data were reduced and are presented as a terrain-corrected Bouguer gravity anomaly map with a contour interval of 1 mgal. To facilitate the interpretation of these gravity values, the following processing and modeling techniques were applied: 1) high-pass frequency filtering; 2) polynomial fitting; 3) pseudomagnetic filtering; 4) strike filtering; 5) upward continuation filtering; and 6) two and one-half dimensional profile modeling.

The reduced aeromagnetic data are presented as a total magnetic field intensity residual anomaly map with a contour interval of 50 gammas. To facilitate the interpretation of these magnetic values, the following processing and modeling techniques were applied: 1) low-pass frequency filtering; 2) polynomial fitting; 3) pseudogravity filtering; 4) strike filtering; and 5) two and one-half dimensional profile modeling.

Combined interpretation of the gravity and aeromagnetic data was based on comparing and contrasting the base maps, processed maps, and geologic cross sections which were produced using the techniques mentioned above. Broad structural features apparent from the interpretation of the gravity and magnetic surveys include: 1) Basin and Range normal faults which strike generally north-south and lie along the eastern and western margins of the Mineral Mountains; 2) the

grabens of Milford and Beaver Valleys which border the Mineral Mountains horst on the west and east, respectively; and 3) an east-northeastward-trending lineation which passes through the County Line fault in the northern Mineral Mountains and probably corresponds to a major structural feature along which intrusive bodies have been emplaced. The Basin and Range normal faulting which occurs along the flanks of the Mineral Mountains is expressed most clearly on the gravity maps by generally north-south trending contours with a large relief. Although the north-south strike-filtered gravity map shows that faulting is probably present along the eastern and western margins of the Mineral Mountains, the northeast-southwest strike-filtered gravity map indicates that the faulting is less extensive along the northern and central portions of the eastern margin of the Mineral Mountains than elsewhere. The Milford Valley graben, which borders the Mineral Mountains horst on the west, has been modeled with a maximum depth of alluvial fill of about 1.5 km for an assumed density contrast of 0.5 g/cc between the bedrock and alluvium. The northern and southern ends of the Mineral Mountains pluton are well-defined by east-west trending magnetic contours with large relief, which correspond well with the County Line and Cave Canyon faults, respectively. The east-west trending magnetic contours which converge and pass through the County Line fault continue westward across the alluvium of Milford Valley. Weaker east-west trends on the gravity maps (emphasized on the east-west strike-filtered gravity map) follow the same trend across Milford Valley, and both trends probably indicate the northern terminus of one

large or several smaller intrusive bodies which form the floor of Milford Valley south of this line. This line, which apparently controlled the emplacement of these intrusive bodies has been recognized as a probable major structural feature and designated the "Black Rock offset" by Crosby (1973).

Quaternary rhyolite domes (including Bearskin, Little Bearskin, North Twin Flat, and South Twin Flat Mountains) and flows (including the Bailey Ridge Flow) are exposed along the crest of the Mineral Mountains. These volcanics are thought to be related to the heat source for the geothermal reservoir at Roosevelt Hot Springs. Roughly corresponding magnetic and gravity lows overlie the exposed volcanics. These lows may be caused by a magma chamber at rather shallow depth, but are more likely caused by the lower density and magentic susceptibility of the rhyolite. A gravity saddle in the area of Ranch Canyon and a roughly corresponding magnetic saddle are also possibilities for a low-density, low-magnetic susceptibility body, but modeling has indicated that the gravity saddle may be caused by overlap of the gravity lows associated with Milford Valley graben and the silicic volcanics. Removal of a different regional gravity could, however, alter this conclusion.

Over the known geothermal reservoir (patterned area on Figs. 4, 8, 10), possible expressions of hydrothermal magnetite alteration (a magnetic low area) and sediment densification (a gravity high area) have been observed. A north-south trending magnetic high, which overlies alluvium, corresponds with the Opal Mound fault, which marks

the westward extent of the reservoir. A pronounced magnetic low, which may represent a sedimentary or metamorphic rock unit lies just south of the high thermal gradient anomaly area and corresponds with the southern boundary of the reservoir.

APPENDIX 1

LOCATION OF ROCK DENSITIES AND MAGNETIC SUSCEPTIBILITY OF ROCK SAMPLES, AS MEASURED BY AUTHOR

Table 4. Location, density, and magnetic susceptibility of rock samples, as measured by the author.

Rock Type	Latitude N. Deg.	Min.	Longitude W. Deg.	Min.	Density (gm/cc)	Magnetic Susceptibility (in units of 10^{-6} cgs)
Intrusive Rocks						
Granitic	38	34.96	112	49.53	2.59	447
Granitic	38	35.55	112	49.34	2.59	3700
Granitic	38	34.90	112	50.46	2.55	841
Granitic	38	35.03	112	49.78	2.71	1518
Granitic	38	35.55	112	49.34*	2.48	1550
Granitic	38	34.96	112	49.53	2.56	283
Granitic	38	34.90	112	50.46	2.58	414
Granitic	38	34.90	112	50.46	2.85	3750
Granitic	38	28.08	112	46.99*	2.45	1027
Granitic	38	28.08	112	46.99*	2.59	--
Granitic	38	28.08	112	46.99*	2.58	1129
Granitic	38	27.23	112	47.31*	2.60	914

Table 4 (cont.)

Rock Type	Latitude N. Deg.	Min.	Longitude W. Deg.	Min.	Density (gm/cc)	Magnetic Susceptibility (in units of 10^{-6} cgs)
Granitic	38	30.48	112	51.13	2.57	38
Granitic	38	29.00	113	4.44	2.64	2200
Granitic	38	26.17	113	3.02	2.77	4300
Granitic	38	25.20	113	5.73	2.63	1417
Granitic	38	31.04	113	6.03	2.64	260
Extrusive Rocks						
Tertiary Volcanic Rocks						
Rhyolite	38	24.06	112	53.15	2.35	868
Qtz. Latite	38	28.16	113	3.60	2.67	1403
Andesite	38	10.65	112	55.04	2.17	44
Andesite	38	12.38	112	50.62	2.52	820
Andesite	38	11.22	112	50.24	2.44	80
Andesite	38	11.51	112	52.22	2.46	578
Basalt	38	12.38	112	48.93	2.42	1067

Table 4 (cont.)

Rock Type	Latitude N. Deg.	Min.	Longitude W. Deg.	Min.	Density (gm/cc)	Magnetic Susceptibility (in units of 10^{-6} cgs)
Quaternary Volcanic Rocks						
Rhyolite	38	27.50	112	47.75	2.36	149
Rhyolite	38	27.23	112	47.31*	2.36	174
Rhyolite	38	27.23	112	47.31*	2.34	227
Rhyolite	38	27.23	112	47.31*	2.38	179
Rhyolite	38	27.23	112	47.31*	2.23	210
Rhyolite	38	27.23	112	47.31*	2.33	202
Rhyolite	38	27.23	112	47.31*	2.22	415
Rhyolite	38	27.23	112	47.31*#	1.65	3
Rhyolite	38	24.41	112	48.81*#	1.76	34
Perlite	38	29.07	112	49.10	1.99	34
Obsidian	38	27.23	112	47.31*	2.32	34
Obsidian	38	29.07	112	49.10	2.35	102
Obsidian	38	24.41	112	48.81	2.32	95

Table 4 (cont.)

Rock Type	Latitude N. Deg.	Min.	Longitude W. Deg.	Min.	Density (gm/cc)	Magnetic Susceptibility (in units of 10^{-6} cgs)
Obsidian	38	24.41	112	48.81	2.23	97
Obsidian	38	24.41	112	48.81	2.15	105
Metamorphic Rocks						
Gneiss	38	30.02	112	51.13	2.69	35
Marble	38	34.90	112	50.46	2.85	20
Quartzite	38	41.98	113	6.51	2.64	8
Quartzite	38	41.61	113	1.66	2.62	14
Quartzite	38	40.09	113	3.16	2.62	0
Quartzite	38	23.75	113	6.21	2.50	12
Quartzite	38	31.03	113	6.03	2.74	6
Sedimentary Rocks						
Limestone	38	34.90	112	50.46	2.57	0
Limestone	38	35.55	112	49.34	2.97	49
Limestone	38	35.03	112	49.78	2.70	11

Table 4 (cont.)

Rock Type	Latitude N. Deg.	Min.	Longitude W. Deg.	Min.	Density (gm/cc)	Magnetic Susceptibility (in units of 10^{-6} cgs)
Limestone	38	18.11	112	49.90	2.68	10
Limestone	38	34.90	112	50.46	2.84	0
Limestone	38	32.23	113	6.07	2.76	19
Limestone	38	33.47	113	6.07	2.70	5
Sandstone	38	22.63	112	46.20	2.76	28
Sandstone	38	18.11	112	49.90	2.47	13
Sandstone	38	34.90	112	50.46	2.62	12

*Rock samples obtained as float, not from outcrop

#Samples regarded as uncharacteristic and not used to compute averages in Table 1.

APPENDIX 2

MAP PROCESSING PROGRAMS

The programs listed in this Appendix were used by the author to implement the wavelength filtering described in "MAP PROCESSING". A flow chart showing the sequence of steps involved in the filtering process is shown in Figure 28. This discussion deals only with the "multiply by filter factor" step in this sequence. The two-dimensional fast Fourier transform, which was used, has been listed and described by Crebs and Cook (1976).

The fundamental element in this filtering system (originally written by Dr. R. T. Shuey and others at the University of Utah) is the subroutine "FILTER", which uses as input the dimensions (must be an even power of two) of the rectangular grid whose values have been fast Fourier transformed and the fast Fourier transformed grid values (real and imaginary parts). For each grid value, the frequencies in each grid direction in cycles/grid interval are calculated and another subroutine (designated "DUMMY" in the listing of subroutine filter) is called. This subroutine uses as inputs the frequencies calculated by subroutine filter and in some cases the transformed grid values. Any of the subroutines (excluding subroutine filter) listed in this appendix may be used with subroutine filter by replacing the "CALL DUMMY" statement with the statements preceding the listing of each subroutine. When the transformed grid values are required, the multiplication of the transformed grid value by the filter factor

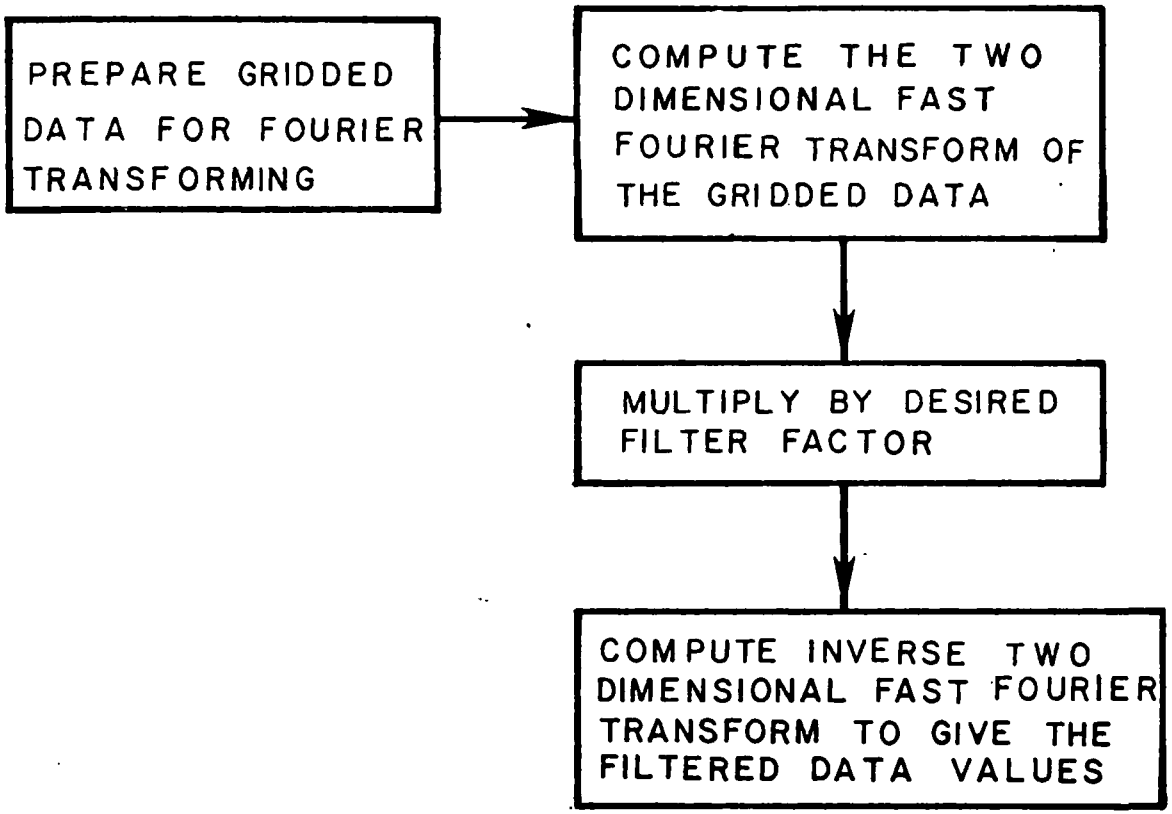

Figure 28. Flow chart showing the wavelength filtering scheme.

calculated in the particular subroutine called is carried out within the subroutine and the transformed filtered grid value is returned to subroutine filter. When the frequencies alone are required as input, the filter factor is returned and the multiplication of the transformed grid value by the filter factor is carried out in subroutine filter. The name of each subroutine which may replace "CALL DUMMY" in subroutine filter, its function, and any additional parameters which are required are specified below:

1) REDPOL--Calculates reduction to the pole of total magnetic field data--requires AI = Inclination of main magnetic field (degrees)
D = Declination of main magnetic field (degrees)
TEST $\leq$ 0.0.

2) STRTUM--Calculates vertical integral filter factor (used to calculate pseudogravity field when applied along with REDPOL)--requires GRID = km/grid interval.

3) RPPSM--Calculates first derivative (used to calculate reduced-to-the-pole pseudomagnetic field)--no additional requirements but field will be in terms of grid intervals rather than km as it is when STRTUM is used.

4) CONTIN--Calculates upward or downward continuation of a field--requires H = desired number of grid intervals of upward (H is negative) or downward (H is positive)

continuation.

5) LOWPAS--Calculates low frequency-passed filter factor--requires FC = cutoff frequency (in cycles/grid interval), DEL = Fraction of end which is tapered, KNT = 0 is inserted in subroutine filter following "DIMENSION" statement.

6) HIPASS--Calculates high frequency-passed filter factor--requires FC = cutoff frequency (in cycles/grid interval), DEL = fraction of end which is tapered, KNT = 1 is inserted in subroutine filter following "DIMENSION" statement.

7) STRIKE--Calculates strike sensitive filter factor--requires A1, A2, W, which are adequately explained in comment cards within the subroutine.

More than one of these subroutines may be placed in the appropriate location in subroutine filter at the same time. For example, if one desires to produce a pseudomagnetic upward continued field, one can perform both operations in succession by calling RPPMS and then CONTIN with the appropriate arguments. Another possibility might be a band-pass-filter operation by calling HIPASS and then LOWPAS.

Listings of the subroutines referred to above follow:

```
      CALL FILTER(2**N,2**M,RGRID,IGRID)

@FOR,ISX FILTER
      SUBROUTINE FILTER(N1,N2,TVR,TVI)
      DIMENSION TVR(1),TVI(1)
C *** VECTOR LENGTH = N1 *N2
C *** NYQUIST FREQUENCY = 0.5
      DO 50 I=1,N2
      F2=FLOAT(I-1)/FLOAT(N2)
      IF (F2.GT.0.5) F2=F2-1
      DO 50 J=1, N1
      F1=FLOAT(J-1)/FLOAT(N1)
      IF (F1.GT.0.5) F1=F1-1
      K=(I-1)*N1+J
      CALL DUMMY(F1,F2,OTHER NECESSARY ARGUMENTS)
   50 CONTINUE
      RETURN
      END
```

```
      DR=TVR(K)
      DI=TVI(K)
      CALL REDPOL(F2,F1,DR,DI)
      TVR(K)=DR
      TVI(K)=DI


@FOR,IS REDPOL
      SUBROUTINE REDPOL(FE,FN,TR,TI)
C* FE=EAST FREQUENCY, FN=NORTH FREQUENCY.
C* DIRECT TRANSFORM WAS DONE WITH MINUS SIGN IN EXPONENT.
      COMPLEX Z,ZD,T
      COMMON/RPFILT/AI,D,TEST
      IF(TEST.GT.0.0) GO TO 1
      PI=3.14159265
      DEGRAD=PI/180.0
      SINI=SIN(AI*DEGRAD)
      COSI=COS(AI*DEGRAD)
      SIND=SIN( D*DEGRAD)
      COSD=COS( D*DEGRAD)
      TEST=1.0
    1 CONTINUE
      F=SQRT(FE**2+FN**2)
      IF(F.LT.1.0E-05) GO TO 2
      DI=COSI*(COSD*FN/F+SIND*FE/F)
      ZD=CMPLX(SINI,DI)
      Z=1.0/(ZD)**2
      T=CMPLX(TR,TI)
      T=T*Z
      TR=REAL(T)
      TI=AIMAG(T)
    2 RETURN
      END
```

```
                CALL STRTUM(F1,F2,RR,RI)
                TVR(K)=TVR(K)*RR
                TVI(K)=TVI(K)*RR


@FOR,ISX STRTUM
      SUBROUTINE STRTUM(F1,F2,RR,RI)
      DATA GRID/.5/
      PI =3.14159265
      RI=0.0
      F=SQRT(F1**2+F2**2)
      IF(F.LT.1E-5) GO TO 1
      RR = GRID/(2.0*PI*F)
      RETURN
    1 RR=0.0
      RETURN
      END
```

```
      DR=TVR(K)
      DI=TVI(K)
      CALL RPPSM(F1,F2,DR,DI)
      TVR(K)=DR
      TVI(K)=DI


@FOR,IS   RPPSM,RPPSM
        SUBROUTINE RPPSM(FE,FN,TR,TI)
C     THE RESULTS OF THIS SUBROUTINE MUST BE MULTIPLIED
C     BY MAGNETIZATION/GRAVITATIONAL CONSTANT*DENSITY)
C     TO GIVE UNITS OF MAGNETIC MAP
        DATA PI/3.141592654/
        FAC=2.*PI*SQRT(FE**2+FN**2)
        TR=TR*FAC
        TI=TI*FAC
        RETURN
        END
```

```
      H=-0.31
      DR=TVR(K)
      DI=TVI(K)
      CALL CONTIN(H,F1,F2,DR,DI)
      TVR(K)=DR
      TVI(K)=DI


@FOR,IS   CONTIN,CONTIN
      SUBROUTINE CONTIN(H,FE,FN,TR,TI)
C     H IS NEGATIVE TO UPWARD CONTINUE, POSITIVE TO
C     DOWNWARD CONTINUE
C     FE=EAST FREQUENCY, FN=NORTH FREQUENCY
C     FORWARD TRANSFORM DONE WITH MINUS SIGN IN EXPONENT
C     H IS IN UNITS OF GRID INTERVAL
      DATA PI/3.141592654/
      FAC=EXP(2.*PI*SQRT(FE**2+FN**2)*H)
      TR=FAC*TR
      TI=FAC*TI
      RETURN
      END
```

```
      CALL LOWPAS(F1,F2,RS,KNT)
      KNT=1
      TVR(K)=TVR(K)*RS
      TVI(K)=TVI(K)*RS


@FOR,IS LOWPAS,LOWPAS
      SUBROUTINE LOWPAS(F1,F2,RR,KNT)
C *** DOES A LOWPASS FILTER WITH COSINE TAPER
C *** FC = CUTOFF FREQUENCY, DEL = FRACTION OF ND
C *** WHICH IS TAPERED
C *** NYQUIST FREQUENCY = 0.5.
      DATA PI/3.141592654/
      DATA FC,DEL/.07,.125/
      F=SQRT(F1**2+F2**2)
      IF (KNT.GT.0) GO TO 70
      TST=(1.-DEL)*FC
      DIF=FC-TST
   70 CONTINUE
      IF (F.GT.TST) GO TO 40
      WF=1.
      GO TO 60
   40 DF=F-TST
      WF= .5*(1.-COS(PI*(DIF-DF)/DIF))
      IF (DF.GT.DIF) WF=0.
   60 CONTINUE
      RR=WF
      RETURN
      END
```

```
      KNT=1


      CALL HIPASS(F1,F2,RR,KNT)
      KNT=0
      TVR(K)=TVR(K)*RR
      TVI(K)=TVI(K)*RR


@FOR,IS   HIPASS,HIPASS
      SUBROUTINE HIPASS(F1,F2,RR,KNT)
      DATA FC,DEL/.056,.125/
      DATA PI/3.141592654/
      F=SQRT(F1**2+F2**2)
      IF(KNT.GT.0) GO TO 70
      TST=(1.-DEL)*FC+.5*DEL
      DIF=TST-FC
   70 CONTINUE
      IF(F.LT.TST) GO TO 40
      WF=1.
      GO TO 60
   40 DF=TST-F
      WF=.5*(1.-COS(PI*(DIF-DF)/DIF))
      IF(DF.GT.DIF) WF=0.
   60 CONTINUE
      RR=WF
      RETURN
      END
```

```
                CALL STRIKE(F2,F1,RR)
                TVI(K)=TVI(K)*RR
                TVR(K)=TVR(K)*RR


@FOR,IS STRIKE, STRIKE
      SUBROUTINE STRIKE (F1,F2,RR)
      DATA A1,A2,W/045.,135.,030./
C *** PERFORMS A STRIKE FILTER OPERATION IN FREQUENCY
C *** DOMAIN
C *** AZIMUTH IS MEASURED FROM 1-AXIS TOWARDS 2-AXIS
C *** WITH EDGES TAPERED BY W AMOUNT
C *** A1, A2, W ARE MEASURED IN DEGREES
C *** NOTE THE INVERSION SYMETRY
C *** REMEMBER CONTOUR LINES ARE PERPENDICULAR TO
C *** FREQUENCY VECTORS
      PI=3.14159265
      RR=0.
      F=SQRT(F1*F1+F2*F2)
      IF (F.LT.1.0E-5) GO TO 2
      WR=W/180.
      F=ATAN2(F2,F1)/PI
      IF (F.LT.0.) F=F+1.
C *** F IS NOW IN CLOSED INTERVAL (0,1)
      A1R=A1/180.-AINT(A1/180.)
      A2R=A2/180.-AINT(A2/180.)
      IF (A2R.LT.A1R) GO TO 1
C *** CASE IF PASS BAND IS IN MIDDLE
      IF (F.GT.A1R) RR=.5*(1.-COS(((F-A1R)*PI)/WR))
      IF (F.GT.(A1R+WR)) RR=1.
      IF (F.GT.(A2R-WR)) RR=.5*(1.-COS(((A2R-F)*
     1PI)/WR))
      IF (F.GT.A2R) RR=0.
      GO TO 2
C *** CASE IF PASS BAND IS AT THE SIDES
    1 RR=1.
      IF (F.GT.(A2R-WR)) RR=0.5*(1.-COS(((A2R-F)*
     1PI)/WR))
      IF (F.GT.A2R) RR=0.
      IF (F.GT.A1R) RR=0.5*(1.-COS(((F-A1R)*PI)/WR))
      IF (F.GT.(A1R+WR)) RR=1.
    2 RETURN
      END
```

APPENDIX 3

TABLE OF DATA FOR GRAVITY

Notes: 1) Units are as follows:

	Units
Latitude	degrees, minutes
Longitude	degrees, minutes
Elevation	feet
Free-air anomaly values	mgal
Simple Bouguer anomaly value [1/]	mgal
Terrain-correction value [1/]	mgal
Terrain-corrected Bouguer anomaly value	mgal

2) Coding is as follows:

WB003 - number designation of gravity station taken by Brumbaugh (1977)

TC001 - number designation of gravity station taken by Crebs (1976).

JC001 - number designation of gravity station taken by the author

7601 - number designation of gravity station taken by the author

RS77 - number designation of gravity station taken by Sawyer (1977) (first page of RS stations)

RS163 - number designation of gravity station taken by Sontag (1965) (second page of RS stations)

IT001 - number designation of gravity station taken by Thangsuphanich (1976)

74103 - number designation of gravity station taken by the Univ. of Utah, GGS521 Class of 1974

[1/] A density contrast of 2.67 g/cc was assumed for both the Bouguer and terrain corrections.

STATION NUMBER	LATITUDE DEG	LATITUDE MIN	LONGITUDE DEG	LONGITUDE MIN	ELEVATION IN FEET	FREE-AIR ANOMALY	SIMPLE BOUGUER	TERRAIN CORRECTION	TERR-CORR BOUGUER
WB003	38.	37.33	112.	38.20	5875.	.90	-199.20	.47	-198.73
WB004	38.	37.01	112.	37.77	5885.	-.59	-201.03	.64	-200.39
WB011	38.	36.79	112.	38.72	5865.	1.89	-197.87	.51	-197.36
WB012	38.	35.97	112.	39.26	5981.	.89	-202.82	.49	-202.33
WB013	38.	35.59	112.	40.02	6047.	1.96	-204.00	1.10	-202.90
WB014	38.	34.03	112.	40.51	6172.	-1.07	-211.29	.71	-210.58
WB015	38.	32.64	112.	39.76	6417.	-3.16	-221.72	2.52	-219.20
WB016	38.	31.68	112.	39.40	6091.	-12.43	-219.89	.91	-218.98
WB017	38.	31.80	112.	38.40	6105.	-16.58	-224.51	1.23	-223.28
WB032	38.	37.63	112.	38.31	5905.	2.96	-198.16	.42	-197.74
WB033	38.	38.16	112.	38.37	5912.	3.57	-197.80	.40	-197.40
WB034	38.	38.53	112.	38.45	5912.	4.60	-196.76	.39	-196.37
WB035	38.	38.79	112.	38.48	5895.	4.30	-196.48	.42	-196.06
WB036	38.	39.12	112.	38.46	5929.	7.81	-194.14	.46	-193.68
WB037	38.	39.38	112.	38.48	5945.	9.34	-193.14	.76	-192.38
WB038	38.	39.67	112.	38.66	5966.	11.01	-192.20	.39	-191.81
WB039	38.	39.78	112.	38.82	5992.	11.43	-192.66	.52	-192.14
WB040	38.	40.09	112.	39.22	6089.	14.04	-193.36	.50	-192.86
WB041	38.	40.26	112.	39.42	6043.	11.16	-194.66	.45	-194.21
WB042	38.	40.50	112.	39.66	6023.	10.16	-194.98	.43	-194.55
WB043	38.	40.74	112.	39.82	5993.	8.08	-196.04	.63	-195.41
WB044	38.	41.48	112.	40.00	5838.	1.46	-197.38	.44	-196.94
WB045	38.	42.05	112.	39.22	5760.	.67	-195.52	.87	-194.65
WB046	38.	41.53	112.	40.93	5674.	-7.83	-201.09	.42	-200.67
WB047	38.	41.46	112.	41.52	5700.	-6.97	-201.11	.36	-200.75
WB048	38.	41.72	112.	42.26	5781.	-4.46	-201.36	.44	-200.92
WB049	38.	42.45	112.	42.62	5806.	5.95	-191.80	.52	-191.28
WB050	38.	42.60	112.	42.54	5621.	-10.06	-201.51	.38	-201.13
WB051	38.	42.81	112.	42.12	5590.	-10.39	-200.79	.39	-200.40
WB052	38.	42.85	112.	41.89	5533.	-11.53	-199.98	.40	-199.58

STATION NUMBER	LATITUDE DEG	LATITUDE MIN	LONGITUDE DEG	LONGITUDE MIN	ELEVATION IN FEET	FREE-AIR ANOMALY	SIMPLE BOUGUER	TERRAIN CORRECTION	TERR-CORR BOUGUER
WB053	38.	42.91	112.	41.53	5493.	-13.46	-200.55	.54	-200.01
WB054	38.	42.75	112.	41.08	5406.	-14.77	-198.90	.80	-198.10
WB055	38.	42.80	112.	41.32	5357.	-22.28	-204.74	.82	-203.92
WB067	38.	41.13	112.	39.75	5914.	5.67	-195.76	.77	-194.99
WB068	38.	42.12	112.	42.32	5734.	-5.80	-201.10	.37	-200.73
WB075	38.	31.62	112.	38.22	6110.	-17.79	-225.89	1.39	-224.50
WB076	38.	31.28	112.	39.24	6223.	-9.31	-221.26	1.16	-220.10
WB077	38.	30.29	112.	39.79	6607.	-2.86	-227.89	2.20	-225.69
WB078	38.	30.88	112.	40.10	6454.	-.69	-220.52	2.46	-218.06
WB079	38.	31.03	112.	40.44	6144.	-7.32	-216.59	.98	-215.61
WB080	38.	31.41	112.	40.59	6096.	-7.76	-215.39	.83	-214.56
WB081	38.	31.72	112.	41.50	6026.	-7.32	-212.57	.91	-211.66
WB082	38.	31.15	112.	41.40	6132.	-2.33	-211.19	.91	-210.28
WB083	38.	30.75	112.	41.51	6242.	3.39	-209.21	.94	-208.27
WB084	38.	31.18	112.	43.81	6209.	-1.30	-212.78	1.11	-211.67
WB085	38.	31.49	112.	44.37	5996.	-5.47	-209.69	1.29	-208.40
WB086	38.	32.31	112.	43.56	5830.	-10.26	-208.83	.94	-207.89
WB087	38.	32.26	112.	42.74	5851.	-9.43	-208.71	.91	-207.80
WB091	38.	41.18	112.	41.52	5701.	-6.36	-200.53	.38	-200.15
WB092	38.	40.89	112.	41.52	5705.	-5.56	-199.87	.45	-199.42
WB093	38.	40.30	112.	41.52	5724.	-3.64	-198.60	.52	-198.08
WB094	38.	40.46	112.	41.52	5718.	-4.47	-199.22	.54	-198.68
WB095	38.	39.36	112.	41.82	5774.	-.87	-197.53	.31	-197.22
WB096	38.	40.47	112.	42.62	6026.	4.13	-201.11	.46	-200.65
WB097	38.	38.10	112.	42.20	5698.	-3.71	-197.78	.33	-197.45
WB098	38.	37.70	112.	41.54	5783.	-2.31	-199.28	.31	-198.97
WB099	38.	37.57	112.	41.27	5749.	-2.51	-198.32	.42	-197.90
WB100	38.	37.70	112.	39.26	5855.	1.32	-198.10	.39	-197.71
WB101	38.	36.63	112.	39.54	5862.	.63	-199.03	.44	-198.59
WB102	38.	36.01	112.	39.81	5915.	.03	-201.44	.63	-200.81

STATION NUMBER	LATITUDE DEG	LATITUDE MIN	LONGITUDE DEG	LONGITUDE MIN	ELEVATION IN FEET	FREE-AIR ANOMALY	SIMPLE BOUGUER	TERRAIN CORRECTION	TERR-CORR BOUGUER
WB103	38.	36.24	112.	40.12	5875.	-.46	-200.56	.62	-199.94
WB104	38.	36.96	112.	38.38	5889.	1.20	-199.38	.46	-198.92
WB105	38.	35.96	112.	40.38	5893.	-.95	-201.67	.50	-201.17
WB106	38.	35.98	112.	40.68	5847.	-2.19	-201.34	.50	-200.84
WB107	38.	35.74	112.	41.19	5824.	-3.90	-202.26	.46	-201.80
WB108	38.	35.31	112.	41.40	5804.	-6.69	-204.37	.57	-203.80
WB109	38.	35.20	112.	41.50	5804.	-6.53	-204.21	.62	-203.59
WB110	38.	35.04	112.	42.12	5800.	-6.08	-203.62	.56	-203.06
WB111	38.	34.79	112.	42.22	5809.	-5.86	-203.71	.52	-203.19
WB112	38.	34.33	112.	41.70	5807.	-9.10	-206.88	.57	-206.31
WB113	38.	34.23	112.	41.50	5888.	-7.75	-208.29	.69	-207.60
WB114	38.	33.68	112.	42.05	5826.	-10.58	-209.02	.62	-208.40
WB115	38.	33.82	112.	41.98	5826.	-10.05	-208.49	.56	-207.93
WB116	38.	32.10	112.	41.58	5958.	-9.21	-212.14	.84	-211.30
WB117	38.	32.51	112.	41.38	5990.	-8.68	-212.70	.76	-211.94
WB118	38.	32.85	112.	41.30	5985.	-8.95	-212.80	.67	-212.13
WB119	38.	33.19	112.	41.09	5979.	-8.26	-211.90	.69	-211.21
WB120	38.	33.25	112.	41.36	5940.	-11.64	-213.96	.72	-213.24
WB121	38.	33.45	112.	42.07	5836.	-10.65	-209.43	.63	-208.80
WB122	38.	34.65	112.	43.07	5681.	-13.98	-207.48	.64	-206.84
WB123	38.	35.32	112.	43.60	5588.	-11.08	-201.41	.63	-200.78
WB124	38.	37.11	112.	43.25	5621.	-6.14	-197.59	.31	-197.28
WB125	38.	37.18	112.	42.67	5628.	-6.67	-198.36	.36	-198.00
WB126	38.	37.41	112.	41.80	5742.	-3.31	-198.89	.36	-198.53
WB230	38.	34.35	112.	38.30	6498.	6.46	-214.86	1.61	-213.25
WB231	38.	32.58	112.	43.47	5796.	-11.29	-208.70	.87	-207.83
WB232	38.	32.73	112.	44.18	5744.	-12.33	-207.97	.95	-207.02
WB233	38.	33.49	112.	44.82	5668.	-13.72	-206.77	.93	-205.84
WB234	38.	31.93	112.	43.94	5829.	-13.00	-211.53	1.50	-210.03
WB235	38.	35.66	112.	43.85	5580.	-10.68	-200.74	.55	-200.19

STATION NUMBER	LATITUDE DEG	MIN	LONGITUDE DEG	MIN	ELEVATION IN FEET	FREE-AIR ANOMALY	SIMPLE BOUGUER	TERRAIN CORRECTION	TERR-CORR BOUGUER
WB236	38.	36.07	112.	43.92	5605.	-9.09	-200.00	.38	-199.62
WB237	38.	36.67	112.	43.86	5638.	-5.78	-197.81	.30	-197.51
WB238	38.	36.28	112.	44.78	5554.	-7.35	-196.52	.39	-196.13
WB239	38.	37.00	112.	44.92	5555.	-4.30	-193.50	.29	-193.21
WB240	38.	37.30	112.	44.93	5563.	-3.15	-192.63	.29	-192.34
WB241	38.	37.66	112.	44.95	5573.	-2.26	-192.07	.27	-191.80
WB242	38.	37.42	112.	44.32	5589.	-3.53	-193.89	.52	-193.37
WB243	38.	37.71	112.	40.38	5858.	1.31	-198.22	.65	-197.57
WB251	38.	42.57	112.	37.60	5750.	1.72	-194.12	1.63	-192.49
WB252	38.	41.63	112.	37.82	6000.	6.34	-198.02	.77	-197.25
WB253	38.	40.80	112.	37.74	6064.	14.03	-192.51	.60	-191.91
WB257	38.	40.36	112.	38.24	6049.	14.03	-192.00	.67	-191.33
WB258	38.	40.14	112.	38.51	6012.	11.98	-192.79	.40	-192.39
WB260	38.	42.00	112.	41.42	5596.	-9.83	-200.43	1.56	-198.87
WB261	38.	40.39	112.	40.84	6217.	22.79	-188.96	.91	-188.05
WB262	38.	39.91	112.	40.30	5952.	8.63	-194.09	.37	-193.72
WB264	38.	38.74	112.	41.94	5740.	-2.24	-197.74	.30	-197.44
WB265	38.	38.28	112.	42.66	5696.	-2.78	-196.79	.30	-196.49
WB266	38.	38.15	112.	39.93	5893.	3.97	-196.75	.38	-196.37
WB267	38.	38.58	112.	39.26	5942.	7.03	-195.36	.42	-194.94
WB268	38.	33.31	112.	39.52	6290.	-2.00	-216.24	.61	-215.63
WB269	38.	33.62	112.	39.80	6253.	-2.09	-215.06	.62	-214.44
WB270	38.	34.35	112.	40.22	6100.	-2.27	-210.03	.63	-209.40
WB271	38.	34.47	112.	40.04	6115.	-2.28	-210.56	.69	-209.87
WB272	38.	34.75	112.	39.82	6101.	-1.66	-209.46	.64	-208.82
WB273	38.	34.97	112.	40.13	5921.	-11.10	-212.77	.64	-212.13
WB274	38.	35.26	112.	40.06	5973.	-1.62	-205.06	.60	-204.46
WB275	38.	35.75	112.	39.80	5951.	.40	-202.29	.70	-201.59
WB276	38.	41.88	112.	39.54	5809.	1.08	-196.77	.58	-196.19
WB277	38.	37.98	112.	39.12	5848.	1.97	-197.21	.42	-196.79

STATION NUMBER	LATITUDE DEG	MIN	LONGITUDE DEG	MIN	ELEVATION IN FEET	FREE-AIR ANOMALY	SIMPLE BOUGUER	TERRAIN CORRECTION	TERR-CORR BOUGUER
WB278	38.	41.18	112.	40.67	5750.	-3.16	-199.00	.74	-198.26
WB279	38.	42.86	112.	38.92	5517.	-5.35	-193.26	.64	-192.62
WB280	38.	42.60	112.	39.22	5600.	-2.97	-193.70	.77	-192.93
WB292	38.	42.44	112.	43.42	5720.	-4.51	-199.33	.52	-198.81
WB293	38.	42.78	112.	43.93	5771.	-6.13	-202.69	.51	-202.18
WB295	38.	42.48	112.	44.51	5857.	-.30	-199.79	.58	-199.21
WB296	38.	41.97	112.	44.42	5950.	3.81	-198.84	.63	-198.21
WB297	38.	41.49	112.	43.75	5949.	2.36	-200.26	.53	-199.73
WB298	38.	41.63	112.	43.15	5914.	-.34	-201.77	.48	-201.29
WB299	38.	42.18	112.	42.80	5714.	-7.21	-201.83	.40	-201.43
WB300	38.	40.88	112.	42.38	5930.	-1.90	-203.87	.44	-203.43
WB301	38.	39.43	112.	42.18	5840.	2.13	-196.78	.38	-196.40
WB302	38.	39.71	112.	42.55	5867.	1.23	-198.60	.45	-198.15
WB303	38.	39.96	112.	43.05	5966.	3.58	-199.63	.39	-199.24
WB304	38.	39.88	112.	43.54	5960.	4.55	-198.45	.40	-198.05
WB305	38.	39.26	112.	43.62	5833.	-.28	-198.95	.67	-198.28
WB306	38.	38.86	112.	43.77	5773.	-.64	-197.27	.50	-196.77
WB307	38.	38.60	112.	43.92	5756.	.25	-195.80	.41	-195.39
WB308	38.	38.30	112.	43.94	5723.	.06	-194.86	.44	-194.42
WB309	38.	37.97	112.	43.90	5677.	-.77	-194.13	.40	-193.73
WB310	38.	37.60	112.	43.95	5615.	-2.85	-194.10	.52	-193.58
WB311	38.	39.50	112.	44.11	5926.	2.40	-199.44	.44	-199.00
WB312	38.	38.41	112.	43.47	5717.	-1.86	-196.58	.31	-196.27
WB313	38.	38.39	112.	43.10	5694.	-3.02	-196.95	.30	-196.65
WB314	38.	39.00	112.	43.08	5783.	-1.81	-198.78	.48	-198.30
WB315	38.	38.00	112.	43.19	5660.	-3.37	-196.15	.34	-195.81
WB316	38.	38.67	112.	44.58	5705.	-.97	-195.28	.31	-194.97
WB317	38.	39.10	112.	44.89	5715.	-1.30	-195.95	.38	-195.57
WB318	38.	38.33	112.	44.96	5617.	-1.61	-192.93	.32	-192.61
WB325	38.	23.10	112.	42.86	6313.	-2.91	-217.93	.82	-217.11

STATION NUMBER	LATITUDE DEG	MIN	LONGITUDE DEG	MIN	ELEVATION IN FEET	FREE-AIR ANOMALY	SIMPLE BOUGUER	TERRAIN CORRECTION	TERR-CORR BOUGUER
WB326	38.	24.10	112.	43.42	6322.	-1.64	-216.97	.97	-216.00
WB327	38.	24.88	112.	43.96	6444.	4.30	-215.18	1.28	-213.90
WB328	38.	25.16	112.	44.08	6518.	7.53	-214.47	1.19	-213.28
WB332	38.	28.82	112.	42.92	7024.	25.54	-213.69	.94	-212.75
WB333	38.	28.32	112.	41.88	7148.	28.80	-214.66	.92	-213.74
WB334	38.	28.60	112.	41.66	7235.	30.86	-215.56	1.08	-214.48
WB335	38.	23.13	112.	43.88	6084.	-6.82	-214.05	1.21	-212.84
WB336	38.	22.50	112.	41.98	6159.	-10.64	-220.41	4.09	-216.32
WB337	38.	24.58	112.	42.62	6680.	9.44	-218.08	1.27	-216.81
WB338	38.	25.14	112.	42.80	6805.	15.69	-216.09	2.30	-213.79
WB339	38.	26.32	112.	43.07	7010.	21.52	-217.24	2.46	-214.78
WB340	38.	25.86	112.	43.00	6951.	19.96	-216.79	2.29	-214.50
WB341	38.	23.26	112.	42.17	6383.	-.63	-218.04	.92	-217.12
WB342	38.	25.09	112.	42.05	7170.	25.24	-218.97	2.52	-216.45
WB343	38.	23.98	112.	42.17	6711.	9.10	-219.47	1.71	-217.76
WB344	38.	25.82	112.	42.29	7344.	31.60	-218.53	2.72	-215.81
WB345	38.	25.65	112.	41.48	7153.	22.30	-221.34	2.25	-219.09
WB346	38.	23.82	112.	44.56	6320.	5.97	-209.28	1.89	-207.39
WB347	38.	25.42	112.	44.76	*****	11.88	-213.83	1.41	-212.42
WB348	38.	25.79	112.	44.38	6649.	11.73	-214.74	1.35	-213.39
WB349	38.	29.10	112.	43.92	7099.	27.94	-213.86	1.34	-212.52
WB350	38.	24.54	112.	41.75	7061.	18.38	-222.11	2.72	-219.39
WB351	38.	26.34	112.	42.15	7240.	27.98	-218.62	1.68	-216.94
WB352	38.	27.09	112.	42.44	7320.	31.80	-217.52	1.72	-215.80
WB353	38.	29.81	112.	42.13	7384.	30.60	-220.90	3.44	-217.46
WB354	38.	27.23	112.	41.70	7292.	28.77	-219.60	1.42	-218.18
WB355	38.	29.62	112.	41.65	6784.	17.11	-213.95	1.76	-212.19
WB356	38.	29.36	112.	42.20	7304.	31.40	-217.38	5.23	-212.15
WB357	38.	29.34	112.	43.01	7074.	27.47	-213.47	1.80	-211.67
WB358	38.	27.64	112.	41.18	6956.	22.31	-214.61	.97	-213.64

STATION NUMBER	LATITUDE DEG	LATITUDE MIN	LONGITUDE DEG	LONGITUDE MIN	ELEVATION IN FEET	FREE-AIR ANOMALY	SIMPLE BOUGUER	TERRAIN CORRECTION	TERR-CORR BOUGUER
WB359	38.	28.27	112.	40.12	7418.	29.93	-222.72	2.11	-220.61
WB360	38.	28.96	112.	39.35	7478.	23.00	-231.70	4.43	-227.27
WB361	38.	28.07	112.	39.62	7396.	26.13	-225.78	1.87	-223.91
WB363	38.	23.05	112.	40.35	6077.	-14.40	-221.38	.88	-220.50
WB364	38.	23.83	112.	40.00	6136.	-12.04	-221.04	1.01	-220.03
WB365	38.	24.46	112.	40.12	6258.	-5.90	-219.04	.97	-218.07
WB366	38.	24.86	112.	40.14	6358.	-2.69	-219.24	1.08	-218.16
WB367	38.	25.50	112.	39.35	6235.	-10.69	-223.06	1.14	-221.92
WB368	38.	25.91	112.	40.14	6412.	.89	-217.50	1.52	-215.98
WB369	38.	26.60	112.	40.44	6808.	14.29	-217.59	1.51	-216.08
WB370	38.	26.43	112.	41.21	7238.	28.49	-210.03	3.64	-206.39
WB371	38.	27.48	112.	39.50	7888.	30.59	-238.08	9.95	-228.13
WB372	38.	27.04	112.	39.52	7394.	22.96	-228.88	4.79	-224.09
WB373	38.	28.88	112.	41.18	7665.	38.43	-222.64	8.64	-214.00
WB374	38.	27.04	112.	40.84	7003.	22.28	-216.24	1.60	-214.64
WB489	38.	30.40	112.	46.00	6855.	28.35	-205.13	2.10	-203.03
WB491	38.	31.12	112.	45.31	6242.	6.51	-206.10	1.80	-204.30
WB493	38.	31.86	112.	45.47	6153.	5.93	-203.64	1.54	-202.10
WB494	38.	32.24	112.	45.52	6028.	.13	-205.19	1.52	-203.67
WB496	38.	33.28	112.	46.12	5865.	.86	-198.90	1.41	-197.49
WB498	38.	32.60	112.	45.31	5873.	-5.97	-206.00	1.26	-204.74
WB499	38.	34.10	112.	46.69	5738.	2.18	-193.26	1.37	-191.89
WB501	38.	34.69	112.	46.78	5630.	-.80	-192.56	1.11	-191.45
WB502	38.	34.71	112.	46.40	5605.	-3.61	-194.51	.89	-193.62
WB503	38.	35.12	112.	45.92	5610.	-6.61	-197.69	.59	-197.10
WB504	38.	35.18	112.	45.18	5773.	-2.58	-199.21	.74	-198.47
WB505	38.	34.25	112.	45.20	5675.	-8.48	-201.77	.73	-201.04
WB506	38.	34.35	112.	46.15	5627.	-4.35	-196.01	.91	-195.10
WB507	38.	33.10	112.	47.46	6825.	36.97	-195.49	.68	-194.81
WB508	38.	33.61	112.	46.90	5995.	13.16	-191.03	2.76	-188.27

STATION NUMBER	LATITUDE DEG	MIN	LONGITUDE DEG	MIN	ELEVATION IN FEET	FREE-AIR ANOMALY	SIMPLE BOUGUER	TERRAIN CORRECTION	TERR-CORR BOUGUER
WB509	38.	34.08	112.	48.04	6610.	34.91	-190.23	6.34	-183.89
WB510	38.	34.46	112.	47.60	5912.	14.75	-186.61	2.09	-184.52
WB511	38.	35.74	112.	45.25	5569.	-8.02	-197.70	.49	-197.21
WB512	38.	35.52	112.	45.48	5590.	-7.41	-197.80	.49	-197.31
WB513	38.	37.78	112.	45.20	5555.	-1.89	-191.09	.32	-190.77
WB514	38.	38.00	112.	45.78	5515.	-2.53	-190.37	.37	-190.00
WB515	38.	38.18	112.	46.35	5486.	-3.99	-190.84	.32	-190.52
WB516	38.	38.50	112.	47.41	5409.	-6.20	-190.43	.35	-190.08
WB517	38.	38.30	112.	46.80	5458.	-5.22	-191.12	.32	-190.80
WB518	38.	38.64	112.	47.92	5398.	-5.73	-189.59	.29	-189.30
WB519	38.	38.68	112.	48.31	5382.	-5.25	-188.56	.32	-188.24
WB520	38.	38.24	112.	48.30	5390.	-3.09	-186.68	.47	-186.21
WB521	38.	37.80	112.	48.30	5409.	.58	-183.66	.70	-182.96
WB522	38.	37.06	112.	48.08	5447.	3.41	-182.12	1.00	-181.12
WB523	38.	36.49	112.	47.82	5468.	1.37	-184.87	1.05	-183.82
WB524	38.	35.81	112.	47.40	5511.	-.95	-188.65	1.05	-187.60
WB525	38.	35.20	112.	47.15	5585.	.18	-190.04	1.08	-188.96
WB526	38.	35.19	112.	48.31	6125.	20.71	-187.91	5.06	-182.85
WB527	38.	38.65	112.	49.81	5383.	1.22	-182.12	.52	-181.60
WB528	38.	38.16	112.	49.64	5632.	12.89	-178.93	2.10	-176.83
WB529	38.	38.58	112.	49.29	5385.	.11	-183.30	.50	-182.80
WB530	38.	38.60	112.	48.78	5368.	-3.27	-186.10	.41	-185.69
WB531	38.	39.01	112.	47.34	5429.	-6.02	-190.93	.28	-190.65
WB532	38.	39.38	112.	47.22	5421.	-7.48	-192.12	.28	-191.84
WB533	38.	39.83	112.	47.12	5430.	-9.23	-194.18	.30	-193.88
WB534	38.	41.70	112.	47.12	5402.	-14.83	-198.83	.62	-198.21
WB535	38.	41.98	112.	47.32	5322.	-15.86	-197.13	.25	-196.88
WB536	38.	41.38	112.	47.36	5331.	-17.26	-198.84	.31	-198.53
WB537	38.	41.00	112.	47.50	5350.	-16.54	-198.76	.30	-198.46
WB538	38.	40.44	112.	47.37	5389.	-14.06	-197.61	.31	-197.30

STATION NUMBER	LATITUDE DEG	LATITUDE MIN	LONGITUDE DEG	LONGITUDE MIN	ELEVATION IN FEET	FREE-AIR ANOMALY	SIMPLE BOUGUER	TERRAIN CORRECTION	TERR-CORR BOUGUER
WB539	38.	41.91	112.	47.81	5274.	-17.51	-197.15	.23	-196.92
WB540	38.	41.92	112.	48.50	5251.	-17.35	-196.20	.19	-196.01
WB541	38.	41.95	112.	49.08	5248.	-14.80	-193.55	.21	-193.34
WB542	38.	41.68	112.	49.38	5243.	-14.34	-192.91	.19	-192.72
WB543	38.	41.28	112.	50.10	5221.	-11.83	-189.65	.17	-189.48
WB544	38.	40.70	112.	49.23	5277.	-14.64	-194.37	.18	-194.19
WB545	38.	40.18	112.	49.10	5326.	-11.73	-193.14	.18	-192.96
WB546	38.	39.56	112.	49.14	5342.	-8.36	-190.31	.24	-190.07
WB547	38.	39.10	112.	49.10	5364.	-5.10	-187.80	.28	-187.52
WB548	38.	40.05	112.	49.42	5335.	-9.50	-191.21	.19	-191.02
WB549	38.	42.30	112.	48.68	5253.	-15.31	-194.23	.19	-194.04
WB550	38.	42.77	112.	48.25	5227.	-14.35	-192.38	.23	-192.15
WB558	38.	42.08	112.	49.62	5325.	-9.94	-191.30	.22	-191.08
WB559	38.	42.29	112.	50.38	5397.	-3.19	-187.02	.26	-186.76
WB560	38.	42.44	112.	50.94	5402.	.03	-183.97	.32	-183.65
WB561	38.	42.48	112.	51.65	5303.	1.06	-179.56	.25	-179.31
WB562	38.	42.04	112.	51.08	5342.	-1.42	-183.37	.28	-183.09
WB563	38.	41.66	112.	52.00	5176.	-1.08	-177.37	.17	-177.20
WB564	38.	40.56	112.	51.00	5158.	-7.81	-183.49	.22	-183.27
WB565	38.	39.60	112.	51.52	5128.	-7.39	-182.05	.22	-181.83
WB566	38.	39.13	112.	51.39	5110.	-10.67	-184.72	.30	-184.42
WB567	38.	38.65	112.	51.32	5144.	-9.61	-184.81	.41	-184.40
WB568	38.	39.28	112.	52.18	5063.	-10.31	-182.76	.29	-182.47
WB569	38.	39.49	112.	52.28	5078.	-8.84	-181.80	.22	-181.58
WB570	38.	40.02	112.	52.25	5090.	-5.90	-179.26	.20	-179.06
WB571	38.	40.41	112.	52.08	5107.	-3.84	-177.78	.20	-177.58
WB572	38.	40.84	112.	52.18	5121.	-3.03	-177.45	.16	-177.29
WB573	38.	41.34	112.	52.12	5140.	-1.71	-176.78	.15	-176.63
WB574	38.	42.08	112.	52.13	5225.	.87	-177.09	.22	-176.87
WB575	38.	42.99	112.	51.64	5435.	5.65	-179.46	.54	-178.92

STATION NUMBER	LATITUDE DEG	MIN	LONGITUDE DEG	MIN	ELEVATION IN FEET	FREE-AIR ANOMALY	SIMPLE BOUGUER	TERRAIN CORRECTION	TERR-CORR BOUGUER
WB580	38.	42.55	112.	46.49	5408.	-15.41	-199.61	.62	-198.99
WB581	38.	42.03	112.	45.26	5873.	.65	-199.39	1.55	-197.84
WB582	38.	40.34	112.	45.41	5993.	6.81	-197.31	1.04	-196.27
WB583	38.	39.95	112.	45.36	6102.	8.39	-199.44	3.50	-195.94
WB584	38.	40.65	112.	45.51	6048.	8.04	-197.96	1.12	-196.84
WB585	38.	39.41	112.	45.34	5741.	.61	-194.93	.67	-194.26
WB586	38.	38.71	112.	45.87	5572.	-2.74	-192.52	.26	-192.26
WB587	38.	37.10	112.	49.62	7110.	49.40	-192.77	17.92	-174.85
WB588	38.	36.94	112.	49.59	7123.	50.63	-191.98	19.81	-172.17
WB589	38.	36.45	112.	49.25	7230.	51.29	-194.97	20.62	-174.35
WB590	38.	36.28	112.	49.20	7100.	49.01	-192.82	16.30	-176.52
WB591	38.	36.00	112.	49.18	6990.	48.84	-189.24	14.17	-175.07
WB592	38.	35.60	112.	48.92	6550.	41.69	-181.40	4.16	-177.24
WB593	38.	35.41	112.	48.87	6655.	42.09	-184.58	5.20	-179.38
WB594	38.	34.88	112.	48.72	7175.	49.26	-195.12	17.58	-177.54
WB600	38.	40.90	112.	50.66	5261.	-6.97	-186.16	.40	-185.76
WB602	38.	37.44	112.	50.70	5495.	10.70	-176.46	2.53	-173.93
WB603	38.	36.90	112.	50.78	5511.	10.46	-177.25	2.09	-175.16
WB604	38.	37.85	112.	51.58	5116.	-9.74	-183.99	.71	-183.28
WB605	38.	36.56	112.	51.28	5305.	-.72	-181.41	1.15	-180.26
WB606	38.	36.10	112.	51.06	5403.	3.32	-180.71	1.17	-179.54
WB607	38.	35.53	112.	51.05	5492.	6.12	-180.94	1.15	-179.79
WB608	38.	35.24	112.	51.12	5505.	7.21	-180.29	1.10	-179.19
WB609	38.	34.88	112.	51.25	5540.	10.39	-178.30	1.13	-177.17
WB610	38.	33.75	112.	51.32	5650.	16.53	-175.91	1.32	-174.59
WB611	38.	36.10	112.	51.50	5315.	-3.81	-184.83	.91	-183.92
WB612	38.	36.98	112.	51.58	5180.	-8.36	-184.79	.93	-183.86
WB613	38.	40.45	112.	52.71	5087.	-4.53	-177.80	.16	-177.64
WB614	38.	42.32	112.	52.69	5104.	-2.77	-176.61	.14	-176.47
WB615	38.	41.08	112.	53.82	5020.	-5.36	-176.34	.13	-176.21

STATION NUMBER	LATITUDE DEG	MIN	LONGITUDE DEG	MIN	ELEVATION IN FEET	FREE-AIR ANOMALY	SIMPLE BOUGUER	TERRAIN CORRECTION	TERR-CORR BOUGUER
WB616	38.	42.22	112.	53.87	5047.	.80	-171.10	.13	-170.97
WB617	38.	42.66	112.	53.84	5048.	1.56	-170.37	.14	-170.23
WB618	38.	42.37	112.	56.14	4952.	-7.74	-176.40	.10	-176.30
WB619	38.	42.53	112.	55.14	4968.	-4.24	-173.45	.11	-173.34
WB620	38.	42.60	112.	54.72	5012.	-.59	-171.30	.11	-171.19
WB621	38.	42.98	112.	54.35	5034.	2.12	-169.34	.12	-169.22
WB629	38.	42.84	112.	57.15	4922.	-5.39	-173.03	.13	-172.90
WB637	38.	41.69	112.	56.96	4932.	-9.52	-177.50	.09	-177.41
WB638	38.	41.01	112.	56.49	4957.	-11.64	-180.47	.09	-180.38
WB639	38.	40.26	112.	56.38	4956.	-13.99	-182.79	.09	-182.70
WB641	38.	42.17	112.	58.25	4858.	-7.75	-173.22	.11	-173.11
WB642	38.	41.33	112.	58.50	4873.	-10.07	-176.04	.10	-175.94
WB643	38.	40.12	112.	58.78	4900.	-13.35	-180.24	.09	-180.15
WB644	38.	39.18	112.	58.87	4898.	-17.20	-184.03	.09	-183.94
WB645	38.	38.32	112.	58.95	4875.	-20.75	-186.80	.12	-186.68
WB646	38.	37.92	112.	58.98	4877.	-22.27	-188.38	.12	-188.26
WB647	38.	39.17	112.	57.14	4944.	-17.57	-185.96	.10	-185.86
WB648	38.	37.40	112.	57.16	4910.	-25.67	-192.91	.14	-192.77
WB649	38.	41.58	112.	54.87	4975.	-6.87	-176.32	.11	-176.21
WB650	38.	37.01	112.	59.07	4872.	-24.78	-190.72	.14	-190.58
WB651	38.	35.24	112.	59.07	4886.	-28.69	-195.11	.17	-194.94
WB652	38.	34.84	112.	59.04	4882.	-30.02	-196.30	.18	-196.12
WB653	38.	38.45	112.	50.29	5351.	3.58	-178.67	2.26	-176.41
WB654	38.	37.85	112.	39.62	5835.	1.83	-196.91	.45	-196.46
WB655	38.	37.15	112.	50.36	5910.	23.89	-177.41	4.26	-173.15
WB656	38.	36.07	112.	50.13	6185.	31.20	-179.46	7.70	-171.76
WB657	38.	35.71	112.	50.13	6170.	27.59	-182.56	5.58	-176.98
WB658	38.	35.35	112.	49.85	6067.	28.88	-177.76	2.95	-174.81
WB659	38.	35.29	112.	50.42	5725.	18.42	-176.57	1.48	-175.09
WB660	38.	34.33	112.	50.39	6110.	29.94	-178.17	4.21	-173.96

STATION NUMBER	LATITUDE DEG	LATITUDE MIN	LONGITUDE DEG	LONGITUDE MIN	ELEVATION IN FEET	FREE-AIR ANOMALY	SIMPLE BOUGUER	TERRAIN CORRECTION	TERR-CORR BOUGUER
WB661	38.	33.48	112.	50.33	6531.	36.67	-185.77	8.26	-177.51
WB662	38.	34.16	112.	51.36	5590.	15.23	-175.16	1.75	-173.41
WB663	38.	35.33	112.	50.07	5800.	20.58	-176.97	1.72	-175.25
WB664	38.	35.10	112.	49.70	6040.	27.05	-178.67	2.60	-176.07
WB665	38.	34.78	112.	49.30	6200.	29.37	-181.80	3.92	-177.88
WB666	38.	34.60	112.	49.42	6905.	45.00	-190.18	11.16	-179.02
WB667	38.	34.27	112.	49.28	7060.	51.02	-189.45	8.41	-181.04
WB668	38.	35.98	112.	48.46	6050.	21.78	-184.28	3.35	-180.93
WB669	38.	34.52	112.	48.53	6985.	43.80	-194.11	12.09	-182.02

STATION NUMBER	LATITUDE DEG	LATITUDE MIN	LONGITUDE DEG	LONGITUDE MIN	ELEVATION IN FEET	FREE-AIR ANOMALY	SIMPLE BOUGUER	TERRAIN CORRECTION	TERR-CORR BOUGUER
JC001	38.	26.91	112.	48.31	8194.	58.50	-220.59	9.15	-211.44
JC002	38.	26.65	112.	49.03	7445.	43.46	-210.12	6.05	-204.07
JC003	38.	26.65	112.	50.57	6690.	24.53	-203.33	4.48	-198.85
JC004	38.	25.79	112.	51.56	6369.	17.01	-199.92	5.51	-194.41
JC005	38.	25.47	112.	46.14	7340.	36.64	-213.36	1.95	-211.41
JC006	38.	25.08	112.	45.88	7290.	34.34	-213.96	4.88	-209.08
JC007	38.	26.12	112.	46.87	8504.	66.71	-222.94	14.02	-208.92
JC008	38.	25.81	112.	47.06	8330.	67.30	-216.42	10.48	-205.94
JC040	38.	31.50	112.	48.41	7575.	57.13	-200.87	8.20	-192.67
JC041	38.	31.41	112.	47.35	7915.	56.56	-213.02	17.20	-195.82
JC042	38.	30.92	112.	45.93	6790.	26.72	-204.55	3.62	-200.93
JC043	38.	31.39	112.	46.89	7355.	43.57	-206.94	10.39	-196.55
JC044	38.	31.51	112.	45.90	6730.	25.10	-204.12	5.23	-198.89
JC045	38.	26.03	112.	49.50	7670.	52.94	-208.30	7.91	-200.39
JC046	38.	26.07	112.	49.83	7732.	51.00	-212.35	13.66	-198.69
JC047	38.	26.03	112.	50.71	7150.	38.48	-205.05	9.51	-195.54
JC048	38.	27.52	112.	49.09	7914.	53.66	-215.89	11.51	-204.38
JC049	38.	24.01	112.	46.07	7567.	43.05	-214.68	7.09	-207.59
JC050	38.	21.47	112.	46.85	6784.	19.94	-211.12	6.75	-204.37
JC051	38.	22.63	112.	46.20	6968.	28.93	-208.40	4.45	-203.95
JC052	38.	27.06	112.	45.96	7572.	41.80	-216.10	4.90	-211.20
JC053	38.	24.41	112.	48.81	7957.	50.07	-220.95	9.06	-211.89
JC054	38.	27.81	112.	46.10	7735.	49.20	-214.25	5.53	-208.72
JC055	38.	26.75	112.	46.27	7795.	48.90	-216.60	7.18	-209.42
JC091	38.	23.41	112.	46.52	7842.	48.29	-218.81	12.36	-206.45
JC092	38.	23.59	112.	47.55	8708.	72.18	-224.41	18.06	-206.35
JC093	38.	23.25	113.	2.63	5042.	-19.98	-191.71	.31	-191.40
JC094	38.	23.30	113.	3.96	5083.	-12.17	-185.29	.37	-184.92
JC095	38.	23.85	113.	3.88	5121.	-13.74	-188.16	.33	-187.83
JC096	38.	24.67	113.	3.93	5198.	-11.32	-188.36	.28	-188.08

STATION NUMBER	LATITUDE DEG	MIN	LONGITUDE DEG	MIN	ELEVATION IN FEET	FREE-AIR ANOMALY	SIMPLE BOUGUER	TERRAIN CORRECTION	TERR-CORR BOUGUER
JC097	38.	25.18	113.	5.86	5374.	2.96	-180.08	.37	-179.71
JC098	38.	24.52	113.	5.41	5284.	-.08	-180.05	.79	-179.26
JC099	38.	23.45	113.	5.10	5171.	-5.49	-181.62	.62	-181.00
JC100	38.	23.54	113.	5.70	5352.	1.17	-181.12	1.00	-180.12
JC101	38.	23.91	113.	1.66	5045.	-24.27	-196.10	.29	-195.81
JC102	38.	25.20	113.	1.83	5102.	-21.18	-194.96	.27	-194.69
JC103	38.	25.60	113.	1.65	5086.	-22.72	-195.95	.27	-195.68
JC104	38.	26.04	113.	.54	5015.	-31.74	-202.55	.32	-202.23
JC105	38.	24.28	113.	.55	4992.	-31.86	-201.89	.37	-201.52
JC106	38.	25.18	113.	.55	5030.	-30.81	-202.13	.33	-201.80
JC107	38.	27.39	113.	.53	4957.	-33.54	-202.38	.34	-202.04
JC108	38.	27.20	113.	2.93	5095.	-13.18	-186.71	.46	-186.25
JC109	38.	27.61	113.	6.06	5437.	1.93	-183.26	.30	-182.96
JC110	38.	26.89	113.	6.05	5418.	2.07	-182.47	.27	-182.20
JC111	38.	26.16	113.	4.61	5303.	-3.22	-183.84	.27	-183.57
JC112	38.	26.62	113.	2.61	5130.	-15.32	-190.04	.30	-189.74
JC113	38.	26.17	113.	2.99	5158.	-11.21	-186.90	.30	-186.60
JC114	38.	28.16	113.	3.60	5180.	-7.18	-183.61	.78	-182.83
JC115	38.	29.00	113.	4.44	5194.	-7.11	-184.02	.55	-183.47
JC116	38.	28.24	113.	1.59	4991.	-26.12	-196.11	.30	-195.81
JC117	38.	28.24	113.	2.76	5031.	-17.05	-188.41	.44	-187.97
JC118	38.	29.12	113.	2.76	5030.	-18.00	-189.32	.33	-188.99
JC119	38.	29.98	113.	2.76	5020.	-18.11	-189.09	.31	-188.78
JC120	38.	29.98	113.	3.88	5103.	-10.33	-184.14	.44	-183.70
JC121	38.	29.98	113.	1.59	4984.	-24.74	-194.50	.27	-194.23
JC122	38.	30.24	113.	1.14	4967.	-27.61	-196.78	.26	-196.52
JC123	38.	32.61	113.	.80	4906.	-27.71	-194.80	.22	-194.58
JC124	38.	33.47	113.	1.37	4899.	-26.43	-193.29	.22	-193.07
JC125	38.	33.83	113.	2.77	4921.	-23.65	-191.26	.26	-191.00
JC126	38.	32.60	113.	2.75	4926.	-19.76	-187.54	.30	-187.24

STATION NUMBER	LATITUDE DEG	LATITUDE MIN	LONGITUDE DEG	LONGITUDE MIN	ELEVATION IN FEET	FREE-AIR ANOMALY	SIMPLE BOUGUER	TERRAIN CORRECTION	TERR-CORR BOUGUER
JC127	38.	32.60	113.	1.65	4921.	-24.19	-191.80	.24	-191.56
JC140	38.	35.16	113.	1.35	4882.	-24.28	-190.56	.17	-190.39
JC141	38.	35.24	113.	2.74	4924.	-21.47	-189.18	.20	-188.98
JC142	38.	35.24	113.	3.86	5026.	-16.32	-187.51	.25	-187.26
JC143	38.	34.34	113.	3.85	4998.	-18.61	-188.85	.31	-188.54
JC144	38.	34.34	113.	4.96	5110.	-10.26	-184.31	.34	-183.97
JC145	38.	32.60	113.	4.93	5215.	2.79	-174.83	.68	-174.15
JC146	38.	33.47	113.	6.07	5275.	6.29	-173.37	.80	-172.57
JC147	38.	33.47	113.	4.96	5094.	-7.37	-180.88	.48	-180.40
JC148	38.	33.84	113.	4.80	5087.	-10.74	-184.00	.41	-183.59
JC149	38.	34.34	113.	2.75	4922.	-23.83	-191.47	.24	-191.23
JC150	38.	42.94	113.	.75	4857.	-4.27	-169.70	.43	-169.27
JC151	38.	35.25	113.	6.10	5215.	-2.17	-179.80	.35	-179.45
JC152	38.	35.25	113.	4.98	5106.	-10.32	-184.23	.28	-183.95
JC153	38.	34.34	113.	1.64	4884.	-26.39	-192.74	.22	-192.52
JC154	38.	32.60	113.	3.86	5015.	-10.50	-181.31	.46	-180.85
JC155	38.	32.23	113.	5.57	5442.	11.47	-173.89	.94	-172.95
JC156	38.	31.60	113.	5.33	5424.	8.31	-176.43	.85	-175.58
JC157	38.	30.94	113.	5.03	5327.	1.13	-180.31	.77	-179.54
JC158	38.	30.16	113.	4.75	5243.	-2.49	-181.07	.61	-180.46
JC159	38.	31.19	113.	5.85	5602.	12.83	-177.97	1.20	-176.77
JC160	38.	31.73	113.	3.86	5025.	-9.07	-180.22	.57	-179.65
JC161	38.	31.73	113.	2.75	4962.	-18.09	-187.10	.32	-186.78
JC162	38.	31.73	113.	1.65	4943.	-24.35	-192.71	.26	-192.45
JC163	38.	30.86	113.	1.65	4902.	-30.00	-196.97	.31	-196.66
JC164	38.	30.86	113.	2.75	4993.	-17.57	-187.63	.31	-187.32
JC170	38.	26.50	113.	1.65	5071.	-23.69	-196.41	.27	-196.14
JC171	38.	27.59	113.	1.65	5018.	-24.86	-195.77	.30	-195.47
JC172	38.	28.39	112.	52.92	5658.	-5.69	-198.40	1.07	-197.33
JC173	38.	36.11	113.	3.86	5009.	-14.63	-185.24	.23	-185.01

STATION NUMBER	LATITUDE DEG	MIN	LONGITUDE DEG	MIN	ELEVATION IN FEET	FREE-AIR ANOMALY	SIMPLE BOUGUER	TERRAIN CORRECTION	TERR-CORR BOUGUER
JC174	38.	36.11	113.	1.08	4877.	-21.60	-187.71	.16	-187.55
JC175	38.	35.45	113.	1.61	4883.	-23.08	-189.40	.19	-189.21
JC176	38.	35.93	113.	2.12	4908.	-18.93	-186.10	.17	-185.93
JC177	38.	34.17	113.	6.25	5245.	.48	-178.17	.48	-177.69
JC178	38.	34.71	113.	6.64	5285.	2.79	-177.22	.42	-176.80
JC179	38.	36.15	113.	5.51	5115.	-6.86	-181.08	.28	-180.80
JC180	38.	37.88	113.	4.47	4956.	-8.18	-176.98	.26	-176.72
JC181	38.	37.86	113.	3.90	4928.	-8.60	-176.45	.22	-176.23
JC182	38.	38.74	113.	3.92	4893.	-5.60	-172.26	.23	-172.03
JC183	38.	38.86	113.	6.21	5054.	4.78	-167.36	.56	-166.80
JC184	38.	38.75	113.	5.00	4947.	-3.81	-172.31	.30	-172.01
JC185	38.	37.34	113.	6.09	5080.	-2.51	-175.54	.36	-175.18
JC186	38.	37.91	113.	6.83	5127.	2.61	-172.01	.57	-171.44
JC187	38.	37.35	113.	4.81	5005.	-8.60	-179.07	.25	-178.82
JC188	38.	37.92	113.	1.06	4861.	-15.17	-180.74	.13	-180.61
JC189	38.	37.88	113.	2.79	4881.	-9.63	-175.87	.17	-175.70
JC190	38.	38.74	113.	1.83	4860.	-11.17	-176.70	.14	-176.56
JC191	38.	38.76	113.	.51	4859.	-14.88	-180.37	.11	-180.26
JC192	38.	40.09	113.	3.16	4864.	-.52	-166.18	.20	-165.98
JC193	38.	39.70	113.	2.87	4854.	-4.90	-170.23	.17	-170.06
JC194	38.	39.87	113.	2.18	4850.	-7.97	-173.16	.14	-173.02
JC195	38.	40.10	112.	59.99	4853.	-12.90	-178.20	.10	-178.10
JC196	38.	33.36	112.	59.79	4898.	-29.55	-196.38	.20	-196.18
JC197	38.	43.00	112.	58.60	4846.	-5.10	-170.15	.14	-170.01
JC198	38.	42.95	112.	59.94	4848.	-3.20	-168.32	.15	-168.17
JC199	38.	42.71	113.	1.72	4922.	1.87	-165.77	.19	-165.58
JC200	38.	42.38	113.	2.60	4989.	4.90	-165.03	.20	-164.83
JC201	38.	42.14	113.	3.76	5071.	7.30	-165.42	.23	-165.19
JC202	38.	41.95	113.	4.88	5140.	10.18	-164.89	.29	-164.60
JC203	38.	41.94	113.	5.36	5215.	12.48	-165.14	.36	-164.78

STATION NUMBER	LATITUDE DEG	MIN	LONGITUDE DEG	MIN	ELEVATION IN FEET	FREE-AIR ANOMALY	SIMPLE BOUGUER	TERRAIN CORRECTION	TERR-CORR BOUGUER
JC204	38.	41.98	113.	6.51	5122.	10.50	-163.95	.86	-163.09
JC205	38.	42.00	113.	2.64	4972.	3.19	-166.16	.18	-165.98
JC206	38.	41.37	113.	2.73	4912.	.84	-166.47	.17	-166.30
JC207	38.	40.96	113.	2.49	4884.	.43	-165.92	.16	-165.76
JC208	38.	41.61	113.	1.66	4858.	-.25	-165.72	.15	-165.57
JC209	38.	40.47	113.	4.95	5021.	5.42	-165.59	.30	-165.29
JC210	38.	40.48	113.	3.84	4907.	-1.85	-168.99	.23	-168.76
JC211	38.	40.13	113.	3.65	4878.	-2.64	-168.79	.21	-168.58
JC212	38.	40.51	113.	2.83	4868.	-1.37	-167.17	.16	-167.01
JC213	38.	39.60	113.	4.97	4953.	-.20	-168.90	.32	-168.58
JC214	38.	28.23	112.	58.31	4995.	-39.42	-209.55	.40	-209.15
JC215	38.	29.11	112.	58.32	4974.	-38.58	-208.00	.37	-207.63
JC219	38.	41.28	113.	4.42	5021.	5.84	-165.18	.25	-164.93
JC220	38.	40.05	113.	5.41	5038.	5.78	-165.81	.39	-165.42
JC221	38.	39.35	113.	5.90	5032.	5.39	-166.00	.53	-165.47
JC222	38.	38.35	113.	6.71	5110.	6.65	-167.40	.68	-166.72
JC223	38.	40.45	113.	6.08	5360.	16.16	-166.40	1.46	-164.94
JC224	38.	41.36	113.	4.95	5120.	9.19	-165.20	.36	-164.84
JC225	38.	41.36	113.	6.05	5377.	17.83	-165.29	1.13	-164.16
JC226	38.	40.36	113.	5.15	5038.	5.81	-165.78	.33	-165.45
JC227	38.	40.27	113.	4.63	4968.	2.07	-167.14	.27	-166.87
JC228	38.	40.19	113.	4.12	4910.	-2.46	-169.70	.24	-169.46
JC229	38.	40.05	113.	3.45	4866.	-1.71	-167.44	.20	-167.24
JC230	38.	39.91	113.	3.03	4854.	-2.64	-167.96	.17	-167.79
JC231	38.	39.78	113.	2.58	4853.	-6.58	-171.88	.16	-171.72
JC232	38.	39.84	113.	1.69	4845.	-9.73	-174.76	.12	-174.64
JC233	38.	39.78	113.	.80	4850.	-12.08	-177.26	.11	-177.15
JC234	38.	38.91	112.	51.69	5095.	-11.28	-184.82	.35	-184.47
JC235	38.	38.42	112.	50.99	5195.	-5.49	-182.43	.69	-181.74
JC236	38.	39.34	112.	52.67	5062.	-11.02	-183.43	.21	-183.22

STATION NUMBER	LATITUDE DEG	MIN	LONGITUDE DEG	MIN	ELEVATION IN FEET	FREE-AIR ANOMALY	SIMPLE BOUGUER	TERRAIN CORRECTION	TERR-CORR BOUGUER
JC237	38.	39.34	112.	53.28	5048.	-12.37	-184.31	.19	-184.12
JC238	38.	39.37	112.	54.30	5003.	-14.89	-185.29	.14	-185.15
JC239	38.	39.39	112.	55.33	4992.	-16.15	-186.18	.12	-186.06
JC240	38.	39.18	112.	58.28	4913.	-18.06	-185.39	.09	-185.30
JC241	38.	40.26	112.	59.33	4878.	-13.28	-179.42	.09	-179.33
JC242	38.	38.74	113.	7.15	5532.	24.21	-164.21	3.38	-160.83
JC243	38.	27.79	113.	6.31	5559.	7.11	-182.23	1.80	-180.43
JC244	38.	27.52	113.	5.74	5407.	.75	-183.42	.31	-183.11
JC245	38.	27.42	113.	5.44	5390.	1.25	-182.33	.29	-182.04
JC246	38.	27.33	113.	5.13	5370.	1.16	-181.75	.36	-181.39
JC247	38.	27.38	113.	4.98	5385.	2.08	-181.33	.41	-180.92
JC248	38.	27.14	113.	4.77	5375.	1.68	-181.39	.52	-180.87
JC249	38.	26.98	113.	4.63	5354.	.87	-181.49	.74	-180.75
JC250	38.	26.88	113.	4.42	5345.	1.45	-180.60	.99	-179.61
JC251	38.	26.85	113.	4.10	5321.	.13	-181.10	.73	-180.37
JC252	38.	26.90	113.	3.92	5293.	-.70	-180.98	.95	-180.03
JC253	38.	26.94	113.	3.76	5252.	-2.59	-181.47	1.01	-180.46
JC254	38.	27.13	113.	3.14	5121.	-10.47	-184.89	.67	-184.22
JC255	38.	27.07	113.	3.36	5161.	-7.66	-183.44	.61	-182.83
JC256	38.	27.01	113.	3.55	5192.	-5.70	-182.53	.69	-181.84
JC257	38.	27.29	113.	2.61	5078.	-16.51	-189.47	.38	-189.09
JC258	38.	27.38	113.	2.30	5063.	-19.07	-191.52	.33	-191.19
JC259	38.	27.48	113.	2.00	5046.	-21.72	-193.59	.31	-193.28
JC260	38.	27.68	113.	1.34	5002.	-27.23	-197.60	.30	-197.30
JC261	38.	27.75	113.	.82	4941.	-32.25	-200.54	.35	-200.19
JC262	38.	27.54	113.	.63	4958.	-32.66	-201.53	.34	-201.19
JC263	38.	27.63	112.	59.89	4970.	-36.65	-205.93	.33	-205.60
JC264	38.	27.81	112.	58.92	4978.	-39.30	-208.85	.37	-208.48
JC265	38.	27.84	112.	57.78	5070.	-38.71	-211.39	.44	-210.95
JC266	38.	28.05	112.	56.65	5138.	-35.99	-210.99	.50	-210.49

STATION NUMBER	LATITUDE DEG	LATITUDE MIN	LONGITUDE DEG	LONGITUDE MIN	ELEVATION IN FEET	FREE-AIR ANOMALY	SIMPLE BOUGUER	TERRAIN CORRECTION	TERR-CORR BOUGUER
JC267	38.	28.21	112.	55.45	5258.	-29.94	-209.03	.63	-208.40
JC268	38.	28.39	112.	54.37	5403.	-21.11	-205.14	.81	-204.33
JC269	38.	28.38	112.	52.59	5735.	-1.85	-197.19	1.09	-196.10
JC270	38.	28.48	112.	50.50	5840.	4.20	-194.71	3.04	-191.67
JC271	38.	28.69	112.	51.69	5870.	6.12	-193.81	1.54	-192.27
JC272	38.	28.96	112.	51.21	6006.	10.73	-193.84	1.54	-192.30
JC273	38.	29.23	112.	50.76	6130.	14.13	-194.66	1.69	-192.97
JC275	38.	29.45	112.	50.42	6230.	14.76	-197.43	1.56	-195.87
JC276	38.	29.53	112.	49.85	6380.	19.88	-197.43	1.94	-195.49
JC277	38.	29.49	112.	50.07	6320.	17.69	-197.57	1.75	-195.82
JC278	38.	29.58	112.	49.12	6390.	16.22	-201.43	2.97	-198.46
JC279	38.	29.65	112.	48.58	6550.	18.97	-204.12	2.93	-201.19
JC280	38.	29.73	112.	48.27	6700.	25.14	-203.06	3.57	-199.49
JC281	38.	29.68	112.	47.70	7060.	36.65	-203.81	2.45	-201.36
JC282	38.	29.66	112.	47.42	7150.	39.54	-203.99	2.00	-201.99
JC283	38.	32.60	113.	6.07	5510.	15.46	-172.21	1.64	-170.57
JC284	38.	32.52	113.	5.83	5440.	11.38	-173.90	1.12	-172.78
JC285	38.	32.54	113.	5.60	5376.	8.94	-174.17	.91	-173.26
JC286	38.	32.56	113.	5.37	5317.	7.04	-174.06	.87	-173.19
JC287	38.	32.60	113.	5.16	5255.	4.48	-174.50	.78	-173.72
JC288	38.	32.60	113.	4.69	5172.	.47	-175.69	.62	-175.07
JC289	38.	32.60	113.	4.48	5120.	-2.90	-177.28	.58	-176.70
JC290	38.	32.60	113.	4.26	5075.	-5.27	-178.12	.52	-177.60
JC291	38.	32.60	113.	4.03	5038.	-8.02	-179.61	.47	-179.14
JC292	38.	32.60	113.	3.63	4987.	-13.19	-183.05	.44	-182.61
JC293	38.	32.60	113.	3.41	4956.	-16.09	-184.89	.39	-184.50
JC294	38.	32.60	113.	3.19	4944.	-17.19	-185.59	.38	-185.21
JC295	38.	32.60	113.	2.96	4933.	-18.46	-186.48	.37	-186.11
JC296	38.	32.60	113.	2.20	4926.	-21.82	-189.60	.25	-189.35
JC297	38.	32.60	113.	1.20	4929.	-25.92	-193.80	.21	-193.59

STATION NUMBER	LATITUDE DEG	MIN	LONGITUDE DEG	MIN	ELEVATION IN FEET	FREE-AIR ANOMALY	SIMPLE BOUGUER	TERRAIN CORRECTION	TERR-CORR BOUGUER
JC298	38.	32.61	112.	59.43	4917.	-30.39	-197.86	.24	-197.62
JC299	38.	32.61	112.	56.64	4948.	-33.12	-201.65	.37	-201.28
JC300	38.	32.61	112.	58.30	4916.	-31.94	-199.38	.24	-199.14
JC301	38.	29.65	112.	46.91	7177.	39.58	-204.86	1.74	-203.12
JC302	38.	29.59	112.	46.59	7090.	35.57	-205.91	2.15	-203.76
JC303	38.	29.46	112.	46.40	7027.	32.78	-206.56	2.88	-203.68
JC304	38.	29.45	112.	46.07	6860.	24.59	-209.06	4.17	-204.89
JC305	38.	29.52	112.	45.74	6930.	28.36	-207.68	2.11	-205.57
JC306	38.	29.53	112.	45.60	6950.	27.50	-209.22	1.97	-207.25
JC307	38.	29.57	112.	45.33	6840.	24.35	-208.62	1.71	-206.91
JC308	38.	33.11	112.	53.85	5142.	-20.36	-195.50	.69	-194.81
JC309	38.	33.11	112.	53.28	5242.	-13.71	-192.25	.69	-191.56
JC310	38.	33.11	112.	52.75	5345.	-6.23	-188.28	.80	-187.48
JC311	38.	33.12	112.	52.19	5443.	1.64	-183.75	.94	-182.81
JC312	38.	33.03	112.	51.52	5578.	10.10	-179.88	1.19	-178.69
JC313	38.	33.03	112.	51.18	5686.	17.36	-176.30	1.25	-175.05
JC314	38.	32.97	112.	50.63	5837.	19.93	-178.87	1.48	-177.39
JC315	38.	32.91	112.	50.46	5873.	19.23	-180.81	1.43	-179.38
JC316	38.	32.85	112.	50.20	5919.	18.89	-182.71	1.63	-181.08
JC317	38.	32.63	112.	50.03	5992.	19.51	-184.57	1.68	-182.89
JC318	38.	24.39	113.	1.65	5085.	-23.22	-196.42	.27	-196.15
JC319	38.	24.73	113.	2.76	5135.	-16.12	-191.01	.27	-190.74
JC320	38.	26.45	112.	53.15	5723.	-7.26	-202.19	1.09	-201.10
JC321	38.	27.17	112.	52.80	5735.	-5.05	-200.38	1.18	-199.20
JC322	38.	27.33	112.	52.73	5742.	-4.66	-200.23	1.19	-199.04
JC323	38.	27.69	112.	52.63	5703.	-4.47	-198.71	1.24	-197.47
JC324	38.	28.02	112.	52.73	5701.	-4.24	-198.42	1.15	-197.27
JC325	38.	28.38	112.	52.73	5700.	-3.58	-197.72	1.09	-196.63
JC326	38.	28.55	112.	52.73	5670.	-3.84	-196.96	1.16	-195.80
JC327	38.	29.07	112.	52.73	5692.	-4.45	-198.32	1.05	-197.27

STATION NUMBER	LATITUDE DEG	LATITUDE MIN	LONGITUDE DEG	LONGITUDE MIN	ELEVATION IN FEET	FREE-AIR ANOMALY	SIMPLE BOUGUER	TERRAIN CORRECTION	TERR-CORR BOUGUER
JC328	38.	22.35	112.	53.15	6144.	12.98	-196.28	1.67	-194.61
JC329	38.	22.53	112.	53.15	6125.	12.63	-195.98	1.69	-194.29
JC330	38.	22.80	112.	53.14	6080.	10.07	-197.01	1.65	-195.36
JC331	38.	22.14	112.	53.15	6145.	12.85	-196.45	1.73	-194.72
JC332	38.	21.15	112.	53.17	6246.	18.91	-193.85	2.04	-191.81
JC333	38.	21.81	112.	53.16	6140.	15.72	-193.43	1.88	-191.55
JC334	38.	25.52	113.	4.18	5260.	-5.51	-184.67	.27	-184.40
JC335	38.	28.25	113.	6.08	5433.	2.18	-182.87	.40	-182.47
JC336	38.	29.09	113.	5.96	5407.	1.80	-182.37	.67	-181.70
JC337	38.	29.11	113.	4.98	5250.	-5.00	-183.81	.52	-183.29
JC338	38.	23.81	113.	6.11	5600.	10.18	-180.55	2.08	-178.47
JC339	38.	24.73	113.	6.12	5520.	9.11	-178.90	.69	-178.21
JC340	38.	11.76	112.	58.31	5228.	-22.23	-200.30	.59	-199.71
JC341	38.	11.53	112.	57.26	5332.	-16.60	-198.21	.67	-197.54
JC342	38.	11.54	112.	59.50	5188.	-20.97	-197.67	.60	-197.07
JC343	38.	11.53	112.	55.03	5588.	-.85	-191.19	1.04	-190.15
JC344	38.	10.65	112.	55.04	5804.	8.92	-188.76	1.33	-187.43
JC345	38.	11.24	112.	56.32	5455.	-10.71	-196.50	.82	-195.68
JC346	38.	10.16	112.	57.16	5519.	-7.05	-195.02	.83	-194.19
JC347	38.	9.76	112.	57.27	5527.	-6.88	-195.13	.92	-194.21
JC348	38.	9.38	112.	57.43	5504.	-8.72	-196.18	1.12	-195.06
JC349	38.	9.27	112.	59.09	5462.	-9.10	-195.13	.90	-194.23
JC350	38.	10.65	112.	57.26	5444.	-10.81	-196.24	.76	-195.48
JC351	38.	12.38	112.	50.62	5880.	9.96	-190.31	3.11	-187.20
JC352	38.	11.90	112.	49.82	6035.	6.55	-199.00	4.08	-194.92
JC353	38.	11.22	112.	50.24	6162.	12.09	-197.79	2.71	-195.08
JC354	38.	9.90	112.	53.80	6293.	12.85	-201.49	2.01	-199.48
JC355	38.	9.79	112.	55.03	5871.	10.64	-189.33	1.35	-187.98
JC356	38.	9.94	112.	56.50	5869.	5.97	-193.93	3.03	-190.90
JC357	38.	10.77	112.	52.55	6635.	38.69	-187.30	2.59	-184.71

STATION NUMBER	LATITUDE DEG	LATITUDE MIN	LONGITUDE DEG	LONGITUDE MIN	ELEVATION IN FEET	FREE-AIR ANOMALY	SIMPLE BOUGUER	TERRAIN CORRECTION	TERR-CORR BOUGUER
JC358	38.	9.29	112.	58.15	5485.	-8.99	-195.81	.91	-194.90
JC359	38.	9.69	112.	58.85	5382.	-12.26	-195.57	.80	-194.77
JC360	38.	10.48	112.	58.70	5320.	-14.48	-195.68	.69	-194.99
JC361	38.	11.61	112.	54.00	5892.	15.22	-185.46	2.13	-183.33
JC362	38.	12.33	112.	47.21	5961.	-10.74	-213.77	.99	-212.78
JC363	38.	11.98	112.	46.26	5980.	-11.08	-214.76	1.18	-213.58
JC364	38.	11.46	112.	46.08	6215.	-4.61	-216.30	1.28	-215.02
JC365	38.	10.85	112.	46.59	6284.	.81	-213.23	1.52	-211.71
JC366	38.	9.30	112.	52.35	6390.	23.46	-194.19	1.82	-192.37
JC367	38.	9.96	112.	51.50	6680.	33.65	-193.87	1.61	-192.26
JC368	38.	10.30	112.	50.92	6360.	20.11	-196.51	2.38	-194.13
JC369	38.	10.61	112.	50.57	6241.	15.10	-197.47	3.28	-194.19
JC370	38.	10.81	113.	2.77	5130.	-14.72	-189.45	.42	-189.03
JC371	38.	10.68	113.	3.28	5138.	-14.41	-189.41	.44	-188.97
JC372	38.	11.53	113.	2.82	5093.	-15.16	-188.62	.37	-188.25
JC373	38.	12.44	113.	2.82	5082.	-15.81	-188.89	.28	-188.61
JC374	38.	13.33	113.	3.37	5070.	-17.40	-190.09	.23	-189.86
JC375	38.	11.26	112.	51.78	7226.	47.51	-198.61	10.53	-188.08
JC376	38.	10.63	112.	51.92	6910.	43.63	-191.73	2.95	-188.78
JC377	38.	11.51	112.	52.22	6866.	40.40	-193.45	7.43	-186.02
JC378	38.	11.32	112.	51.25	6640.	32.98	-193.18	2.78	-190.40
JC379	38.	10.76	112.	51.34	6695.	35.98	-192.05	1.92	-190.13
JC380	38.	11.95	113.	.77	5128.	-19.59	-194.25	.45	-193.80
JC381	38.	11.55	113.	1.72	5109.	-16.82	-190.84	.42	-190.42
JC38A	38.	30.13	112.	47.52	7494.	51.37	-203.88	3.96	-199.92
JC382	38.	10.25	112.	49.62	7064.	32.85	-207.75	3.32	-204.43
7601	38.	25.03	112.	53.14	5815.	-3.43	-201.49	1.49	-200.00
7602	38.	25.13	112.	53.15	5660.	-8.31	-201.09	1.96	-199.13
7603	38.	25.25	112.	53.15	5625.	-9.73	-201.31	1.79	-199.52
7604	38.	25.36	112.	53.15	5771.	2.12	-194.44	1.98	-192.46

STATION NUMBER	LATITUDE DEG MIN	LONGITUDE DEG MIN	ELEVATION IN FEET	FREE-AIR ANOMALY	SIMPLE BOUGUER	TERRAIN CORRECTION	TERR-CORR BOUGUER
7605	38. 25.46	112. 53.15	5784.	-5.82	-202.83	1.30	-201.53
7606	38. 25.57	112. 53.15	5779.	-5.82	-202.65	1.16	-201.49
7607	38. 25.69	112. 53.16	5775.	-6.09	-202.79	1.14	-201.65
7608	38. 25.79	112. 53.16	5764.	-6.14	-202.46	1.15	-201.31
7609	38. 25.88	112. 53.17	5754.	-6.63	-202.61	1.12	-201.49
7610	38. 26.00	112. 53.17	5743.	-7.13	-202.73	1.12	-201.61
7611	38. 26.03	112. 53.18	5735.	-7.23	-202.56	1.13	-201.43
7612	38. 26.21	112. 53.18	5719.	-7.72	-202.51	1.10	-201.41
7613	38. 26.31	112. 53.19	5716.	-7.77	-202.45	1.10	-201.35

STATION NUMBER	LATITUDE DEG MIN	LONGITUDE DEG MIN	ELEVATION IN FEET	FREE-AIR ANOMALY	SIMPLE BOUGUER	TERRAIN CORRECTION	TERR-CORR BOUGUER
TC001	38. 22.30	112. 56.70	5269.	-22.30	-201.77	.90	-200.87
TC002	38. 22.88	112. 56.38	5278.	-23.43	-203.20	.87	-202.33
TC003	38. 24.84	112. 55.45	5364.	-22.59	-205.29	.90	-204.39
TC004	38. 25.97	112. 54.00	5604.	-13.08	-203.96	1.00	-202.96
TC005	38. 26.02	112. 53.01	5775.	-5.50	-202.20	1.17	-201.03
TC007	38. 25.46	112. 51.46	6110.	9.34	-198.77	1.80	-196.97
TC008	38. 25.02	112. 51.05	6358.	17.14	-199.42	2.08	-197.34
TC009	38. 24.95	112. 50.60	6370.	16.36	-200.60	2.50	-198.10
TC010	38. 24.94	112. 49.95	6511.	17.55	-204.22	3.28	-200.94
TC011	38. 24.87	112. 49.13	6760.	20.99	-209.25	5.42	-203.83
TC012	38. 24.72	112. 48.52	6953.	24.99	-211.83	5.00	-206.83
TC013	38. 24.32	112. 48.24	7115.	30.73	-211.61	4.56	-207.05
TC014	38. 27.94	112. 57.39	5091.	-38.30	-211.70	.50	-211.20
TC015	38. 31.72	112. 51.63	5703.	7.61	-186.63	1.24	-185.39
TC017	38. 31.72	112. 52.05	5596.	2.50	-188.10	1.02	-187.08
TC019	38. 31.72	112. 52.46	5508.	-2.86	-190.47	.91	-189.56
TC020	38. 31.72	112. 52.66	5473.	-5.34	-191.75	.89	-190.86
TC021	38. 31.72	112. 52.88	5440.	-7.94	-193.23	.86	-192.37
TC022	38. 31.72	112. 53.08	5394.	-10.91	-194.63	.82	-193.81
TC023	38. 31.72	112. 53.30	5348.	-13.80	-195.95	.80	-195.15
TC024	38. 31.72	112. 53.50	5303.	-16.51	-197.13	.78	-196.35
TC025	38. 31.72	112. 53.71	5278.	-17.75	-197.52	.75	-196.77
TC026	38. 31.72	112. 53.92	5230.	-21.05	-199.18	.72	-198.46
TC027	38. 31.72	112. 54.13	5193.	-23.17	-200.05	.69	-199.36
TC028	38. 31.72	112. 54.34	5165.	-24.90	-200.82	.67	-200.15
TC029	38. 31.72	112. 54.54	5131.	-26.74	-201.50	.63	-200.87
TC030	38. 31.72	112. 54.75	5110.	-28.09	-202.13	.61	-201.52
TC031	38. 31.72	112. 54.96	5096.	-29.12	-202.69	.58	-202.11
TC033	38. 31.72	112. 55.58	5035.	-32.54	-204.03	.50	-203.53
TC034	38. 31.72	112. 55.99	4999.	-33.82	-204.08	.44	-203.64

STATION NUMBER	LATITUDE DEG	MIN	LONGITUDE DEG	MIN	ELEVATION IN FEET	FREE-AIR ANOMALY	SIMPLE BOUGUER	TERRAIN CORRECTION	TERR-CORR BOUGUER
TC035	38.	31.72	112.	56.57	4972.	-34.39	-203.73	.38	-203.35
TC036	38.	31.72	112.	57.16	4948.	-34.73	-203.26	.37	-202.89
TC037	38.	30.56	112.	51.63	5851.	10.27	-189.02	1.45	-187.57
TC042	38.	31.72	112.	51.22	5812.	11.68	-186.27	1.49	-184.78
TC045	38.	30.56	112.	50.19	6257.	18.95	-194.17	1.62	-192.55
TC044	38.	30.56	112.	49.98	6332.	20.63	-195.04	1.65	-193.39
TC046	38.	30.56	112.	50.39	6180.	17.24	-193.25	1.60	-191.65
TC048	38.	30.56	112.	50.81	6056.	15.24	-191.03	1.58	-189.45
TC050	38.	30.56	112.	51.21	5926.	13.32	-188.52	1.52	-187.00
TC053	38.	30.56	112.	52.05	5766.	5.83	-190.56	1.31	-189.25
TC054	38.	30.56	112.	52.27	5718.	2.99	-191.76	1.28	-190.48
TC058	38.	30.56	112.	53.09	5515.	-8.67	-196.51	1.00	-195.51
TC059	38.	30.56	112.	53.30	5469.	-11.46	-197.74	.92	-196.82
TC060	38.	30.56	112.	53.50	5424.	-14.13	-198.87	.90	-197.97
TC061	38.	30.56	112.	53.70	5385.	-16.49	-199.91	.85	-199.06
TC062	38.	30.56	112.	53.92	5346.	-18.59	-200.68	.80	-199.88
TC063	38.	30.56	112.	54.12	5281.	-21.34	-201.21	.79	-200.42
TC064	38.	30.56	112.	54.34	5278.	-22.28	-202.05	.75	-201.30
TC065	38.	30.56	112.	54.54	5254.	-23.70	-202.65	.70	-201.95
TC066	38.	30.56	112.	54.75	5230.	-24.94	-203.08	.67	-202.41
TC067	38.	30.56	112.	54.96	5195.	-26.73	-203.68	.61	-203.07
TC070	38.	30.56	112.	51.92	5798.	7.47	-190.01	1.39	-188.62
TC073	38.	30.56	112.	52.18	5735.	3.93	-191.40	1.29	-190.11
TC075	38.	30.56	112.	51.50	5877.	11.54	-188.63	1.50	-187.13
TC076	38.	30.56	112.	51.36	5898.	12.45	-188.43	1.50	-186.93
TC079	38.	30.56	112.	51.08	5964.	14.16	-188.97	1.54	-187.43
TC080	38.	30.56	112.	50.95	6006.	14.36	-190.20	1.56	-188.64
TC083	38.	31.72	112.	51.77	5665.	6.15	-186.80	1.18	-185.62
TC084	38.	31.72	112.	51.91	5629.	4.19	-187.53	1.09	-186.44
TC087	38.	31.72	112.	52.18	5563.	.73	-188.74	.97	-187.77

STATION NUMBER	LATITUDE DEG	MIN	LONGITUDE DEG	MIN	ELEVATION IN FEET	FREE-AIR ANOMALY	SIMPLE BOUGUER	TERRAIN CORRECTION	TERR-CORR BOUGUER
TC088	38.	31.72	112.	52.32	5529.	-1.36	-189.68	.92	-188.76
TC090	38.	31.72	112.	51.08	5846.	12.91	-186.20	1.58	-184.62
TC093	38.	31.72	112.	51.35	5777.	10.10	-186.67	1.39	-185.28
TC93B	38.	31.72	112.	51.49	5738.	8.65	-186.78	1.31	-185.47
TC095	38.	28.53	112.	51.63	5876.	5.27	-194.87	1.65	-193.22
TC096	38.	28.53	112.	51.71	5865.	4.82	-194.94	1.60	-193.34
TC098	38.	28.53	112.	51.85	5837.	3.92	-194.89	1.50	-193.39
TC100	38.	28.53	112.	51.98	5834.	4.49	-194.22	1.42	-192.80
TC102	38.	28.53	112.	52.12	5827.	3.79	-194.68	1.40	-193.28
TC104	38.	28.53	112.	52.25	5782.	1.65	-195.28	1.38	-193.90
TC106	38.	28.53	112.	52.40	5751.	-.11	-195.99	1.35	-194.64
TC108	38.	28.53	112.	52.52	5731.	-1.50	-196.70	1.30	-195.40
TC110	38.	28.53	112.	52.66	5700.	-3.05	-197.20	1.29	-195.91
TC113	38.	28.53	112.	51.50	5909.	5.94	-195.32	1.73	-193.59
TC115	38.	28.53	112.	51.35	5955.	6.70	-196.13	1.81	-194.32
TC117	38.	28.53	112.	51.22	6009.	8.52	-196.15	1.90	-194.25
TC119	38.	28.53	112.	51.09	6067.	10.72	-195.93	2.00	-193.93
TC120	38.	28.53	112.	52.87	5656.	-5.53	-198.17	1.23	-196.94
TC121	38.	28.53	112.	53.09	5625.	-7.72	-199.30	1.19	-198.11
TC122	38.	28.53	112.	53.29	5584.	-10.10	-200.30	1.14	-199.16
TC123	38.	28.53	112.	53.50	5551.	-12.17	-201.24	1.10	-200.14
TC124	38.	28.53	112.	53.70	5503.	-15.10	-202.53	1.02	-201.51
TC125	38.	28.53	112.	53.91	5468.	-17.23	-203.47	1.00	-202.47
TC126	38.	28.53	112.	54.12	5433.	-19.28	-204.32	.95	-203.37
TC127	38.	28.53	112.	54.32	5398.	-21.24	-205.10	.90	-204.20
TC128	38.	28.53	112.	54.54	5365.	-23.10	-205.83	.85	-204.98
TC129	38.	28.53	112.	54.75	5337.	-24.74	-206.52	.80	-205.72
TC130	38.	28.53	112.	54.95	5312.	-26.25	-207.18	.78	-206.40
TC131	38.	28.53	112.	55.37	5249.	-29.49	-208.27	.71	-207.56
TC132	38.	28.53	112.	55.79	5203.	-32.09	-209.30	.69	-208.61

STATION NUMBER	LATITUDE DEG	MIN	LONGITUDE DEG	MIN	ELEVATION IN FEET	FREE-AIR ANOMALY	SIMPLE BOUGUER	TERRAIN CORRECTION	TERR-CORR BOUGUER
TC133	38.	28.53	112.	56.20	5164.	-34.27	-210.15	.61	-209.54
TC134	38.	28.53	112.	56.61	5111.	-36.52	-210.60	.59	-210.01
TC135	38.	28.53	112.	57.24	5052.	-38.63	-210.70	.50	-210.20
TC137	38.	28.53	112.	50.81	6192.	14.75	-196.15	2.25	-193.90
TC138	38.	28.53	112.	50.60	6311.	18.26	-196.69	2.46	-194.23
TC139	38.	28.53	112.	50.39	6420.	21.15	-197.52	2.50	-195.02
TC140	38.	28.53	112.	50.25	6488.	21.68	-199.31	2.54	-196.77
TC142	38.	27.34	112.	51.98	5853.	2.88	-196.48	1.65	-194.83
TC144	38.	27.34	112.	52.12	5813.	.51	-197.49	1.60	-195.89
TC146	38.	27.34	112.	52.26	5807.	-.42	-198.21	1.54	-196.67
TC148	38.	27.34	112.	52.39	5789.	-1.80	-198.97	1.48	-197.49
TC150	38.	27.34	112.	52.52	5770.	-3.07	-199.60	1.42	-198.18
TC152	38.	27.34	112.	52.65	5748.	-4.22	-200.00	1.38	-198.62
TC154	38.	27.34	112.	51.85	5895.	4.27	-196.51	1.75	-194.76
TC156	38.	27.34	112.	51.71	5940.	5.72	-196.60	1.85	-194.75
TC158	38.	27.34	112.	51.56	5985.	7.21	-196.63	1.95	-194.68
TC159	38.	27.34	112.	51.49	6009.	8.04	-196.62	2.20	-194.42
TC161	38.	27.34	112.	51.35	6064.	9.91	-196.63	2.60	-194.03
TC162	38.	27.34	112.	52.85	5712.	-5.78	-200.33	1.31	-199.02
TC163	38.	27.34	112.	53.06	5685.	-7.26	-200.89	1.23	-199.66
TC164	38.	27.34	112.	53.27	5634.	-9.89	-201.78	1.18	-200.60
TC165	38.	27.34	112.	53.47	5595.	-12.16	-202.72	1.10	-201.62
TC166	38.	27.34	112.	53.67	5563.	-14.21	-203.68	1.01	-202.67
TC167	38.	27.34	112.	53.89	5538.	-15.80	-204.42	.96	-203.46
TC168	38.	27.34	112.	54.10	5507.	-17.75	-205.32	.90	-204.42
TC169	38.	27.34	112.	54.30	5483.	-19.47	-206.22	.84	-205.38
TC170	38.	27.34	112.	54.50	5451.	-21.30	-206.96	.79	-206.17
TC171	38.	27.34	112.	54.71	5412.	-23.30	-207.63	.76	-206.87
TC172	38.	27.34	112.	54.92	5385.	-24.86	-208.28	.75	-207.53
TC173	38.	22.95	112.	58.58	5038.	-34.06	-205.66	.60	-205.06

STATION NUMBER	LATITUDE DEG	MIN	LONGITUDE DEG	MIN	ELEVATION IN FEET	FREE-AIR ANOMALY	SIMPLE BOUGUER	TERRAIN CORRECTION	TERR-CORR BOUGUER
TC174	38.	22.95	112.	59.43	4985.	-35.04	-204.83	.43	-204.40
TC175	38.	21.59	112.	54.50	5813.	3.59	-194.40	1.65	-192.75
TC176	38.	21.27	112.	53.72	6069.	13.87	-192.84	1.90	-190.94
TC177	38.	20.85	112.	52.09	6634.	30.42	-195.53	3.00	-192.53
TC178	38.	20.85	112.	51.25	7020.	43.23	-195.87	3.40	-192.47
TC179	38.	21.59	112.	51.67	6758.	32.51	-197.67	2.70	-194.97
TC180	38.	22.30	112.	53.46	6034.	10.04	-195.48	1.70	-193.78
TC181	38.	22.62	112.	51.20	6775.	31.41	-199.34	2.23	-197.11
TC182	38.	22.70	112.	51.99	6514.	24.82	-197.04	2.00	-195.04
TC183	38.	22.75	112.	52.81	6206.	15.74	-195.63	1.80	-193.83
TC184	38.	23.28	112.	52.23	6334.	18.22	-197.51	1.80	-195.71
TC185	38.	23.82	112.	51.16	6586.	23.57	-200.75	2.30	-198.45
TC186	38.	24.44	112.	50.15	6957.	32.83	-204.13	3.00	-201.13
TC187	38.	24.09	112.	52.14	6138.	9.57	-199.49	1.62	-197.87
TC188	38.	25.00	112.	54.49	5448.	-17.28	-202.84	1.14	-201.70
TC189	38.	24.30	112.	55.79	5285.	-25.50	-205.51	.90	-204.61
TC190	38.	27.82	112.	58.40	5011.	-39.34	-210.01	.40	-209.61
TC191	38.	28.12	112.	56.97	5198.	-33.16	-210.21	.50	-209.71
TC192	38.	28.27	112.	54.97	5332.	-25.67	-207.28	.80	-206.48
TC193	38.	28.40	112.	53.54	5528.	-11.64	-199.92	1.00	-198.92
TC194	38.	28.37	112.	52.30	5815.	2.15	-195.91	1.30	-194.61
TC195	38.	28.77	112.	51.52	5909.	7.92	-193.34	1.50	-191.84
TC196	38.	29.06	112.	51.04	6057.	12.57	-193.73	1.60	-192.13
TC197	38.	28.30	112.	51.05	6070.	10.08	-196.66	2.10	-194.56
TC198	38.	27.94	112.	51.13	6115.	12.26	-196.01	2.40	-193.61
TC199	38.	27.40	112.	57.85	5050.	-39.88	-211.88	.50	-211.38
TC200	38.	27.10	112.	56.20	5233.	-33.51	-211.75	.60	-211.15
TC201	38.	27.05	112.	55.80	5289.	-30.53	-210.68	.60	-210.08
TC202	38.	26.90	112.	55.15	5387.	-24.21	-207.69	.70	-206.99
TC203	38.	26.40	112.	54.12	5563.	-14.57	-204.05	1.00	-203.05

STATION NUMBER	LATITUDE DEG	MIN	LONGITUDE DEG	MIN	ELEVATION IN FEET	FREE-AIR ANOMALY	SIMPLE BOUGUER	TERRAIN CORRECTION	TERR-CORR BOUGUER
TC204	38.	26.15	112.	52.00	5950.	3.81	-198.84	1.50	-197.34
TC205	38.	26.70	112.	51.11	6170.	10.58	-199.57	2.31	-197.26
TC206	38.	26.65	112.	51.70	6019.	7.53	-197.48	1.80	-195.68
TC207	38.	27.12	112.	51.65	5949.	6.22	-196.40	1.90	-194.50
TC208	38.	27.49	112.	51.52	6023.	9.70	-195.44	2.00	-193.44
TC209	38.	26.86	112.	52.94	5747.	-5.56	-201.31	1.20	-200.11
TC210	38.	27.00	112.	54.37	5495.	-18.31	-205.47	.90	-204.57
TC212	38.	27.87	112.	52.98	5639.	-8.08	-200.14	1.20	-198.94
TC213	38.	27.99	112.	53.52	5551.	-13.22	-202.29	1.00	-201.29
TC214	38.	27.52	112.	54.25	5461.	-19.65	-205.65	.90	-204.75
TC215	38.	27.76	112.	54.97	5362.	-25.42	-208.05	.80	-207.25
TC216	38.	27.77	112.	56.07	5221.	-32.80	-210.63	.60	-210.03
TC217	38.	25.77	112.	59.27	4957.	-38.30	-207.13	.50	-206.63
TC218	38.	25.59	112.	58.30	5039.	-38.41	-210.04	.50	-209.54
TC219	38.	25.40	112.	57.04	5141.	-34.93	-210.03	.60	-209.43
TC220	38.	26.14	112.	56.30	5229.	-32.03	-210.13	.55	-209.58
TC221	38.	26.31	112.	55.55	5330.	-26.57	-208.11	.70	-207.41
TC222	38.	26.40	112.	55.04	5405.	-22.34	-206.43	.79	-205.64
TC223	38.	25.90	112.	55.04	5450.	-20.24	-205.87	.90	-204.97
TC224	38.	26.46	112.	57.19	5104.	-38.61	-212.46	.50	-211.96
TC225	38.	26.46	112.	58.30	5004.	-39.94	-210.38	.51	-209.87
TC226	38.	19.59	112.	51.00	7249.	51.05	-195.85	4.21	-191.64
TC227	38.	19.34	112.	50.75	7408.	56.02	-196.30	4.07	-192.23
TC228	38.	19.06	112.	50.47	7189.	48.58	-196.28	3.50	-192.78
TC229	38.	18.64	112.	50.34	6892.	40.43	-194.32	2.76	-191.56
TC230	38.	18.08	112.	49.31	6236.	17.21	-195.19	3.80	-191.39
TC231	38.	18.21	112.	48.12	5968.	1.74	-201.53	2.00	-199.53
TC232	38.	17.99	112.	47.65	5862.	-7.28	-206.94	1.34	-205.60
TC233	38.	18.04	112.	47.35	6042.	3.46	-202.33	2.00	-200.33
TC234	38.	19.54	112.	47.11	6036.	3.35	-202.24	2.00	-200.24

STATION NUMBER	LATITUDE DEG	LATITUDE MIN	LONGITUDE DEG	LONGITUDE MIN	ELEVATION IN FEET	FREE-AIR ANOMALY	SIMPLE BOUGUER	TERRAIN CORRECTION	TERR-CORR BOUGUER
TC235	38.	20.30	112.	46.79	6243.	9.15	-203.48	1.95	-201.53
TC236	38.	21.16	112.	46.06	6334.	7.93	-207.80	1.90	-205.90
TC237	38.	22.03	112.	46.06	6505.	14.84	-206.72	1.80	-204.92
TC238	38.	20.29	112.	45.42	6042.	-5.44	-211.23	1.00	-210.23
TC239	38.	18.77	112.	45.47	5678.	-23.71	-217.10	.90	-216.20
TC240	38.	17.29	112.	46.47	5599.	-24.43	-215.13	1.00	-214.13
TC242	38.	28.48	112.	56.97	5074.	-37.49	-210.31	.50	-209.81
TC243	38.	28.72	112.	56.47	5112.	-35.92	-210.04	.50	-209.54
TC244	38.	28.94	112.	56.12	5142.	-33.57	-208.71	.60	-208.11
TC245	38.	29.50	112.	54.97	5225.	-25.90	-203.86	.70	-203.16
TC246	38.	29.25	112.	54.97	5264.	-25.77	-205.07	.70	-204.37
TC247	38.	29.88	112.	53.62	5444.	-14.63	-200.06	.90	-199.16
TC248	38.	28.89	112.	52.20	5828.	3.60	-194.91	1.30	-193.61
TC249	38.	29.17	112.	51.75	5941.	9.86	-192.49	1.30	-191.19
TC250	38.	29.75	112.	51.00	6161.	16.78	-193.06	1.50	-191.56
TC251	38.	29.82	112.	47.17	7262.	42.01	-205.33	1.79	-203.54
TC252	38.	23.62	112.	55.20	5690.	-5.31	-199.12	1.40	-197.72
TC253	38.	23.80	112.	57.19	5131.	-31.90	-206.66	.70	-205.96
TC254	38.	24.72	112.	57.19	5119.	-34.91	-209.27	.57	-208.70
TC257	38.	16.34	112.	44.89	5660.	-32.85	-225.63	.61	-225.02
TC258	38.	19.14	112.	44.30	5747.	-22.20	-217.95	.80	-217.15
TC259	38.	19.96	112.	43.20	5800.	-22.41	-219.95	.80	-219.15
TC260	38.	21.09	112.	43.22	5882.	-16.64	-216.98	.90	-216.08
TC261	38.	22.06	112.	43.23	5950.	-13.36	-216.02	1.10	-214.92
TC262	38.	23.13	112.	43.62	6084.	-7.18	-214.40	1.30	-213.10
TC263	38.	23.42	112.	45.51	6690.	20.60	-207.26	1.71	-205.55
TC264	38.	24.55	112.	45.24	6684.	16.33	-211.33	1.60	-209.73
TC265	38.	24.97	112.	45.06	6643.	14.07	-212.19	1.50	-210.69
TC266	38.	26.66	112.	44.29	6822.	14.32	-218.04	1.20	-216.84
TC267	38.	27.27	112.	44.31	6902.	19.69	-215.40	1.17	-214.23

STATION NUMBER	LATITUDE DEG	MIN	LONGITUDE DEG	MIN	ELEVATION IN FEET	FREE-AIR ANOMALY	SIMPLE BOUGUER	TERRAIN CORRECTION	TERR-CORR BOUGUER
TC268	38.	28.71	112.	44.72	7226.	34.06	-212.06	1.29	-210.77
TC269	38.	29.47	112.	45.95	6823.	24.85	-207.54	3.35	-204.19
TC270	38.	28.54	112.	45.25	7315.	36.55	-212.60	1.49	-211.11
TC271	38.	23.85	112.	59.42	4955.	-37.09	-205.86	.50	-205.36
TC272	38.	24.73	112.	58.31	5010.	-38.36	-209.00	.50	-208.50
TC273	38.	24.72	112.	59.33	4949.	-37.51	-206.08	.48	-205.60
TC274	38.	24.33	112.	57.19	5119.	-34.00	-208.35	.60	-207.75
TC275	38.	23.79	112.	56.08	5263.	-25.52	-204.78	.80	-203.98
TC277	38.	23.18	112.	57.18	5160.	-28.75	-204.50	.70	-203.80
TC278	38.	22.49	112.	57.19	5189.	-25.92	-202.66	.80	-201.86
TC279	38.	22.92	112.	57.18	5164.	-27.89	-203.78	.70	-203.08
TC280	38.	22.85	112.	55.98	5341.	-21.20	-203.11	1.00	-202.11
TC281	38.	22.79	112.	55.20	5484.	-14.85	-201.63	1.20	-200.43
TC282	38.	23.79	112.	52.72	5980.	5.89	-197.79	1.60	-196.19
TC283	38.	24.72	112.	52.72	5892.	.25	-200.43	1.40	-199.03
TC284	38.	24.72	112.	53.83	5597.	-9.75	-200.38	1.20	-199.18
TC285	38.	25.14	112.	52.99	5666.	-7.14	-200.13	1.30	-198.83
TC286	38.	24.49	112.	51.59	6243.	13.58	-199.06	1.80	-197.26
TC287	38.	22.05	112.	52.71	6289.	18.06	-196.14	2.00	-194.14
TC288	38.	21.77	112.	52.33	6479.	25.31	-195.36	2.20	-193.16
TC289	38.	22.10	112.	51.08	6860.	33.06	-200.60	2.60	-198.00
TC290	38.	21.75	112.	50.80	7095.	40.82	-200.83	3.00	-197.83
TC291	38.	22.32	112.	50.16	6990.	34.44	-203.64	4.43	-199.21
TC292	38.	22.98	112.	51.98	6500.	22.73	-198.66	1.90	-196.76
TC293	38.	23.55	112.	51.49	6489.	22.36	-198.66	2.10	-196.56
TC294	38.	24.18	112.	50.40	6770.	28.33	-202.26	2.93	-199.33
TC295	38.	25.78	112.	52.20	5935.	3.25	-198.89	1.40	-197.49
TC296	38.	29.35	112.	50.60	6178.	14.67	-195.76	1.68	-194.08
TC297	38.	29.60	112.	49.56	6329.	16.73	-198.84	2.68	-196.16
TC298	38.	29.54	112.	48.86	6429.	17.10	-201.87	3.10	-198.77

STATION NUMBER	LATITUDE DEG	MIN	LONGITUDE DEG	MIN	ELEVATION IN FEET	FREE-AIR ANOMALY	SIMPLE BOUGUER	TERRAIN CORRECTION	TERR-CORR BOUGUER
TC299	38.	29.07	112.	48.32	6670.	23.64	-203.54	3.33	-200.21
TC300	38.	28.73	112.	48.37	6790.	27.92	-203.35	5.01	-198.34
TC301	38.	28.77	112.	46.50	7930.	57.68	-212.42	6.09	-206.33
TC302	38.	29.32	112.	47.38	7476.	49.46	-205.17	3.51	-201.66
TC303	38.	28.17	112.	46.64	8087.	58.82	-216.62	8.10	-208.52
TC304	38.	28.07	112.	46.74	8230.	65.03	-215.29	8.18	-207.11
TC305	38.	27.91	112.	47.67	8230.	66.99	-213.33	7.74	-205.59
TC306	38.	28.01	112.	48.74	8298.	63.79	-218.84	16.24	-202.60
TC307	38.	28.61	112.	45.74	7580.	45.85	-212.33	3.82	-208.51
TC308	38.	27.30	112.	47.51	8725.	68.78	-228.40	12.08	-216.32
TC309	38.	27.23	112.	46.78	9090.	75.02	-234.58	19.54	-215.04
TC310	38.	26.84	112.	46.82	8788.	70.72	-228.60	18.04	-210.56
TC311	38.	26.50	112.	47.08	8874.	77.66	-224.59	14.57	-210.02
TC312	38.	26.30	112.	47.34	8940.	80.00	-224.50	14.40	-210.10
TC313	38.	27.22	112.	50.03	7390.	42.28	-209.43	11.49	-197.94
TC314	38.	28.44	112.	49.32	7505.	48.00	-207.62	9.44	-198.18
TC315	38.	21.17	112.	52.84	6350.	22.66	-193.62	2.11	-191.51
TC316	38.	20.95	112.	52.37	6534.	27.47	-195.08	2.50	-192.58
TC317	38.	21.38	112.	53.52	7239.	45.25	-201.31	3.91	-197.40
TC318	38.	21.32	112.	50.10	7294.	44.21	-204.22	6.21	-198.01
TC319	38.	21.50	112.	51.02	7063.	40.33	-200.24	3.00	-197.24
TC320	38.	20.37	112.	51.77	6740.	35.73	-193.83	3.20	-190.63
TC321	38.	19.90	112.	51.36	7050.	44.80	-195.32	3.30	-192.02
TC322	38.	18.32	112.	50.34	6783.	37.13	-193.90	2.90	-191.00
TC323	38.	18.11	112.	49.90	6470.	25.10	-195.27	3.35	-191.92
TC325	38.	27.74	112.	59.48	4968.	-38.22	-207.43	.32	-207.11
TC326	38.	29.16	112.	58.97	4958.	-38.21	-207.07	.33	-206.74
TC327	38.	30.58	112.	58.99	4941.	-35.86	-204.15	.29	-203.86
TC328	38.	30.95	112.	58.99	4934.	-35.12	-203.17	.30	-202.87
TC329	38.	31.80	112.	59.00	4919.	-32.88	-200.42	.29	-200.13

STATION NUMBER	LATITUDE DEG	MIN	LONGITUDE DEG	MIN	ELEVATION IN FEET	FREE-AIR ANOMALY	SIMPLE BOUGUER	TERRAIN CORRECTION	TERR-CORR BOUGUER
TC330	38.	29.99	112.	56.08	5076.	-33.97	-206.86	.50	-206.36
TC331	38.	29.99	112.	57.20	5005.	-36.63	-207.10	.41	-206.69
TC332	38.	29.99	112.	58.32	4952.	-37.72	-206.39	.30	-206.09
TC333	38.	27.76	112.	50.24	6457.	18.78	-201.15	2.66	-198.49
TC334	38.	27.36	112.	50.58	6937.	34.24	-202.04	7.09	-194.95
TC335	38.	28.35	112.	50.59	6693.	27.06	-200.90	7.27	-193.63
TC336	38.	25.44	112.	51.16	6187.	10.84	-199.89	2.10	-197.79
TC337	38.	25.76	112.	48.21	8188.	59.83	-219.06	7.83	-211.23
TC338	38.	25.93	112.	48.54	8404.	63.71	-222.53	13.53	-209.00
TC339	38.	25.60	112.	48.94	8196.	57.96	-221.19	12.51	-208.68
TC340	38.	30.21	112.	47.24	7425.	48.81	-204.09	3.10	-200.99
TC341	38.	30.80	112.	47.85	7918.	62.80	-206.89	10.61	-196.28
TC342	38.	31.56	112.	47.68	7875.	63.07	-205.15	10.26	-194.89
TC343	38.	29.20	112.	49.80	6449.	20.55	-199.11	2.50	-196.61
TC345	38.	29.75	112.	47.86	6999.	35.43	-202.96	3.17	-199.79
TC346	38.	30.22	112.	46.04	6813.	26.57	-205.49	1.51	-203.98
TC347	38.	30.44	112.	55.82	5076.	-32.86	-205.75	.50	-205.25
TC348	38.	30.76	112.	55.63	5086.	-32.12	-205.35	.52	-204.83
TC349	38.	31.10	112.	55.90	5130.	-29.68	-204.40	.50	-203.90
TC350	38.	30.74	112.	54.82	5215.	-25.57	-203.19	.60	-202.59
TC351	38.	30.51	112.	54.30	5291.	-21.48	-201.69	.70	-200.99
TC352	38.	30.20	112.	53.62	5428.	-14.90	-199.78	.90	-198.88
TC354	38.	29.39	112.	53.58	5487.	-13.29	-200.18	.90	-199.28
TC356	38.	30.86	112.	53.84	5330.	-18.39	-199.93	.84	-199.09
TC357	38.	31.29	112.	53.85	5280.	-19.71	-199.54	.80	-198.74
TC360	38.	30.99	112.	51.54	5810.	9.05	-188.84	1.40	-187.44
TC361	38.	31.10	112.	51.18	5925.	13.89	-187.91	1.50	-186.41
TC362	38.	31.14	112.	50.59	6150.	19.77	-189.70	1.67	-188.03
TC363	38.	30.56	112.	49.28	6600.	27.34	-197.45	2.38	-195.07
TC365	38.	32.01	112.	54.46	5125.	-25.91	-200.47	.60	-199.87

STATION NUMBER	LATITUDE DEG	MIN	LONGITUDE DEG	MIN	ELEVATION IN FEET	FREE-AIR ANOMALY	SIMPLE BOUGUER	TERRAIN CORRECTION	TERR-CORR BOUGUER
TC366	38.	32.25	112.	54.21	5150.	-23.34	-198.75	.62	-198.13
TC367	38.	33.02	112.	53.85	5149.	-20.28	-195.65	.60	-195.05
TC368	38.	32.68	112.	52.82	5345.	-7.49	-189.54	.89	-188.65
TC369	38.	33.26	112.	54.97	5002.	-29.14	-199.51	.50	-199.01
TC370	38.	33.49	112.	55.52	4978.	-30.39	-199.95	.43	-199.52
TC371	38.	33.49	112.	56.33	4959.	-31.57	-200.48	.30	-200.18
TC372	38.	32.60	112.	57.32	4922.	-33.34	-200.98	.29	-200.69
TC373	38.	32.60	112.	58.14	4916.	-32.41	-199.85	.30	-199.55
TC374	38.	32.28	112.	56.86	4948.	-33.27	-201.80	.40	-201.40
TC375	38.	31.37	112.	57.12	4965.	-34.55	-203.65	.40	-203.25
TC376	38.	30.86	112.	57.31	4974.	-35.65	-205.07	.40	-204.67
TC377	38.	30.86	112.	58.31	4936.	-36.12	-204.24	.30	-203.94
TC380	38.	31.51	112.	52.16	5596.	1.59	-189.01	1.10	-187.91
TC381	38.	31.09	112.	52.56	5564.	-2.70	-192.21	1.10	-191.11
TC382	38.	31.95	112.	49.93	6232.	23.87	-188.39	2.32	-186.07
TC383	38.	31.96	112.	49.01	6600.	33.80	-190.99	2.84	-188.15
TC384	38.	32.79	112.	49.72	6075.	21.58	-185.34	2.00	-183.34
TC385	38.	32.48	112.	48.92	6460.	29.49	-190.53	2.10	-188.43
TC386	38.	32.49	112.	50.28	5915.	18.04	-183.43	1.54	-181.89
TC387	38.	30.04	112.	50.93	6080.	16.20	-190.89	1.62	-189.27
TC388	38.	33.10	112.	51.68	5540.	8.67	-180.02	1.20	-178.82
TC389	38.	33.02	112.	50.92	5770.	19.21	-177.32	1.37	-175.95
TC390	38.	33.26	112.	49.28	6310.	28.90	-186.02	2.01	-184.01
TC391	38.	33.47	112.	48.33	6753.	41.91	-188.09	3.77	-184.32
TC392	38.	30.56	112.	47.28	7450.	54.86	-198.88	10.17	-188.71
TC393	38.	18.76	112.	48.55	6312.	15.82	-199.17	5.67	-193.50
TC394	38.	19.48	112.	47.55	6360.	15.04	-201.58	3.02	-198.56
TC395	38.	20.64	112.	47.47	6600.	21.00	-203.80	4.09	-199.71
TC396	38.	29.53	112.	45.22	6746.	21.19	-208.58	2.96	-205.62
TC397	38.	25.65	112.	44.32	6600.	9.41	-215.38	1.18	-214.20

STATION NUMBER	LATITUDE DEG	MIN	LONGITUDE DEG	MIN	ELEVATION IN FEET	FREE-AIR ANOMALY	SIMPLE BOUGUER	TERRAIN CORRECTION	TERR-CORR BOUGUER
TC398	38.	24.36	112.	47.22	8340.	66.01	-218.05	10.86	-207.19
TC399	38.	24.81	112.	47.56	8248.	65.18	-215.75	8.08	-207.67
TC400	38.	25.08	112.	47.68	8224.	64.75	-215.36	8.28	-207.08
TC401	38.	25.40	112.	46.97	8134.	63.49	-213.55	6.48	-207.07
TC402	38.	24.72	112.	45.98	6950.	24.92	-211.80	3.77	-208.03
TC403	38.	31.40	112.	45.43	6282.	8.21	-205.75	1.42	-204.33
TC404	38.	32.56	112.	45.76	5970.	.62	-202.72	1.50	-201.22
TC405	38.	33.59	112.	46.31	5785.	-.01	-197.05	1.30	-195.75
TC406	38.	33.17	112.	46.67	6155.	15.08	-194.56	3.33	-191.23
TC407	38.	34.44	112.	46.74	5677.	.63	-192.73	.99	-191.74
TC408	38.	25.48	112.	51.54	6089.	8.06	-199.33	1.70	-197.63
TC409	38.	25.00	112.	51.73	6118.	9.04	-199.34	1.70	-197.64
TC410	38.	25.10	112.	51.04	6379.	16.93	-200.34	2.08	-198.26
TC411	38.	25.58	112.	50.51	6400.	16.35	-201.63	4.09	-197.54
TC412	38.	30.10	112.	46.76	7337.	44.14	-205.76	3.23	-202.53
TC413	38.	29.00	112.	45.06	7156.	33.94	-209.79	1.70	-208.09
TC414	38.	25.55	112.	45.68	6932.	22.12	-213.99	2.16	-211.83
TC416	38.	27.44	112.	51.63	5978.	7.74	-195.87	2.07	-193.80
TC417	38.	27.54	112.	51.63	6044.	10.33	-195.53	2.20	-193.33
TC418	38.	27.65	112.	51.63	5959.	8.00	-194.96	2.05	-192.91
TC419	38.	27.75	112.	51.63	5926.	6.70	-195.14	1.89	-193.25
TC420	38.	27.86	112.	51.63	5934.	6.39	-195.72	1.74	-193.98
TC421	38.	27.97	112.	51.63	5940.	6.56	-195.76	1.61	-194.15
TC422	38.	28.08	112.	51.63	5935.	6.49	-195.66	1.61	-194.05
TC424	38.	28.20	112.	51.63	5925.	6.39	-195.41	1.62	-193.79
TC425	38.	28.31	112.	51.63	5910.	5.96	-195.34	1.63	-193.71
TC426	38.	28.42	112.	51.63	5895.	5.73	-195.05	1.64	-193.41
TC427	38.	28.62	112.	51.63	5869.	5.67	-194.23	1.64	-192.59
TC428	38.	28.85	112.	51.63	5879.	6.03	-194.21	1.58	-192.63
TC429	38.	28.96	112.	51.63	5891.	6.53	-194.12	1.54	-192.58

STATION NUMBER	LATITUDE DEG	MIN	LONGITUDE DEG	MIN	ELEVATION IN FEET	FREE-AIR ANOMALY	SIMPLE BOUGUER	TERRAIN CORRECTION	TERR-CORR BOUGUER
TC430	38.	29.06	112.	51.63	5908.	7.28	-193.94	1.50	-192.44
TC431	38.	29.17	112.	51.63	5920.	7.95	-193.68	1.46	-192.22
TC432	38.	28.71	112.	51.63	5870.	5.74	-194.19	1.61	-192.58
TC434	38.	31.67	112.	51.63	5710.	7.72	-186.76	1.25	-185.51
TC435	38.	31.56	112.	51.63	5726.	7.92	-187.11	1.26	-185.85
TC436	38.	31.45	112.	51.63	5742.	7.91	-187.67	1.27	-186.40
TC437	38.	31.35	112.	51.63	5760.	8.07	-188.12	1.28	-186.84
TC438	38.	31.24	112.	51.63	5774.	8.24	-188.43	1.28	-187.15
TC439	38.	31.12	112.	51.63	5766.	7.91	-188.48	1.29	-187.19
TC440	38.	31.02	112.	51.63	5785.	8.37	-188.67	1.31	-187.36
TC441	38.	30.90	112.	51.63	5793.	8.51	-188.80	1.36	-187.44
TC442	38.	30.80	112.	51.63	5794.	8.69	-188.66	1.40	-187.26
TC443	38.	30.69	112.	51.63	5819.	9.57	-188.63	1.43	-187.20
TC446	38.	30.36	112.	51.63	5872.	10.31	-189.69	1.56	-188.13
TC447	38.	30.25	112.	51.63	5859.	9.76	-189.80	1.61	-188.19
TC448	38.	30.14	112.	51.63	5792.	7.51	-189.76	1.65	-188.11
TC449	38.	30.03	112.	51.63	5817.	7.90	-190.22	1.71	-188.51
TC450	38.	29.28	112.	51.63	5952.	9.59	-193.14	1.42	-191.72
TC451	38.	29.38	112.	51.63	5978.	10.40	-193.21	1.39	-191.82
TC453	38.	29.60	112.	51.63	5956.	10.06	-192.80	1.50	-191.30
TC454	38.	29.71	112.	51.63	5949.	10.50	-192.12	1.56	-190.56
TC455	38.	29.85	112.	51.63	5944.	10.51	-191.94	1.62	-190.32
TC456	38.	29.93	112.	51.63	5938.	10.61	-191.63	1.68	-189.95
TC474	38.	27.86	112.	51.84	5876.	4.01	-196.13	1.64	-194.49
TC476	38.	27.86	112.	51.70	5912.	5.56	-195.80	1.71	-194.09
TC477	38.	27.86	112.	51.97	5843.	2.69	-196.33	1.57	-194.76
TC479	38.	27.86	112.	52.11	5811.	1.56	-196.36	1.50	-194.86
TC481	38.	27.86	112.	52.25	5787.	.38	-196.73	1.44	-195.29
TC483	38.	27.86	112.	52.38	5752.	-1.41	-197.33	1.37	-195.96
TC485	38.	27.86	112.	52.54	5723.	-3.07	-198.00	1.30	-196.70

STATION NUMBER	LATITUDE DEG	MIN	LONGITUDE DEG	MIN	ELEVATION IN FEET	FREE-AIR ANOMALY	SIMPLE BOUGUER	TERRAIN CORRECTION	TERR-CORR BOUGUER
TC487	38.	27.86	112.	52.66	5698.	-4.60	-198.67	1.23	-197.44
TC491	38.	27.86	112.	51.49	5978.	6.76	-196.85	1.94	-194.91
TC493	38.	27.86	112.	51.28	6042.	8.85	-196.94	2.23	-194.71
TC495	38.	27.86	112.	51.14	6092.	11.44	-196.06	2.43	-193.63
TC498	38.	30.08	112.	52.73	5609.	-5.00	-196.04	1.30	-194.74
TC500	38.	30.19	112.	52.73	5583.	-5.47	-195.63	1.35	-194.28
TC501	38.	29.93	112.	52.73	5627.	-4.81	-196.47	1.24	-195.23
TC502	38.	30.41	112.	52.73	5578.	-5.17	-195.16	1.15	-194.01
TC504	38.	30.30	112.	52.73	5503.	-7.41	-194.84	1.25	-193.59
TC509	38.	30.63	112.	52.73	5582.	-4.61	-194.74	1.05	-193.69
TC512	38.	30.79	112.	52.73	5565.	-4.85	-194.40	1.04	-193.36
TC515	38.	29.82	112.	52.73	5635.	-4.71	-196.64	1.20	-195.44
TC517	38.	29.71	112.	52.73	5641.	-4.52	-196.66	1.16	-195.50
TC519	38.	29.60	112.	52.73	5647.	-4.37	-196.71	1.12	-195.59
TC521	38.	29.49	112.	52.73	5656.	-4.27	-196.91	1.08	-195.83
TC522	38.	29.49	112.	52.86	5626.	-5.80	-197.42	1.05	-196.37
TC523	38.	29.49	112.	53.01	5595.	-7.56	-198.13	1.02	-197.11
TC524	38.	29.49	112.	53.15	5564.	-9.17	-198.68	.99	-197.69
TC525	38.	29.49	112.	53.28	5540.	-10.49	-199.18	.97	-198.21
TC526	38.	29.49	112.	53.42	5510.	-11.94	-199.61	.94	-198.67
TC527	38.	29.49	112.	53.56	5479.	-13.48	-200.10	.91	-199.19
TC528	38.	29.49	112.	53.70	5455.	-14.80	-200.60	.88	-199.72
TC529	38.	29.49	112.	53.83	5430.	-16.24	-201.18	.85	-200.33
TC531	38.	29.49	112.	52.59	5693.	-2.31	-196.21	1.12	-195.09
TC533	38.	29.49	112.	52.46	5734.	-.27	-195.57	1.17	-194.40
TC535	38.	29.49	112.	52.32	5777.	1.93	-194.83	1.21	-193.62
TC537	38.	29.49	112.	52.11	5841.	5.47	-193.47	1.28	-192.19
TC539	38.	29.49	112.	51.97	5881.	7.53	-192.77	1.32	-191.45
TC541	38.	29.49	112.	51.83	5919.	9.34	-192.26	1.36	-190.90
TC543	38.	29.49	112.	51.56	5975.	10.66	-192.84	1.42	-191.42

STATION NUMBER	LATITUDE DEG	MIN	LONGITUDE DEG	MIN	ELEVATION IN FEET	FREE-AIR ANOMALY	SIMPLE BOUGUER	TERRAIN CORRECTION	TERR-CORR BOUGUER
TC544	38.	29.49	112.	51.43	6002.	10.92	-193.51	1.40	-192.11
TC547	38.	23.89	112.	53.15	5853.	1.20	-198.16	1.95	-196.21
TC552	38.	24.00	112.	53.15	5962.	3.80	-199.26	3.55	-195.71
TC563	38.	23.78	112.	53.15	5945.	3.40	-199.09	1.82	-197.27
TC566	38.	23.68	112.	53.15	5971.	4.23	-199.15	1.51	-197.64
TC567	38.	24.93	112.	53.15	5809.	-2.75	-200.61	1.32	-199.29
TC569	38.	24.82	112.	53.15	5802.	-2.19	-199.81	1.35	-198.46
TC571	38.	24.71	112.	53.15	5795.	-2.13	-199.51	1.38	-198.13
TC573	38.	24.61	112.	53.15	5785.	-2.29	-199.33	1.41	-197.92
TC575	38.	24.49	112.	53.15	5810.	-1.61	-199.49	1.45	-198.04
TC577	38.	24.39	112.	53.15	5846.	-.70	-199.81	1.48	-198.33
TC579	38.	24.30	112.	53.15	5870.	-.02	-199.95	1.50	-198.45
TC583	38.	24.20	112.	53.15	5905.	1.65	-199.47	1.53	-197.94
TC588	38.	24.10	112.	53.15	5992.	3.98	-200.11	2.99	-197.12
TC589	38.	23.79	112.	54.41	5627.	-6.85	-198.51	1.30	-197.21
TC591	38.	23.79	112.	54.51	5567.	-10.07	-199.68	1.27	-198.41
TC593	38.	23.79	112.	54.65	5534.	-13.24	-201.73	1.22	-200.51
TC595	38.	23.79	112.	54.78	5508.	-15.26	-202.86	1.17	-201.69
TC597	38.	23.79	112.	54.92	5472.	-17.07	-203.45	1.13	-202.32
TC599	38.	23.79	112.	55.05	5443.	-18.37	-203.76	1.08	-202.68
TC601	38.	23.79	112.	55.18	5416.	-19.63	-204.09	1.04	-203.05
TC603	38.	23.79	112.	55.32	5395.	-20.55	-204.31	.99	-203.32
TC604	38.	23.79	112.	55.46	5366.	-21.67	-204.44	.94	-203.50
TC608	38.	23.79	112.	54.30	5656.	-5.13	-197.77	1.32	-196.45
TC610	38.	23.79	112.	54.16	5691.	-3.60	-197.43	1.34	-196.09
TC612	38.	23.79	112.	54.03	5724.	-2.48	-197.44	1.37	-196.07
TC614	38.	23.79	112.	53.88	5760.	-1.52	-197.70	1.39	-196.31
TC616	38.	23.79	112.	53.75	5786.	-.99	-198.06	1.42	-196.64
TC618	38.	23.79	112.	53.61	5824.	-.05	-198.42	1.44	-196.98
TC620	38.	23.57	112.	53.15	5985.	4.93	-198.92	1.52	-197.40

STATION NUMBER	LATITUDE DEG MIN	LONGITUDE DEG MIN	ELEVATION IN FEET	FREE-AIR ANOMALY	SIMPLE BOUGUER	TERRAIN CORRECTION	TERR-CORR BOUGUER
TC622	38. 23.46	112. 53.15	5984.	5.51	-198.30	1.53	-196.77
TC624	38. 23.35	112. 53.15	5995.	6.32	-197.87	1.54	-196.33
TC626	38. 23.24	112. 53.15	6017.	7.40	-197.54	1.55	-195.99

STATION NUMBER	LATITUDE DEG	MIN	LONGITUDE DEG	MIN	ELEVATION IN FEET	FREE-AIR ANOMALY	SIMPLE BOUGUER	TERRAIN CORRECTION	TERR-CORR BOUGUER
IT001	38.	22.08	112.	59.68	4986.	-32.03	-201.86	.47	-201.39
IT002	38.	21.70	112.	59.45	4992.	-31.44	-201.46	.53	-200.93
IT003	38.	21.20	112.	59.45	4997.	-29.79	-199.98	.56	-199.42
IT004	38.	20.77	112.	59.45	4999.	-28.53	-198.79	.57	-198.22
IT005	38.	20.33	112.	59.45	5005.	-27.18	-197.65	.58	-197.07
IT006	38.	19.44	112.	58.23	5098.	-18.83	-192.46	1.20	-191.26
IT007	38.	19.44	112.	57.19	5304.	-9.87	-190.53	1.68	-188.85
IT008	38.	20.31	112.	57.19	5233.	-16.44	-194.68	1.30	-193.38
IT009	38.	20.77	112.	56.04	5521.	-5.22	-193.26	1.48	-191.78
IT010	38.	21.01	112.	55.64	5588.	-3.54	-193.87	1.50	-192.37
IT011	38.	22.05	112.	57.19	5229.	-23.21	-201.31	.81	-200.50
IT013	38.	22.08	112.	58.33	5074.	-29.48	-202.30	.62	-201.68
IT014	38.	19.45	112.	59.45	5021.	-25.17	-196.19	.59	-195.60
IT015	38.	19.45	113.	.00	5016.	-25.22	-196.06	.52	-195.54
IT016	38.	18.58	112.	59.45	5043.	-23.23	-195.00	.60	-194.40
IT017	38.	17.26	112.	59.45	5078.	-22.17	-195.12	.58	-194.54
IT018	38.	17.26	113.	.00	5073.	-22.69	-195.47	.52	-194.95
IT019	38.	16.81	112.	58.33	5143.	-18.64	-193.81	.80	-193.01
IT020	38.	16.77	112.	57.70	5224.	-13.97	-191.90	1.00	-190.90
IT021	38.	17.84	112.	58.06	5210.	-13.57	-191.03	1.10	-189.93
IT022	38.	19.06	112.	58.18	5136.	-16.35	-191.28	1.20	-190.08
IT023	38.	17.33	112.	58.00	5198.	-14.74	-191.78	1.00	-190.78
IT024	38.	14.38	112.	56.23	5350.	-8.01	-190.23	.71	-189.52
IT025	38.	14.16	112.	56.14	5320.	-9.09	-190.28	.71	-189.57
IT026	38.	13.80	112.	55.84	5289.	-9.89	-190.03	.72	-189.31
IT028	38.	13.20	112.	54.33	5336.	-4.81	-186.56	2.20	-184.36
IT029	38.	12.93	112.	51.85	5395.	-7.41	-191.17	2.90	-188.27
IT030	38.	15.71	112.	58.61	5123.	-20.38	-194.87	.60	-194.27
IT031	38.	14.17	112.	58.45	5178.	-19.43	-195.80	.47	-195.33
IT032	38.	14.19	112.	59.73	5145.	-21.15	-196.39	.33	-196.06

STATION NUMBER	LATITUDE DEG	MIN	LONGITUDE DEG	MIN	ELEVATION IN FEET	FREE-AIR ANOMALY	SIMPLE BOUGUER	TERRAIN CORRECTION	TERR-CORR BOUGUER
RS77	38.	21.29	113.	4.83	5109.	-9.58	-183.59	.70	-182.89
RS78	38.	20.51	113.	5.38	5074.	-9.66	-182.48	.72	-181.76
RS79	38.	19.66	113.	6.26	5130.	-7.83	-182.56	.76	-181.80
RS82	38.	19.45	113.	6.14	5086.	-9.25	-182.48	.60	-181.88
RS83	38.	19.60	113.	5.73	5042.	-11.00	-182.73	.55	-182.18
RS84	38.	19.93	113.	5.48	5030.	-12.10	-183.43	.55	-182.88
RS85	38.	20.78	113.	4.76	5013.	-12.95	-183.69	.55	-183.14
RS86	38.	21.68	113.	4.19	5016.	-15.23	-186.08	.55	-185.53
RS87	38.	22.10	113.	3.89	5023.	-14.75	-185.83	.50	-185.33
RS89	38.	21.65	113.	2.15	4970.	-23.44	-192.72	.26	-192.46
RS90	38.	21.63	113.	2.67	4973.	-21.52	-190.90	.27	-190.63
RS91	38.	21.83	113.	3.04	4978.	-20.18	-189.73	.28	-189.45
RS92	38.	20.11	113.	3.41	4985.	-18.56	-188.35	.27	-188.08
RS93	38.	19.20	113.	4.16	4991.	-17.80	-187.80	.27	-187.53
RS94	38.	17.86	113.	5.26	5004.	-17.50	-187.93	.25	-187.68
RS97	38.	22.48	113.	5.24	5232.	-4.11	-182.31	.90	-181.41
RS99	38.	22.08	113.	6.13	5415.	2.13	-182.30	1.05	-181.25
RS100	38.	21.59	113.	5.90	5534.	6.44	-182.05	1.03	-181.02
RS102	38.	20.34	113.	6.13	5240.	-3.59	-182.07	.85	-181.22
RS110	38.	20.52	113.	3.28	4976.	-18.93	-188.41	.27	-188.14
RS127	38.	22.03	113.	4.51	5088.	-10.78	-184.08	.70	-183.38
RS132	38.	18.08	113.	5.95	5000.	-15.32	-185.62	.35	-185.27
RS133	38.	16.86	113.	6.10	5005.	-18.16	-188.63	.25	-188.38
RS135	38.	18.55	113.	4.71	4995.	-17.55	-187.68	.25	-187.43
RS136	38.	21.21	113.	3.89	4995.	-16.87	-187.00	.40	-186.60
RS137	38.	19.45	113.	5.28	5002.	-14.26	-184.63	.40	-184.23

STATION NUMBER	LATITUDE DEG	MIN	LONGITUDE DEG	MIN	ELEVATION IN FEET	FREE-AIR ANOMALY	SIMPLE BOUGUER	TERRAIN CORRECTION	TERR-CORR BOUGUER
RS163	38.	16.61	112.	38.39	5898.	-24.73	-225.62	1.10	-224.52
RS164	38.	16.86	112.	38.42	5916.	-25.05	-226.55	1.05	-225.50
RS165	38.	16.50	112.	39.21	5869.	-31.91	-231.81	.89	-230.92
RS166	38.	16.67	112.	39.22	5858.	-32.23	-231.75	.92	-230.83
RS167	38.	16.65	112.	39.78	5839.	-36.12	-235.00	.80	-234.20
RS168	38.	16.49	112.	39.78	5850.	-35.48	-234.73	.76	-233.97
RS169	38.	17.13	112.	39.78	5868.	-35.45	-235.31	.73	-234.58
RS170	38.	17.32	112.	39.78	5885.	-34.68	-235.12	.69	-234.43
RS171	38.	17.32	112.	39.22	5909.	-31.34	-232.60	.81	-231.79
RS172	38.	17.33	112.	38.85	5925.	-28.96	-230.77	.89	-229.88
RS173	38.	17.13	112.	39.22	5890.	-31.80	-232.41	.92	-231.49
RS177	38.	15.98	112.	40.33	5788.	-38.21	-235.35	.75	-234.60
RS178	38.	16.43	112.	40.33	5766.	-39.88	-236.27	.48	-235.79
RS180	38.	15.75	112.	44.50	5667.	-35.06	-228.08	.72	-227.36
RS181	38.	15.28	112.	43.33	5678.	-38.05	-231.44	.55	-230.89
RS182	38.	15.28	112.	43.90	5658.	-37.35	-230.06	.61	-229.45
RS183	38.	15.35	112.	44.76	5644.	-34.99	-227.22	.68	-226.54
RS184	38.	15.62	112.	40.12	5779.	-36.79	-233.62	.83	-232.79
RS185	38.	15.19	112.	39.18	5822.	-29.70	-228.00	1.04	-226.96
RS186	38.	15.19	112.	38.73	5850.	-25.54	-224.79	1.13	-223.66
RS187	38.	15.42	112.	37.98	6025.	-18.50	-223.71	1.27	-222.44
RS188	38.	16.20	112.	39.06	5834.	-30.93	-229.64	1.01	-228.63
RS189	38.	17.18	112.	37.74	5985.	-21.88	-225.73	1.08	-224.65
RS190	38.	17.62	112.	38.30	5985.	-25.24	-229.09	.99	-228.10
RS203	38.	18.54	112.	38.29	6055.	-24.47	-230.70	.90	-229.80
RS259	38.	15.33	112.	40.87	5736.	-38.43	-233.80	.70	-233.10
RS260	38.	15.28	112.	42.07	5684.	-40.17	-233.77	.50	-233.27

STATION NUMBER	LATITUDE DEG	MIN	LONGITUDE DEG	MIN	ELEVATION IN FEET	FREE-AIR ANOMALY	SIMPLE BOUGUER	TERRAIN CORRECTION	TERR-CORR BOUGUER
IT033	38.	13.74	112.	59.09	5164.	-20.91	-196.80	.37	-196.43
IT034	38.	13.31	112.	58.20	5191.	-21.18	-197.99	.47	-197.52
IT035	38.	13.31	112.	57.53	5208.	-20.23	-197.61	.56	-197.05
IT036	38.	13.00	112.	57.48	5211.	-21.03	-198.52	.56	-197.96
IT037	38.	12.77	112.	57.47	5219.	-21.23	-198.99	.57	-198.42
IT038	38.	12.84	112.	57.83	5208.	-21.91	-199.29	.52	-198.77
IT039	38.	13.31	112.	59.20	5165.	-21.68	-197.60	.36	-197.24
IT040	38.	12.43	112.	59.48	5160.	-22.99	-198.74	.33	-198.41
IT041	38.	12.19	112.	55.86	5345.	-12.45	-194.50	.69	-193.81
IT042	38.	12.18	112.	56.53	5306.	-16.30	-197.02	.64	-196.38
IT043	38.	12.19	112.	56.99	5287.	-18.48	-198.55	.60	-197.95
IT044	38.	21.18	112.	57.20	5244.	-19.43	-198.04	1.00	-197.04
IT045	38.	20.31	112.	56.09	5537.	-2.99	-191.58	1.67	-189.91
IT046	38.	18.51	112.	57.19	5453.	-2.47	-188.20	1.69	-186.51
IT047	38.	18.51	112.	58.32	5158.	-15.92	-191.61	1.10	-190.51
IT048	38.	16.30	112.	55.77	5705.	7.37	-186.94	2.30	-184.64
IT049	38.	16.55	112.	55.07	6019.	17.55	-187.46	2.91	-184.55
IT050	38.	15.90	112.	56.11	5526.	.67	-187.55	1.75	-185.80
IT051	38.	16.68	112.	54.29	6328.	27.58	-187.95	3.00	-184.95
IT052	38.	17.64	112.	54.82	5781.	10.93	-185.97	2.64	-183.33
IT053	38.	17.64	112.	57.19	5422.	-2.83	-187.51	1.35	-186.16
IT054	38.	15.02	112.	56.08	5448.	-1.99	-187.55	1.30	-186.25
IT055	38.	15.82	112.	55.17	5783.	8.20	-188.77	2.40	-186.37
IT056	38.	16.07	112.	55.08	5846.	11.99	-187.12	2.60	-184.52
IT057	38.	15.41	112.	55.20	5731.	6.32	-188.88	2.12	-186.76
IT059	38.	12.85	112.	49.96	5506.	-10.89	-198.42	2.38	-196.04
IT060	38.	13.28	112.	48.93	5569.	-17.30	-206.98	.98	-206.00
IT061	38.	15.48	112.	47.33	5521.	-25.51	-213.55	.87	-212.68
IT062	38.	15.49	112.	47.77	5533.	-22.22	-210.68	.95	-209.73
IT063	38.	16.15	112.	47.42	5581.	-22.08	-212.17	.98	-211.19

STATION NUMBER	LATITUDE DEG	LATITUDE MIN	LONGITUDE DEG	LONGITUDE MIN	ELEVATION IN FEET	FREE-AIR ANOMALY	SIMPLE BOUGUER	TERRAIN CORRECTION	TERR-CORR BOUGUER
IT064	38.	17.26	112.	47.77	5758.	-11.22	-207.34	1.24	-206.10
IT065	38.	15.50	112.	46.61	5541.	-28.75	-217.48	.75	-216.73
IT066	38.	14.58	112.	47.23	5565.	-25.77	-215.31	.74	-214.57
IT067	38.	14.14	112.	47.64	5585.	-24.28	-214.51	.75	-213.76
IT068	38.	21.15	112.	58.33	5079.	-26.88	-199.87	.68	-199.19
IT069	38.	20.72	112.	58.80	5032.	-27.04	-198.43	.98	-197.45
IT070	38.	20.32	112.	58.33	5069.	-23.77	-196.42	.91	-195.51
IT071	38.	18.16	112.	56.25	5814.	11.19	-186.83	2.30	-184.53
IT072	38.	16.77	112.	54.81	5595.	4.31	-186.25	2.30	-183.95
IT073	38.	15.67	112.	57.13	5298.	-11.13	-191.58	.85	-190.73
IT074	38.	13.25	112.	54.80	5291.	-11.18	-191.39	1.57	-189.82
IT075	38.	12.84	112.	52.64	5346.	-5.77	-187.86	3.02	-184.84
IT076	38.	13.08	112.	50.74	5400.	-13.82	-197.74	2.74	-195.00
IT077	38.	12.38	112.	47.75	5836.	-10.26	-209.04	1.40	-207.64
IT078	38.	14.15	112.	47.05	5626.	-24.96	-216.58	.66	-215.92
IT079	38.	13.64	112.	46.91	5654.	-24.70	-217.28	.60	-216.68
IT080	38.	13.45	112.	46.33	5714.	-24.77	-219.39	.70	-218.69
IT081	38.	12.53	112.	46.07	5855.	-18.32	-217.74	.74	-217.00
IT084	38.	20.66	112.	53.38	6361.	24.37	-192.29	3.00	-189.29
IT085	38.	19.95	112.	52.68	7566.	57.55	-200.15	13.70	-186.45
IT087	38.	20.32	112.	53.82	6438.	26.87	-192.41	3.57	-188.84
IT088	38.	19.73	112.	55.48	6045.	15.75	-190.14	5.09	-185.05
IT089	38.	19.24	112.	55.99	5900.	14.58	-186.37	4.59	-181.78
IT090	38.	19.12	112.	56.36	5722.	6.81	-188.08	3.70	-184.38
IT091	38.	18.51	112.	56.08	6133.	21.12	-187.77	4.49	-183.28
IT092	38.	17.91	112.	55.38	6425.	36.44	-182.40	8.75	-173.65
IT093	38.	18.19	112.	55.20	6743.	37.17	-192.50	8.03	-184.47
IT094	38.	18.36	112.	55.32	6190.	21.40	-189.44	7.90	-181.54
IT095	38.	15.66	112.	52.75	6665.	36.82	-190.19	4.68	-185.51
IT096	38.	15.93	112.	52.84	6757.	39.66	-190.48	5.60	-184.88

STATION NUMBER	LATITUDE DEG	MIN	LONGITUDE DEG	MIN	ELEVATION IN FEET	FREE-AIR ANOMALY	SIMPLE BOUGUER	TERRAIN CORRECTION	TERR-CORR BOUGUER
IT097	38.	15.84	112.	53.20	6601.	34.63	-190.20	6.62	-183.58
IT098	38.	14.23	112.	54.62	5568.	-.64	-190.29	.95	-189.34
IT099	38.	14.91	112.	54.18	5767.	8.91	-187.51	1.06	-186.45
IT100	38.	16.00	112.	53.84	6203.	23.31	-187.96	2.85	-185.11
IT101	38.	16.32	112.	52.95	6585.	34.49	-189.79	3.97	-185.82
IT102	38.	17.08	112.	52.54	6939.	44.64	-191.71	4.24	-187.47
IT103	38.	15.63	112.	54.60	5892.	15.08	-185.60	2.14	-183.46
IT104	38.	14.16	112.	55.00	5528.	-2.28	-190.56	.93	-189.63
IT105	38.	15.12	112.	53.08	6317.	27.90	-187.26	3.18	-184.08
IT106	38.	14.51	112.	53.41	6307.	26.72	-188.10	4.67	-183.43
IT107	38.	13.75	112.	53.47	6098.	17.99	-189.71	7.84	-181.87
IT108	38.	13.51	112.	54.08	5475.	.17	-186.30	1.60	-184.70
IT109	38.	13.51	112.	51.46	6084.	9.14	-198.08	5.47	-192.61
IT110	38.	13.93	112.	51.64	6228.	18.10	-194.02	4.09	-189.93
IT111	38.	15.07	112.	48.73	5653.	-14.88	-207.42	2.86	-204.56
IT112	38.	13.81	112.	50.32	5768.	-7.38	-203.83	1.82	-202.01
IT113	38.	15.86	112.	51.11	6975.	40.16	-197.41	.00	-197.41
IT114	38.	15.18	112.	51.88	6590.	33.71	-190.75	3.20	-187.55
IT115	38.	14.65	112.	51.93	6487.	30.14	-190.80	3.57	-187.23
IT116	38.	17.58	112.	51.10	7711.	61.13	-201.50	11.30	-190.20
IT117	38.	17.95	112.	51.24	7950.	67.17	-203.61	15.70	-187.91
IT118	38.	18.69	112.	55.23	6716.	38.94	-189.81	7.86	-181.95
IT119	38.	16.94	112.	51.75	7358.	53.05	-197.56	9.53	-188.03
IT120	38.	16.8.	112.	52.25	7104.	49.04	-192.92	7.01	-185.91
IT121	38.	16.65	112.	53.58	7091.	46.88	-194.64	9.45	-185.19
IT122	38.	17.16	112.	53.38	7132.	48.93	-193.99	7.37	-186.62
IT123	38.	17.47	112.	53.01	7264.	53.58	-193.83	6.98	-186.85
IT124	38.	13.46	112.	55.34	5469.	-5.84	-192.12	2.38	-189.74
IT125	38.	12.46	112.	55.00	5423.	-8.04	-192.75	2.00	-190.75
IT126	38.	16.73	112.	51.15	7441.	52.01	-201.43	9.86	-191.57

STATION NUMBER	LATITUDE DEG	MIN	LONGITUDE DEG	MIN	ELEVATION IN FEET	FREE-AIR ANOMALY	SIMPLE BOUGUER	TERRAIN CORRECTION	TERR-CORR BOUGUER
IT097	38.	15.84	112.	53.20	6601.	34.63	-190.20	6.62	-183.58
IT098	38.	14.23	112.	54.62	5568.	-.64	-190.29	.95	-189.34
IT099	38.	14.91	112.	54.18	5767.	8.91	-187.51	1.06	-186.45
IT100	38.	16.00	112.	53.84	6203.	23.31	-187.96	2.85	-185.11
IT101	38.	16.32	112.	52.95	6585.	34.49	-189.79	3.97	-185.82
IT102	38.	17.08	112.	52.54	6939.	44.64	-191.71	4.24	-187.47
IT103	38.	15.63	112.	54.60	5892.	15.08	-185.60	2.14	-183.46
IT104	38.	14.16	112.	55.00	5528.	-2.28	-190.56	.93	-189.63
IT105	38.	15.12	112.	53.08	6317.	27.90	-187.26	3.18	-184.08
IT106	38.	14.51	112.	53.41	6307.	26.72	-188.10	4.67	-183.43
IT107	38.	13.75	112.	53.47	6098.	17.99	-189.71	7.84	-181.87
IT108	38.	13.51	112.	54.08	5475.	.17	-186.30	1.60	-184.70
IT109	38.	13.51	112.	51.46	6084.	9.14	-198.08	5.47	-192.61
IT110	38.	13.93	112.	51.64	6228.	18.10	-194.02	4.09	-189.93
IT111	38.	15.07	112.	48.73	5653.	-14.88	-207.42	2.86	-204.56
IT112	38.	13.81	112.	50.32	5768.	-7.38	-203.83	1.82	-202.01
IT113	38.	15.86	112.	51.11	6975.	40.16	-197.41	.00	-197.41
IT114	38.	15.18	112.	51.88	6590.	33.71	-190.75	3.20	-187.55
IT115	38.	14.65	112.	51.93	6487.	30.14	-190.80	3.57	-187.23
IT116	38.	17.58	112.	51.10	7711.	61.13	-201.50	11.30	-190.20
IT117	38.	17.95	112.	51.24	7950.	67.17	-203.61	15.70	-187.91
IT118	38.	18.69	112.	55.23	6716.	38.94	-189.81	7.86	-181.95
IT119	38.	16.94	112.	51.75	7358.	53.05	-197.56	9.53	-188.03
IT120	38.	16.85	112.	52.25	7104.	49.04	-192.92	7.01	-185.91
IT121	38.	16.65	112.	53.58	7091.	46.88	-194.64	9.45	-185.19
IT122	38.	17.15	112.	53.38	7132.	48.93	-193.99	7.37	-186.62
IT123	38.	17.47	112.	53.01	7264.	53.58	-193.83	6.98	-186.85
IT124	38.	13.46	112.	55.34	5469.	-5.84	-192.12	2.38	-189.74
IT125	38.	12.46	112.	55.00	5423.	-8.04	-192.75	2.00	-190.75
IT126	38.	16.73	112.	51.15	7441.	52.01	-201.43	9.86	-191.57

STATION NUMBER	LATITUDE DEG	MIN	LONGITUDE DEG	MIN	ELEVATION IN FEET	FREE-AIR ANOMALY	SIMPLE BOUGUER	TERRAIN CORRECTION	TERR-CORR BOUGUER
IT127	38.	16.27	112.	52.15	7315.	51.66	-197.49	10.08	-187.41
IT128	38.	19.77	112.	54.67	6641.	32.68	-193.52	8.29	-185.23
IT129	38.	17.36	112.	55.08	6865.	41.67	-192.15	10.63	-181.52
IT130	38.	12.95	112.	53.76	5494.	1.72	-185.41	3.76	-181.65
IT131	38.	13.42	112.	52.70	5933.	13.21	-188.86	4.41	-184.45
IT132	38.	16.90	112.	48.53	5886.	-3.41	-203.89	1.29	-202.60
IT135	38.	16.52	112.	45.19	5669.	-28.62	-221.70	.65	-221.05
IT136	38.	14.97	112.	49.38	5950.	-5.42	-208.08	3.46	-204.62
IT137	38.	14.36	112.	46.39	5610.	-27.85	-218.92	.64	-218.28
IT138	38.	14.36	112.	45.84	5643.	-29.00	-221.20	.63	-220.57
IT139	38.	18.36	112.	52.83	7813.	68.63	-197.48	10.62	-186.86
IT140	38.	18.28	112.	53.40	7585.	62.06	-196.28	10.56	-185.72
IT141	38.	18.06	112.	53.88	7716.	63.49	-199.32	14.46	-184.86
IT142	38.	17.87	112.	54.52	8011.	63.93	-208.93	23.82	-185.11
IT143	38.	19.25	112.	53.20	8784.	82.95	-216.23	31.23	-185.00
IT144	38.	19.14	112.	53.00	8797.	85.45	-214.17	27.40	-186.77
IT145	38.	17.70	112.	59.45	5068.	-21.87	-194.49	.60	-193.89
IT146	38.	15.71	112.	59.45	5119.	-20.83	-195.18	.46	-194.72
IT147	38.	15.71	113.	.04	5110.	-20.84	-194.88	.37	-194.51
IT148	38.	15.05	112.	59.45	5136.	-21.14	-196.07	.40	-195.67
IT149	38.	15.05	112.	58.33	5154.	-19.11	-194.65	.57	-194.08
IT150	38.	16.40	112.	59.45	5100.	-21.24	-194.95	.52	-194.43
IT151	38.	12.79	112.	55.84	5255.	-14.05	-193.04	.70	-192.34
IT152	38.	12.77	112.	56.91	5235.	-19.10	-197.41	.65	-196.76
IT153	38.	15.78	112.	51.40	6732.	33.92	-195.37	1.84	-193.53
IT154	38.	15.96	112.	50.64	6866.	31.26	-202.59	6.77	-195.82
IT155	38.	15.40	112.	51.31	7035.	39.06	-200.56	8.94	-191.62
IT163	38.	16.71	112.	47.77	5700.	-14.05	-208.19	1.18	-207.01
IT164	38.	18.53	112.	51.93	8139.	76.23	-200.98	14.39	-186.59
IT165	38.	18.12	112.	51.97	7748.	67.85	-196.05	9.49	-186.56

STATION NUMBER	LATITUDE DEG	MIN	LONGITUDE DEG	MIN	ELEVATION IN FEET	FREE-AIR ANOMALY	SIMPLE BOUGUER	TERRAIN CORRECTION	TERR-CORR BOUGUER
IT166	38.	17.69	112.	51.99	7711.	62.44	-200.20	12.13	-188.07
IT167	38.	18.09	112.	49.20	6204.	15.48	-195.83	3.64	-192.19
IT168	38.	18.08	112.	49.07	6170.	14.08	-196.07	3.44	-192.63
IT169	38.	18.06	112.	48.93	6150.	13.08	-196.39	3.20	-193.19
IT170	38.	18.10	112.	48.80	6136.	11.76	-197.23	3.00	-194.23
IT171	38.	18.10	112.	48.66	6106.	9.78	-198.19	2.78	-195.41
IT172	38.	18.13	112.	48.53	6072.	7.86	-198.95	2.56	-196.39
IT173	38.	18.03	112.	48.40	6038.	6.07	-199.59	2.37	-197.22
IT174	38.	18.18	112.	48.27	6006.	3.83	-200.73	2.15	-198.58
IT175	38.	18.21	112.	48.13	5969.	1.73	-201.58	1.90	-199.68
IT176	38.	18.20	112.	48.00	5943.	-.28	-202.70	1.78	-200.92
IT177	38.	18.13	112.	47.89	5916.	-2.56	-204.06	1.64	-202.42
IT178	38.	18.07	112.	47.78	5891.	-4.80	-205.45	1.51	-203.94
IT179	38.	17.94	112.	47.56	5840.	-8.76	-207.67	1.31	-206.36
IT180	38.	17.88	112.	47.46	5811.	-10.46	-208.38	1.27	-207.11
IT181	38.	17.81	112.	47.35	5786.	-11.96	-209.03	1.25	-207.78
IT182	38.	17.75	112.	47.25	5760.	-13.58	-209.77	1.21	-208.56
IT183	38.	17.86	112.	47.13	5738.	-15.28	-210.72	1.17	-209.55
IT184	38.	17.61	112.	47.03	5719.	-16.48	-211.27	1.14	-210.13
IT185	38.	17.54	112.	46.91	5699.	-18.01	-212.12	1.10	-211.02
IT186	38.	17.06	112.	42.80	5859.	-34.22	-233.78	.48	-233.30
IT187	38.	17.33	112.	43.15	5854.	-32.95	-232.34	.49	-231.85
IT188	38.	17.49	112.	43.63	5822.	-31.11	-229.41	.55	-228.86
IT189	38.	17.88	112.	44.03	5895.	-27.46	-228.25	.66	-227.59
IT190	38.	18.20	112.	43.20	5926.	-29.54	-231.38	.57	-230.81
IT191	38.	18.41	112.	42.55	6001.	-29.94	-234.33	.49	-233.84
IT192	38.	18.73	112.	42.03	6195.	-18.45	-229.46	.55	-228.91
IT193	38.	18.76	112.	41.41	6035.	-31.44	-236.99	.60	-236.39
IT194	38.	18.91	112.	40.59	6058.	-31.24	-237.57	.68	-236.89
IT195	38.	18.71	112.	40.05	5981.	-32.38	-236.09	.74	-235.35

STATION NUMBER	LATITUDE DEG	MIN	LONGITUDE DEG	MIN	ELEVATION IN FEET	FREE-AIR ANOMALY	SIMPLE BOUGUER	TERRAIN CORRECTION	TERR-CORR BOUGUER
IT196	38.	19.54	112.	39.98	6058.	-30.35	-236.68	.75	-235.93
IT197	38.	19.26	112.	41.08	5900.	-33.87	-234.82	.65	-234.17
IT198	38.	19.13	112.	41.48	5877.	-33.68	-233.85	.60	-233.25
IT199	38.	20.13	112.	40.19	5975.	-31.95	-235.46	.75	-234.71
IT200	38.	19.83	112.	40.68	5948.	-32.23	-234.82	.70	-234.12
IT201	38.	18.08	112.	39.15	5961.	-29.49	-232.52	.81	-231.71
IT202	38.	18.07	112.	38.31	6018.	-24.55	-229.52	.90	-228.62
IT203	38.	16.33	112.	43.70	5727.	-35.76	-230.83	.58	-230.25
IT205	38.	16.93	112.	44.49	5758.	-33.49	-229.61	.60	-229.01
IT206	38.	16.44	112.	42.50	5782.	-36.68	-233.61	.59	-233.02
IT207	38.	16.44	112.	41.66	5766.	-39.82	-236.21	.59	-235.62
IT208	38.	16.89	112.	40.35	5837.	-37.53	-236.34	.71	-235.63
IT209	38.	17.56	112.	41.35	5850.	-38.01	-237.26	.60	-236.66
IT210	38.	17.93	112.	40.46	5987.	-33.37	-237.29	.70	-236.59
IT211	38.	20.95	112.	40.22	6058.	-26.75	-233.09	.80	-232.29
IT212	38.	21.40	112.	40.22	6083.	-24.91	-232.10	.80	-231.30
IT213	38.	22.18	112.	40.98	5993.	-19.07	-223.19	.88	-222.31
IT214	38.	21.93	112.	41.55	6042.	-18.27	-224.06	.94	-223.12
IT216	38.	19.15	112.	44.30	5747.	-22.08	-217.82	.80	-217.02
IT217	38.	21.09	112.	43.24	5882.	-16.47	-216.81	.90	-215.91
IT219	38.	20.28	112.	44.29	5970.	-11.47	-214.81	.64	-214.17
IT220	38.	22.08	113.	.55	4969.	-29.91	-199.16	.39	-198.77
IT221	38.	21.63	113.	.55	4974.	-28.47	-197.89	.42	-197.47
IT222	38.	21.21	113.	.55	4982.	-27.25	-196.94	.45	-196.49
IT223	38.	20.76	113.	.55	4989.	-26.50	-196.43	.45	-195.98
IT224	38.	20.33	113.	.55	4991.	-25.93	-195.92	.45	-195.47
IT225	38.	19.90	113.	.55	5002.	-25.29	-195.65	.46	-195.19
IT226	38.	19.46	113.	.55	5014.	-24.64	-195.42	.46	-194.96
IT227	38.	18.58	113.	.56	5030.	-24.25	-195.58	.47	-195.11
IT228	38.	20.20	113.	.55	5054.	-26.78	-198.92	.47	-198.45

STATION NUMBER	LATITUDE DEG	MIN	LONGITUDE DEG	MIN	ELEVATION IN FEET	FREE-AIR ANOMALY	SIMPLE BOUGUER	TERRAIN CORRECTION	TERR-CORR BOUGUER
IT229	38.	17.27	113.	.55	5065.	-22.88	-195.39	.45	-194.94
IT230	38.	16.82	113.	.55	5072.	-22.59	-195.34	.41	-194.93
IT231	38.	15.94	113.	.55	5095.	-21.13	-194.67	.35	-194.32
IT232	38.	15.94	113.	.29	5099.	-20.99	-194.66	.35	-194.31
IT233	38.	15.94	113.	1.68	5089.	-22.42	-195.75	.26	-195.49
IT234	38.	16.82	113.	1.20	5060.	-23.42	-195.77	.35	-195.42
IT235	38.	16.82	113.	1.68	5053.	-24.36	-196.46	.30	-196.16
IT236	38.	17.27	113.	1.68	5045.	-24.58	-196.42	.32	-196.10
IT237	38.	17.70	113.	1.68	5036.	-24.40	-195.93	.33	-195.60
IT238	38.	18.58	113.	1.68	5023.	-23.71	-194.79	.33	-194.46
IT239	38.	18.58	113.	1.11	5032.	-24.08	-195.47	.40	-195.07
IT240	38.	19.45	113.	1.67	5005.	-23.47	-193.94	.32	-193.62
IT241	38.	19.90	113.	1.66	4997.	-23.54	-193.73	.33	-193.40
IT242	38.	20.33	113.	1.66	4989.	-23.49	-193.42	.33	-193.09
IT243	38.	20.80	113.	1.66	4981.	-23.64	-193.30	.33	-192.97
IT244	38.	21.23	113.	1.66	4976.	-23.94	-193.42	.33	-193.09
IT247	38.	20.34	113.	2.23	4984.	-21.87	-191.62	.26	-191.36
IT248	38.	20.45	113.	2.78	4982.	-20.35	-190.04	.21	-189.83
IT249	38.	19.46	113.	2.23	5002.	-22.25	-192.62	.26	-192.36
IT250	38.	19.23	113.	2.78	4998.	-20.94	-191.17	.21	-190.96
IT251	38.	18.56	113.	2.78	5010.	-21.51	-192.15	.21	-191.94
IT252	38.	18.56	113.	2.23	5018.	-22.74	-193.65	.26	-193.39
IT253	38.	18.13	113.	2.78	5008.	-22.53	-193.11	.21	-192.90
IT254	38.	17.69	113.	2.78	5019.	-23.26	-194.20	.21	-193.99
IT255	38.	17.69	113.	3.35	5018.	-21.74	-192.65	.21	-192.44
IT256	38.	17.47	113.	3.90	4998.	-21.52	-191.75	.20	-191.55
IT257	38.	16.80	113.	3.90	5023.	-22.61	-193.70	.20	-193.50
IT258	38.	16.81	113.	3.35	5024.	-24.15	-195.26	.21	-195.05
IT259	38.	16.82	113.	2.79	5034.	-24.90	-196.36	.21	-196.15
IT260	38.	15.94	113.	2.80	5053.	-25.64	-197.74	.21	-197.53

STATION NUMBER	LATITUDE DEG	MIN	LONGITUDE DEG	MIN	ELEVATION IN FEET	FREE-AIR ANOMALY	SIMPLE BOUGUER	TERRAIN CORRECTION	TERR-CORR BOUGUER
IT261	38.	15.94	113.	3.35	5042.	-26.22	-197.95	.21	-197.74
IB262	38.	15.28	113.	3.91	5045.	-25.73	-197.57	.20	-197.37
IA262	38.	15.93	113.	3.91	5037.	-25.51	-197.07	.20	-196.87
IT263	38.	15.06	113.	3.91	5045.	-25.32	-197.15	.20	-196.95
IT264	38.	15.93	113.	4.46	5029.	-24.50	-195.79	.20	-195.59
IT265	38.	15.93	113.	5.00	5027.	-23.08	-194.30	.20	-194.10
IT266	38.	15.51	113.	5.02	5030.	-23.95	-195.27	.19	-195.08
IT267	38.	15.93	113.	6.12	5015.	-19.59	-190.40	.19	-190.21
IT268	38.	15.05	113.	6.13	5025.	-21.68	-192.84	.18	-192.66
IT269	38.	13.31	113.	.56	5128.	-19.97	-194.63	.26	-194.37
IT270	38.	13.34	113.	6.18	5036.	-21.87	-193.39	.15	-193.24
IT271	38.	13.34	113.	5.19	5040.	-23.30	-194.97	.17	-194.80
IT272	38.	14.17	113.	6.13	5027.	-24.39	-195.61	.16	-195.45
IT273	38.	14.16	113.	5.02	5039.	-23.96	-195.59	.18	-195.41
IT274	38.	14.19	113.	3.90	5050.	-23.37	-195.37	.20	-195.17
IT275	38.	14.19	113.	2.80	5073.	-20.11	-192.89	.22	-192.67
IT276	38.	13.33	113.	1.69	5104.	-18.50	-192.34	.20	-192.14
IT277	38.	14.19	113.	.55	5122.	-21.42	-195.88	.27	-195.61
IT278	38.	17.19	112.	46.30	5592.	-25.84	-216.31	.94	-215.37
IT279	38.	17.08	112.	46.13	5597.	-26.71	-217.34	.89	-216.45
IT280	38.	16.98	112.	45.95	5635.	-27.03	-218.95	.85	-218.10
IT281	38.	16.87	112.	45.78	5663.	-26.97	-219.85	.80	-219.05
IT282	38.	16.76	112.	45.60	5692.	-26.99	-220.86	.76	-220.10
IT283	38.	16.66	112.	45.43	5702.	-27.64	-221.85	.71	-221.14
IT284	38.	16.55	112.	45.25	5657.	-29.33	-222.01	.67	-221.34
IT285	38.	17.35	112.	46.58	5624.	-22.58	-214.14	1.01	-213.13
IT286	38.	17.42	112.	46.69	5658.	-20.61	-213.32	1.05	-212.27
IT287	38.	17.49	112.	46.80	5686.	-18.71	-212.37	1.07	-211.30
IT288	38.	21.70	112.	55.04	5662.	-4.20	-197.05	1.47	-195.58
IT289	38.	21.89	112.	55.54	5521.	-11.60	-199.65	1.30	-198.35

STATION NUMBER	LATITUDE DEG	MIN	LONGITUDE DEG	MIN	ELEVATION IN FEET	FREE-AIR ANOMALY	SIMPLE BOUGUER	TERRAIN CORRECTION	TERR-CORR BOUGUER
IT290	38.	22.08	112.	56.03	5400.	-17.16	-201.09	1.12	-199.97

STATION NUMBER	LATITUDE DEG	LATITUDE MIN	LONGITUDE DEG	LONGITUDE MIN	ELEVATION IN FEET	FREE-AIR ANOMALY	SIMPLE BOUGUER	TERRAIN CORRECTION	TERR-CORR BOUGUER
741 3	38.	35.23	112.	54.04	4997.	-27.46	-197.66	.40	-197.26
741 4	38.	35.23	112.	54.26	4987.	-28.31	-198.17	.30	-197.87
741 5	38.	35.23	112.	54.48	4980.	-29.23	-198.85	.30	-198.55
741 6	38.	35.24	112.	54.70	4978.	-29.78	-199.33	.30	-199.03
741 7	38.	35.24	112.	54.92	4982.	-29.57	-199.26	.30	-198.96
741 8	38.	35.24	112.	55.15	4976.	-29.93	-199.42	.20	-199.22
741 9	38.	35.24	112.	55.36	4960.	-31.39	-200.33	.20	-200.13
74110	38.	35.22	112.	55.59	4939.	-30.81	-199.03	.20	-198.83
74111	38.	35.23	112.	55.80	4932.	-31.10	-199.09	.20	-198.89
74112	38.	35.23	112.	56.04	4921.	-32.29	-199.90	.20	-199.70
74116	38.	35.18	112.	52.97	5105.	-18.47	-192.35	.60	-191.75
74118	38.	35.18	112.	52.56	5190.	-13.12	-189.89	.60	-189.29
74120	38.	35.20	112.	52.16	5275.	-7.69	-187.36	.80	-186.56
74121	38.	35.21	112.	51.95	5325.	-4.19	-185.56	.90	-184.66
74123	38.	35.23	112.	51.64	5390.	.08	-183.50	1.20	-182.30
74124	38.	35.23	112.	51.43	5430.	2.62	-182.33	1.10	-181.23
74127	38.	35.23	112.	50.90	5570.	11.56	-178.15	1.40	-176.75
74128	38.	35.24	112.	50.68	5627.	14.58	-177.08	1.50	-175.58
74130	38.	34.34	112.	53.85	5067.	-22.70	-195.28	.40	-194.88
74132	38.	32.61	112.	55.73	4997.	-32.02	-202.22	.40	-201.82
742 2	38.	35.22	112.	53.82	5011.	-26.07	-196.75	.40	-196.35
742 3	38.	36.10	112.	53.81	5003.	-26.15	-196.55	.30	-196.25
74204	38.	36.54	112.	53.81	5007.	-24.85	-195.39	.30	-195.09
742 5	38.	37.18	112.	53.80	5020.	-23.17	-194.15	.30	-193.85
742 6	38.	38.72	112.	53.82	5015.	-16.64	-187.45	.30	-187.15
742 7	38.	37.85	112.	53.81	4982.	-23.93	-193.62	.30	-193.32
742 8	38.	39.35	112.	53.83	5022.	-14.07	-185.12	.90	-184.22
742 9	38.	40.05	112.	53.82	5041.	-10.45	-182.14	.20	-181.94
74210	38.	40.05	112.	54.92	5001.	-13.30	-183.64	.40	-183.24
74211	38.	39.38	112.	54.70	5996.	78.61	-125.62	.20	-125.42

STATION NUMBER	LATITUDE DEG	MIN	LONGITUDE DEG	MIN	ELEVATION IN FEET	FREE-AIR ANOMALY	SIMPLE BOUGUER	TERRAIN CORRECTION	TERR-CORR BOUGUER
74212	38.	39.23	112.	55.97	4959.	-18.11	-187.01	.20	-186.81
74213	38.	38.84	112.	55.95	4961.	-20.03	-189.00	.20	-188.80
74214	38.	37.88	112.	56.04	4941.	-23.59	-191.88	.20	-191.68
74217	38.	35.82	112.	56.45	4909.	-30.85	-198.05	.20	-197.85
74219	38.	37.15	112.	52.34	5062.	-18.45	-190.67	.73	-190.14
74222	38.	38.19	112.	50.91	5231.	-2.62	-180.79	1.00	-179.79
74226	38.	38.74	112.	52.61	5059.	-14.47	-186.78	.30	-186.48
74227	38.	32.59	112.	53.84	5142.	-24.25	-199.39	.69	-198.70
74245	38.	32.63	112.	59.02	4906.	-31.43	-198.53	.20	-198.33
74246	38.	33.09	112.	59.02	4901.	-31.48	-198.41	.20	-198.21
74247	38.	34.34	112.	59.04	4884.	-30.77	-197.12	.20	-196.92
74248	38.	36.47	112.	59.08	4867.	-26.52	-192.29	.20	-192.09
74250	38.	36.55	112.	57.16	4911.	-27.99	-195.26	.20	-195.06

REFERENCES

Abou-Zied, M. S., 1968, Geology and mineralogy of the Milford Flat quadrangle and the Old Moscow Mine, Star District, Beaver County, Utah; unpublished Ph.D. dissertation, University of Utah, 150 p.

Anderson, P. N., and Axtell, L. H., 1972, Geothermal resources in California: Geothermal overviews of the western United States. Published by Geothermal Resources Council, Davis, California.

Armstrong, R. L., 1970, Geochronology of Tertiary igneous rocks, eastern Basin and Range province, western Utah, eastern Nevada, and vicinity, U.S.A.: Geochim. et Cosmochim. Acta, vol. 34, p. 203-232.

Baer, J. L., 1962, Geology of the Star Range, Beaver County, Utah: Brigham Young University Geology Studies, v. 9, pt. 2, p. 29-52.

_____, 1973, Summary of stratigraphy and structure of the Star Range, Beaver County, Utah: Utah Geological Association Publication 3, p. 33-38.

Baetcke, G. B., 1969, Stratigraphy of the Star Range and reconnaissance study of three selected mines; unpublished Ph.D. dissertation, University of Utah, 184 p.

Barosh, P. J., 1960, Beaver Lake Mountains, Beaver County Utah: Utah Geol. Min. Survey Bull. 68.

Biehler, S., and Combs, J., 1972, Correlations of gravity and geothermal anomalies in the Imperial Valley, Southern California (abs). Geol. Soc. America Abstracts with Programs, v. 4, no. 3, p. 128.

Bryant, N. L., and Parry, W. T., 1977, Hydrothermal alteration at Roosevelt Hot Springs KGRA - DDH 1976-1: Technical Report ERDA Grant EY-76-S-07-1601, v. 77-5, 87 p.

Brumbaugh, W. D., and Cook, K. L., 1977, Gravity survey of the Cove Fort - Sulphurdale KGRA and North Mineral Mountains area, Millard and Beaver counties, Utah: Technical Report ERDA Grant EY-76-S-07-1601, v. 77-4, 131 p.

Butler, B. S., Loughlin, G. F., Heikes, V. C., and others, 1920, The ore deposits of Utah: U.S. Geol. Survey Prof. Paper 111, 672 p.

Cady, J. W., 1977, Calculation of gravity and magnetic anomalies along profiles with end corrections and inverse solutions for density and magnetization: USGS open file report.

Chapman, R. H., 1975, Geophysical study of the Clear Lake region: California Special Report 116, California Div. of Mines and Geology.

Cook, K. L., Nilsen, T. H., Lambert, J. F., 1971, Gravity base station network in Utah-1967: Utah Geol. and Min. Survey Bull. 92.

Crawford, A. L., and Buranek, A. M., 1945, Tungsten deposits of the Mineral Range, Beaver County, Utah; Utah Eng. Exp. Sta. Bull. 25, p. 6-48.

Crebs, T. J., and Cook, K. L., 1976, Gravity and ground magnetic surveys of the central Mineral Mountains, Utah: Final Report, NSF Grant GI-43741, v. 6, 129 p.

Crosby, G. W., 1973, Regional structure in southwestern Utah; Geology of the Milford area, Hintze, L. F., and Whelan, J. A., Editors, Utah Geol. Assoc. Publication no. 3, 94 p.

Earll, F. N., 1957, Geology of the central Mineral Range, Beaver County, Utah: unpublished Ph.D. thesis, University of Utah.

Erickson, M. P., 1973, Volcanic rocks of the Milford area, Beaver County, Utah: Utah Geological Association Publication 3, p. 13-22.

Erickson, M. P., and Dasch, E.J., 1963, Geology and hydrothermal alteration in northwestern Black Mountains and southern Shauntie Hills, Beaver and Iron counties, Utah: Utah Geological and Mineralogical Survey Special Studies 6, 32 p.

_____, 1968, Volcanic stratigraphy, magnetic data and alteration geologic map and sections of the Jarloose mining district southeast of Minersville, Beaver County, Utah: Utah Geol. and Min. Survey map no. 26.

Evans, S. H., 1977 (compiler), Geologic map of the central and northern Mineral Mountains: Department of Geology and Geophysics, University of Utah.

Fuller, B. D., 1967, Two-dimensional frequency analysis and design of grid operators: Mining Geophysics, v. 2, Society of Exploration Geophysicists, Tulsa, p. 658-708.

Grant, F. S., 1972, Review of data processing and interpretation methods in gravity and magnetics, 1964-71: Geophysics, v. 37, no. 4, p. 647-661.

Hansen, G. H. and Scoville, H. C., 1955, Drilling records for oil and gas in Utah: Utah Geol. Min. Survey Bull. 50.

Hardman, Elwood, 1964, Regional gravity survey of central Iron and Washington counties, Utah; unpublished M. S. thesis, University of Utah, 107 p.

Hintze, L. F., 1963 (compiler), Geologic map of southwestern Utah: Utah Geological and Mineralogical Survey.

Isherwood, W. F., 1975, Gravity and magnetic studies of the Geysers Clear Lake geothermal region, California, Department of the Interior, Geol. Survey. Open-file report 73-368, 1975.

Kane, M. F., 1962, A comprehensive system of terrain corrections using a digital computer: Geophysics, v. 27, no. 4, p. 455-462.

Lemmon, D. M., Silberman, M. L. and Kistler, R. W., 1973, Some K-Ar ages of extrusive and intrusive rocks of the San Francisco and Wah Wah Mountains, Utah: Utah Geological Association Publication 3, p. 23-26.

Liese, H. C., 1957, Geology of the northern Mineral Range, Millard and Beaver Counties, Utah; unpublished M. S. thesis, Univ. of Utah, 88 p.

Mudgett, P. M., 1963, Regional gravity survey of parts of Beaver and Millard Counties, Utah: unpublished M. S. thesis, University of Utah, 19 p.

Mundorff, J. C., 1970, Major thermal springs of Utah: Utah Geol. and Mineral Survey Water Resources Bull. 13.

Nettleton, L. L., 1976, Gravity and magnetics in oil prospecting: McGraw-Hill, New York.

Oppenheim, A. V., and Schafer, R. W., 1975, Digital Signal Processing, Prentice-Hall Inc., New Jersey, 585 p.

Park, G. M., 1968, Some geochemical and geochronologic studies of the beryllium deposits in western Utah: unpublished M. S. thesis, University of Utah.

Parry, W. T., Benson, N. L., and Miller, C. D., 1976, Geochemistry and hydrothermal alteration at selected Utah hot springs: Final Report, NSF Grant GI-43741, vol. 3, 131 p.

Parry, W. T., and Dedolph, R. E., 1976, Geologic map of the Roosevelt Hot Springs, Utah: Department of Geology and Geophysics, University of Utah.

Parry, W. T., Nash, W. P., Bowman, J. R., Truesdell, A. H., Ward, S. H., Whelan, J. A., Bryant, N. L., Dedolph, R. E., and Evans, S. H., 1978, Geology and geochemistry of the Roosevelt Hot Springs thermal area, Utah: manuscript in preparation.

Petersen, C. A., 1973, Summary of stratigraphy in the Mineral Range, Beaver and Millard Counties, Utah: Utah Geol. and Min. Survey Report of Investigation No. 84, 7 p.

_____, 1975a, Geology of the Roosevelt area, Beaver county, Utah; unpublished M. S. thesis, Univ. of Utah, 49 p.

_____, 1975b, Geology of the Roosevelt Hot Springs area, Beaver County, Utah: Utah Geology, v. 2, no. 2, p. 109-116.

Peterson, D. L., 1972, Complete Bouguer anomaly map of parts of Beaver Iron, and Millard counties, southwestern Utah; U.S. Geol. Survey Open-File Map.

Sawyer, R. F. and Cook, K. L., 1977, Gravity and ground magnetic surveys of the Thermo Hot Springs KGRA region Beaver County, Utah: Technical Report ERDA Grant EY-76-S-07-1601, v. 77-6, 142 p.

Schmoker, J. W., 1972, Analysis of gravity and aeromagnetic data, San Francisco Mountains and vicinity, southwestern Utah: Utah Geological and Mineralogical Survey Bulletin 98, 24 p.

Shuey, R. T., and Pasquale, A. S., 1973, End corrections in magnetic profile interpretation: Geophysics, v. 38,no. 3, p. 507-512.

Sill, W. R. and Bodell, J., 1977, Thermal gradients and heat flow at Roosevelt Hot Springs: Technical Report ERDA Grant EY-76-S-07-1601, v. 77-3, 46 p.

Snow, J. H., 1977, Gravity and magnetic interpretation using one-dimensional direct search and Marquardt linear inversion: University of Utah GGS 628 class project, 56 p.

Sontag, R. J., 1965, Regional gravity survey of parts of Beaver, Millard, Piute, and Sevier Counties, Utah; unpublished M. S. thesis, University of Utah, 32 p.

Swick, C. H., 1942, Pendulum gravity measurements and isostatic reductions: U. S. Coast and Geodetic Survey Spec. Pub. 232.

Thangsuphanich, I., 1976, Regional gravity survey of the southern Mineral Mountains, Beaver County, Utah; unpublished M. S. thesis, University of Utah, 38 p.

Ward, S. H., and Sill, W. R., 1976, Dipole-dipole resistivity

surveys, Roosevelt Hot Springs KGRA; Final Report, NSF Grant GI-43741, vol. 2, 29 p.

Welsh, J. E., 1973, Paleozoic and Mesozoic stratigraphy of the Milford area, Beaver County, Utah: Utah Geological Association Publication 3, p. 9-12.

Whelan, J. A., 1973, Geology of the Rocky Range, Beaver County, Utah; Geology of the Milford area, Hintze, L. F., and Whelan, J. A., Editors, Utah Geol. Assoc. Publication no. 3, 94 p.

_____, 1977, Geologic map of the Wildcat Creek area, eastern Beaver County, Utah: map in preparation.

Zietz, I., Shuey, R. T., Kirby, J. R., Jr., 1976, Aeromagnetic map of Utah; U. S. Geol. Survey Geophys. Invest. Map GP-907.

VITA

Name	James Allen Carter
Birthdate	January 26, 1947
Birthplace	Berea, Ohio
High School	East Jefferson High School Metairie, Louisiana
University 1965-1969	Miami University Oxford, Ohio
Degree 1969	B.A. in mathematics, Miami University, Oxford, Ohio
Military Service 1969-1974	U.S. Navy
Research Assistant 1976-1978	Department of Geology and Geophysics, University of of Utah, Salt Lake City, Utah
Professional Organization	Society of Exploration Geophysicists

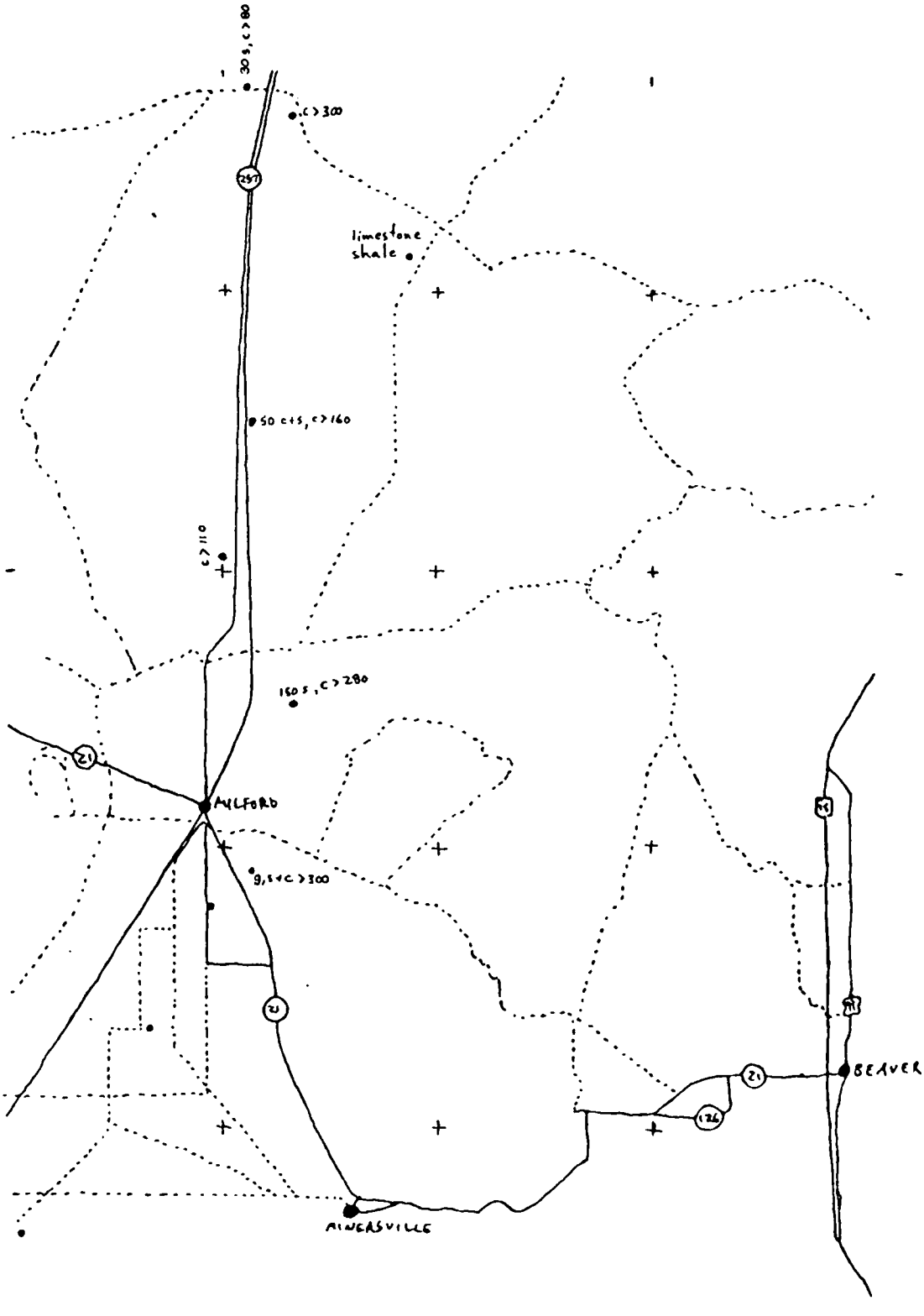
30 s, c > 280
c > 300
267
limestone
shale
50 c+s, c > 160
c > 110
150 s, c > 280
21
AYLFORD
g, s+c > 300
77
77
21
BEAVER
126
AINGERSVILLE


Original
to be copy
onto transparency
BEAVER MOUNTAINS
BLACK ROCK
BLACK ROCK ROAD
MILLARD CO.
BEAVER CO.
BEAVER LAKE MOUNTAINS
ROCKY RANGE
MINERAL MOUNTAINS
COUNTY LINE FAULT
ROOSEVELT HOT SPRINGS
POLE LINE ROAD
OPAL MOUND FAULT
MILFORD VALLEY
MILFORD
HOT SPRINGS FAULT
BEARSKIN MTN.
LITTLE BEARSKIN MTN.
NORTH TWIN FLAT MTN.
SOUTH TWIN FLAT MTN.
GRANITE PEAK
RANCHO CANYON
CORRAL CANYON
THE PASS ROAD
PINE CANYON FAULT
BEAVER VALLEY
ADAMSVILLE
BEAVER
SCALE
TRUE NORTH
MAGNETIC NORTH
OVERLAY
113°00'
112°45'
38°30'
38°15'

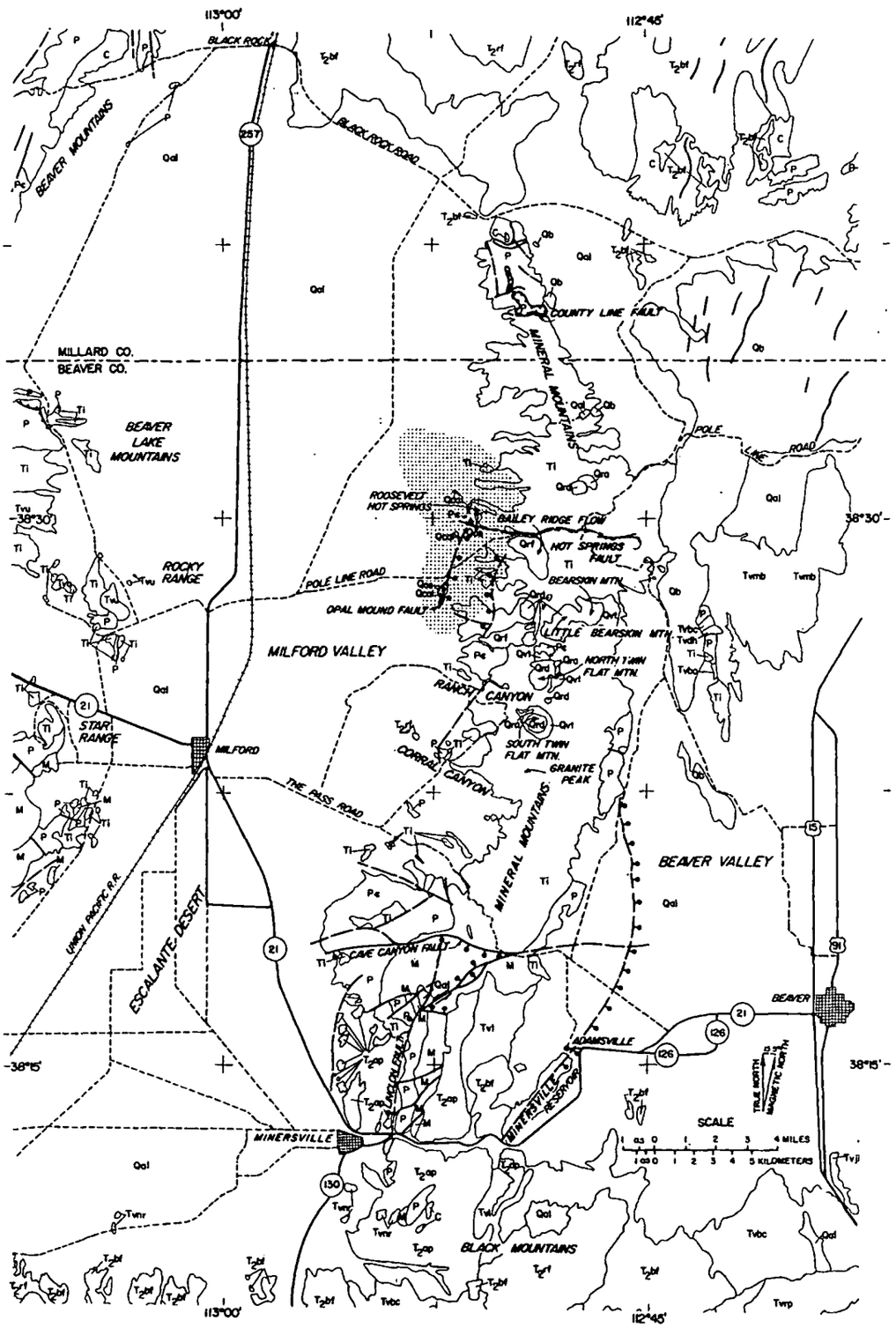

PLATE I. GEOLOGY MAP OVERLAY